NASA CONTRACTOR REPORT

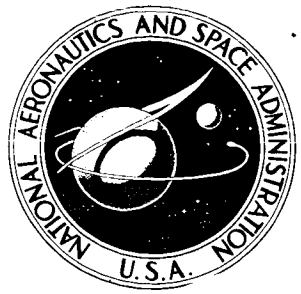

NASA CR-532

NASA CR-532

HUMAN TRACKING PERFORMANCE IN UNCOUPLED AND COUPLED TWO-AXIS SYSTEMS

by E. P. Todosiev, R. E. Rose, G. A. Bekey, and H. L. Williams

Prepared by
TRW SYSTEMS
Redondo Beach, Calif.
for Langley Research Center

FACILITY FORM 602
N66 33981 (ACCESSION NUMBER)
190 (PAGES)
CR-532 (NASA CR OR TMX OR AD NUMBER)
1 (THRU)
05 (CODE)
(CATEGORY)

NATIONAL AERONAUTICS AND SPACE ADMINISTRATION • WASHINGTON, D. C. • AUGUST 1966

NASA CR-532

HUMAN TRACKING PERFORMANCE IN UNCOUPLED AND COUPLED TWO-AXIS SYSTEMS

By E. P. Todosiev, R. E. Rose, G. A. Bekey,
and H. L. Williams

Distribution of this report is provided in the interest of information exchange. Responsibility for the contents resides in the author or organization that prepared it.

Prepared under Contract No. NAS 1-4419 by
TRW SYSTEMS
Redondo Beach, Calif.

for Langley Research Center

NATIONAL AERONAUTICS AND SPACE ADMINISTRATION

For sale by the Clearinghouse for Federal Scientific and Technical Information
Springfield, Virginia 22151 – Price $5.00

33981

ABSTRACT

This report presents the results of an experimental and analytical study of human performance in uncoupled and coupled control systems conducted under NASA Contract NAS 1-4419, monitored by the NASA Langley Research Center.

Human pilot performance in single and two-axis systems was mathematically modeled by linear second-order describing functions. Model parameters were determined using model matching techniques. Analysis of the models showed that the amplitude ratio and phase lead of the describing function increased with training indicating an increase in open loop bandwidth. The phase margin also decreased with training. Increasing the plant lag time constant resulted in an increase in the model lead time constant and a decrease in the zero frequency gain. No significant difference was found to exist in the normalized tracking error per axis between the two-axis tasks and the single-axis tasks. However the model lead time constant was significantly greater in two-axis tracking.

Manual tracking of two-axis systems with cross-coupling was studied experimentally and analytically. Approximate methods for modeling two-axis performance were developed and checked using a precise spectral analysis approach. Coupled and uncoupled, symmetrical and asymmetrical two-axis performance was compared. The results show that modeling of cross-coupled systems is feasible and that trained subjects are capable of decoupling the axes of some systems.

A methodology study compared the identification performance of continuous, iterative, and extrapolation model matching techniques. An iterative technique employing sensitivity equations for the generation of influence coefficients was found to be the best technique due to its excellent identification accuracy and ease of implementation. Convergence in iterative techniques can be improved substantially by equalizing the parameter adjustment rates and limiting the maximum correction per iteration.

PRECEDING PAGE BLANK NOT FILMED.

TABLE OF CONTENTS

PRECEDING PAGE BLANK NOT FILMED.

PRECEDING PAGE BLANK NOT FILMED.

LIST OF FIGURES

LIST OF TABLES

1. INTRODUCTION

This report presents the results of the second phase of a two year study program on model matching techniques for the determination of parameters in human pilot models. Model matching techniques refer to a method of system identification where the parameters of an assumed methematical model are adjusted so as to minimize an appropriate function of the difference between system and model outputs. The first year of the study concentrated on testing the feasibility of applying the method to identification of human pilot performance in a variety of manual tracking systems. The results are reported in NASA CR-143 (Reference 5).

The objective of the research reported here was to apply model matching techniques to study human performance in more realistic control situations, with an emphasis on two-axis tracking. While the first year study concentrated on feasibility, the present study was directed toward obtaining statistically meaningful data on human performance, in both single and two-axis manual control systems. An additional objective was the further development of the modeling techniques and evaluation of their accuracy.

The report is divided into three major sections. The first of these is concerned with the effects of such variables as task difficulty and training on human performance in both single and uncoupled two-axis compensatory tracking systems. The effects of training and task difficulty were evaluated by examining the parameters of mathematical models. Analyses of variance were performed in order to obtain statistical significance levels for the major results.

The second section of the report is devoted to reporting the results of a study of human performance in two-axis manual control systems with cross-coupling. Very little background exists in the area and consequently techniques for determining the mathematical models had to be developed. Model matching techniques were applied and their accuracy was tested by means of a theoretically exact spectral analysis technique which was developed for the purpose. In the spectral analysis technique developed, the human operator is

represented by a matrix whose elements are determined from a knowledge of the system plant dynamics and the spectral matrices of the system excitation and tracking error signals. This portion of the study had two major objectives, namely, to apply modeling methods to the cross-coupled system and to find whether the human operator was capable of decoupling the system. Analysis of variance was again employed to test the significance of the conclusions.

The third section of the report deals with modeling methodology. It includes the results of studies on the effect of excitation bandwidth and model form on parameter accuracy, on approximate techniques for computation of time delay and higher order terms in the model and on certain situations in which parameters cannot be determined precisely. It includes a derivation of the theoretically exact spectral analysis technique developed for mathematical modeling of human performance in coupled tracking systems. Identification accuracy and general performance of continuous and various iterative model matching techniques are compared for both open and closed loop formulations, with the objective being the selection of an optimum technique.

2. HUMAN PERFORMANCE IN SINGLE AND TWO AXIS SYSTEMS

2.1 Introduction

This section presents the results of a study of human tracking performance in single axis and uncoupled two-axis manual control systems. Controlled element dynamics were selected to approximate a realistic aircraft control task. The major objective of this phase of the work was the collection and evaluation of statistically meaningful data on the effects of training, task difficulty, and single vs two-axis tracking.

The evaluation was performed by first obtaining describing function models for each control configuration using a continuous model matching technique and then analyzing the parameters of the describing function to determine the functional relationship between the parameters and task difficulty or training. This analysis was conducted in the frequency domain using conventional control system theory. Single and two-axis tracking systems were compared through the use of describing function parameters and Bode diagrams. Both the analysis and comparison were subjected to an analysis of variance to determine the significance of the results obtained. The above analysis and comparison were used as the basis for specifying the characteristics of human performance in the single and two-axis tracking tasks investigated.

2.2 Experimental Design

2.2.1 Experimental Outline

Training and performance experiments were performed on two manual control systems. Both experiments were concerned with compensatory tracking of a spot on a CRT display using a fingertip controller. One system was restricted to single-axis control and the other to two-axis control with symmetrical uncoupled plant dynamics. The specific objectives were to obtain data for study of the following problems:

1) Evaluation of the effect of training on tracking performance.

2) Evaluation of the effect of task difficulty on tracking performance.

3) Determination of human pilot models.

4) Comparison of single and two-axis tracking.

The plant dynamics were chosen to simulate the roll dynamics of a fighter-type jet aircraft. A previous study by Creer et al (Ref. 1) on pilot opinion ratings of the lateral control characteristics of such aircraft was used to obtain the parameters of the plant dynamics.

Input disturbance signals for the tracking systems were obtained by filtering the output of a gaussian noise generator with a third-order filter. The input amplitude to the system was held constant at 3.5 cm RMS deflection on the CRT display.

The control task difficulty was adjusted by choosing the time constant in the plant dynamics and the break frequency of the input filter.

The experimental design was a nested factorial with subjects nested within single axis versus two-axis tracking. The within group variables were task difficulty and number of sessions. There were four replications within each session. A random sample of three subjects was used within each group. The a priori reasons for the choice of nesting subjects within number of axes was that there might be a transfer of training effect when a subject goes from a single to a two-axis task or vice versa. Subjects with former tracking experience were used. Experimental runs were of 3 minutes duration and only the central 2 minutes were scored.

2.2.2 System Configuration

Figure 2-1 illustrates the configuration of the single axis compensatory tracking system used. This system was a simulation of the roll attitude control system typical of fighter-type aircraft as discussed in Reference 1 and consequently represents a realistic control task.

Two alternate plant dynamics were chosen from Reference 1 to give satisfactory and unsatisfactory control respectively. With a time constant (T) of 0.3 sec the control is satisfactory (Cooper rating = 3) while a 3 sec time constant results in unsatisfactory control (Cooper rating = 5). An unsatisfactory control configuration was used to increase the control task difficulty for purposes of assessing the human operator's performance in a more difficult task. The plant dynamics used had the following form:

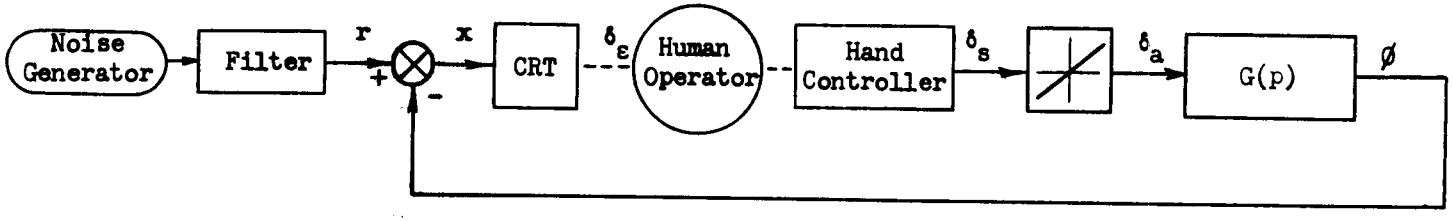

r = input roll angular disturbance (roll degrees)

x = tracking error (roll degrees)

ϕ = roll angle (roll degrees)

δ_ε = visual angle (eye degrees)

δ_s = angular stick deflection (stick degrees)

δ_a = angular aileron deflection (aileron degrees)

Figure 2-1

Single Axis Tracking System

$$G(s) = \frac{\phi}{\delta_a}(s) = \frac{K}{s(Ts + 1)}$$

K $\left(\frac{\text{roll rads/sec}}{\text{aileron rad}}\right)$	T (sec)
5.15	0.3
5.15	3.0

where

$K = TL_{\delta_a}\left(\frac{\text{roll rad/sec}}{\text{aileron rad}}\right)$

L_{δ_a} = roll angular acceleration per unit aileron angular deflection $\left(\frac{\text{roll rad/sec}^2}{\text{aileron rad}}\right)$

δ_a = aileron angular deflection (aileron rad)

ϕ = roll angle (roll rads)

δ_s = stick angular deflection (stick rads)

δ_s max. = 20 degrees

The operating gains were chosen from Figure 11 of Reference 1 under the assumption that $\delta_s = \delta_a$.

In the two-axis experiment, two channels identical to the system shown in Figure 2-1 were used. Although the realism of such a task is questionable, it was used nevertheless to obtain performance data on two-axis tracking for comparison with the performance of the human operator in a similar single axis task.

2.2.3 Task Definitions

Four control tasks were formulated for the experiment and were common to both the single and two-axis phases. The four tasks were designed to exhibit a progressive increase in control difficulty. Specifically the tasks were defined as follows:

TASK	1	2	3	4
$\omega_b\left(\frac{\text{rad}}{\text{sec}}\right)$	0.2	0.2	1.0	1.0
T (sec)	0.3	3.0	0.3	3.0

The variable ω_b represents the break frequency of the third-order input filter while T represents the time constant of the plant dynamics. In two-axis tracking, a separate gaussian noise generator was used for each axis to insure that the correlation between the two inputs would be zero.

2.2.4 Run Schedule

The run schedule for the single axis group was divided into 8 sessions, where the first 6 sessions constituted the training period while the last 2 sessions were the performance sessions. In half of the training and performance periods, the single axis experiment was performed with the system error (x) displayed vertically on the CRT while in the other half, the error was displayed horizontally. A vertical error required that the operator manipulate his fingertip controller in a vertical plane while a horizontal error required a horizontal response.

The experimental conditions may be summarized as follows:

Experimental Conditions

System Configuration (SC)

a) Single axis b) Two-axis

Plant Dynamics (G)

a) T = 0.3 b) T = 3.0

Filter Break Frequency (F)

a) ω_b = 0.2 rad/sec b) ω_b = 1.0 rad/sec

Subjects (S)

S = 3

Replication (R)

R = 4

Each session consisted of 48 runs: each subject performed four replications of the task for each of the plant dynamics and each filter break frequency, i.e., G x F x S x R = 48. The order of presentation of the tasks was randomized for each subject and each session. Subject fatigue was kept at a minimum by using a rest

period of approximately 3 minutes after each replication. It was also found necessary to limit the continuous experimentation period to half a session.

Since training was one of the main variables of the experiment, the subject was given a performance score upon the completion of each replication. The MS value of the system tracking error was used as the performance measure. Normalization of the error with respect to the input signal was not performed as the RMS value of the input signal amplitude was kept approximately constant during the replication period.

In the training sessions the second replication of each task was recorded on FM tape for future analysis by model matching techniques. All replications of the performance session were recorded.

The run schedule for the two-axis phase differed from the schedule given above for the single axis phase in that five sessions were used for training instead of six. This constituted the only difference between the two schedules.

2.3 Determination of Human Describing Function Parameters

The human operator response data obtained in the manner outlined in Section 2.2 was analyzed by using the continuous model matching technique. In using this method to determine human describing functions for the response data, it was assumed that the human operator behaved as a second-order linear system governed by the equation

$$\ddot{z} + \alpha_1 \dot{z} + \alpha_2 z = \alpha_3 \dot{x} + \alpha_4 x \tag{2.1}$$

where x is the input to the human, z is the model output and α_1, α_2, α_3, α_4 are the differential equation parameters to be determined. Equation 2.1 may be transformed to the complex frequency domain and rewritten in describing function notation

$$\frac{Z(s)}{X(s)} = \frac{K(T_1 s + 1)}{(T_2 s + 1)(T_3 s + 1)} \tag{2.2}$$

where s is the Laplace operator, K is the zero frequency gain, and T_1, T_2, T_3 are the describing function time constants.

Since the primary purpose of the human performance study was to evaluate the effects of task difficulty, training, and system configuration on the describing function parameters, modeling of a large number of experimental runs was required. The continuous model matching method described in Section 4.2 was the most rapid and economical method available at the time the study was performed. The technique is readily implemented on a conventional analog computer and requires only the time functions x and y, the input and output of the human operator, respectively. These signals were recorded on magnetic tape during the experimentation period and were later analyzed to obtain the desired models of human response. A block diagram of the basic open loop continuous method is presented in Fig. 4-2 of Section 4.2. The modified error criterion function discussed in Section 4.2 was used to optimize the performance of the continuous technique. Operational constants used in the model matching technique described above are listed in Table 2-1. A typical time history of the model parameters obtained for one subject's performance in the vertical axis is shown in Figure C-1. A similar history was obtained for his performance in the horizontal axis.

Table 2-1

Operational Constants for the Continuous Model Matching Technique

Task Number		1	2	3	4
Parameter Adjustment Gain, K		15	15	15	15
Rate Compensation Coefficient, q(sec)		0.5	0.5	0.5	0.5
Error Limit, L (degrees)		.0033	.0033	.02	.08
Initial Parameter Values	a_1	20	20	20	20
	a_2	20	20	20	20
	a_3	0	0	0	0
	a_4	0	0	0	0

The analysis of task difficulty and operator training was aided by the use of several performance evaluation criteria as well as the parameter mean values. The performance measures were the mean squared values of the tracking error $x(t)$, the human output $y(t)$, the modeling error $\varepsilon(t)$ and the power match P. The power match, defined by

$$P = \left[1 - \frac{\overline{\varepsilon^2}}{\overline{y^2}}\right] \times 100\% \qquad (2.3)$$

indicates the percentage of human output power matched by the model.

A one minute period was found to be a sufficient length of time for the parameters to converge to their approximate steady state values. Therefore, the first minute of the modeling of each two minute human response tracking run was utilized for parameter convergence. The adjustment loop gain was then automatically reduced by a factor of 10 in order to minimize the effect of short term time variations in the parameter values. The performance measures were computed during the final minute of each run.

The performance of the model matching technique is indicated by the power match obtained for each of the run replications as shown in Fig. 2-2. Response models for Tasks 3 and 4 normally gave a power match from 70 to 80 percent while Task 2 response data yielded a power match of 50 to 60 percent. Models for the Task 1 response data could not be successfully obtained. This result was caused by operator output signals of very low frequency which produced unstable operation of the parameter adjustment loop. For Tasks 3 and 4, the power match is approximately constant over the whole range of replications R. Consequently, since model matching accuracy remains invariant during the experimental series it may be concluded that any changes in model parameters were in fact due to training of operators. The power match for Task 2 exhibits considerably greater variability and consequently Task 2 results must be interpreted more cautiously.

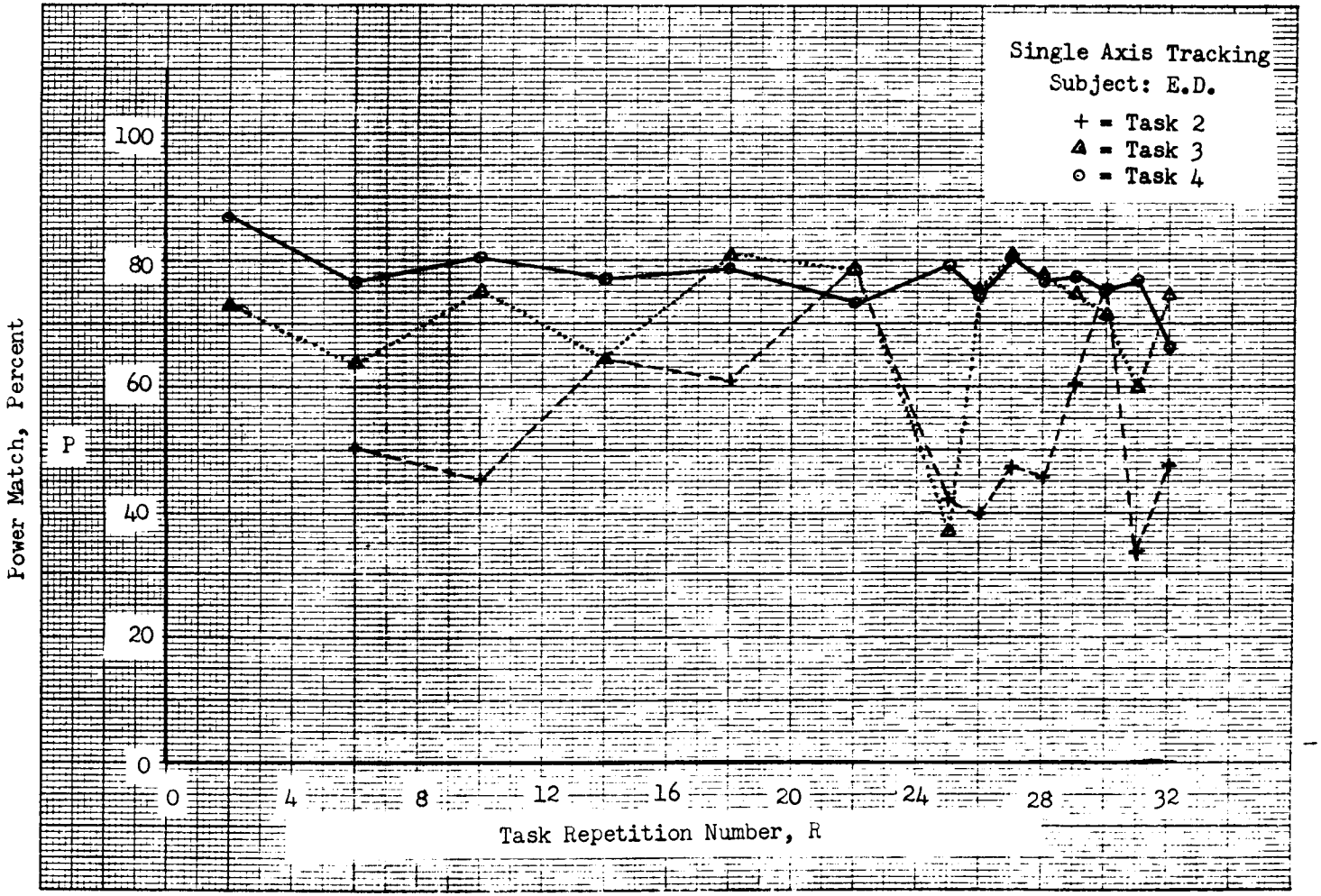

Figure 2-2 Model Matcher Performance

2.4 Effect of Training and Task Difficulty on System Tracking Error

In order to analyze the system tracking error, the normalized mean square error was used as a performance measure. Specifically, this measure is defined by

$$\overline{x_N^2} \triangleq \frac{\int_0^2 x^2 dt}{\int_0^2 r^2 dt} \tag{2.4}$$

which indicates that the integral square error is normalized by the integral square input signal over the two minute scoring period. Such a normalization is necessary to take into account the run to run variations in input power which take place when the input signals are not deterministic but consist of sample functions of random processes. The analysis of system tracking error was performed only for those trials from which model matching results were obtained.

In order to compare single axis tracking with two-axis tracking only one of the two-axis error scores could be chosen. Therefore an analysis was performed to determine if there was any significant difference between the horizontal and vertical axes for both the single and two-axis data. Using the Students t-test no significant difference was found. Therefore a score was chosen alternately from the horizontal or the vertical axis of the two-axis tracking scores for testing against the single axis score.

Two analyses of variance tests were conducted to determine significant differences between the variables. The first analysis tested differences during the learning period while the second analysis tested differences during the performance period.

In the first analysis the variables were training, number of axes, and task difficulty. For this test the second replicate of the system tracking error for each of the first seven training sessions was used as the test score. The result of this test is shown in Table 2-2. This table indicates that task difficulty, training and training-task difficulty interaction were significant. There was no significant difference between one and two-axis tracking To further evaluate the effect of training, the error scores

Table 2-2

Analysis of Variance of the Normalized Mean Square Error

Source	Degrees of Freedom	Sum of Squares	Mean Square MS	F-ratio
TRAINING PERIOD				
Axis (A)	1	241	241	<1
Subjects within Axis (S(A))	4	2744	686	
Tasks (T)	2	10098	5048	17.02**
Training (L)	6	3168	528	6.44***
A x T	2	202	101	<1
A x L	6	542	90	1.10
T x L	12	3232	269	4.95***
T x S(A)	8	2373	297	
L x S(A)	24	1966	82	
A x T x L	12	612	51	<1
T x L x S(A)	48	2610	54	
PERFORMANCE PERIOD				
Axis (A)	1	8	8	<1
Subjects within Axis (S(A))	4	681	170	
Tasks (T)	2	3459	1729	23.78***
Replicates (R)	7	79	11	<1
A x T	2	3	2	<1
A x R	7	69	10	<1
T x R	14	114	8	<1
T x S(A)	8	582	73	
R x S(A)	28	283	101	
A x T x R	14	118	84	1.13
T x R x S(A)	56	416	74	

** Significant at .01 level (1%)
*** Significant at .001 level (0.1%)

were determined for each task and training session by averaging across subjects. These scores are shown in Figure 2-3 and indicate that the task difficulty varies directly with the task code number, i.e., Task 4 was the most difficult and Task 2 the least difficult. These scores show that the amount of learning that occurred varied with task difficulty, i.e., for the more difficult tasks, the amount of learning was greater. This relationship would explain the significant interaction.

The variables of the second analysis were replicates of the performance period, number of axes and task difficulty. For this test the four replicates of each of the last two sessions were used as test scores. Table 2-2 shows that for this test the only significant difference was due to task difficulty. The levels of task difficulty, averaged across subjects and replicates are apparent from Figure 2-3. It should be noted that in this test as in the previous training analysis there was no significant difference between single and two-axis tracking.

2.5 Effect of Training on Human Describing Function Parameters

It has been shown in Section 2.4 that the system tracking error decreased as the subjects became more experienced or trained in controlling the tracking system. In this section, the human describing function parameters are examined using conventional control system theory to determine which parameters a human operator changes to achieve greater tracking accuracy. Both the single and two-axis control tasks are analyzed and emphasis is placed on describing the human operator's performance in the frequency domain. An analysis of variance to determine the significance level of the results obtained is presented in Section 2.6.

2.5.1 Single-Axis Tracking

Human describing function parameters were evaluated for single axis control tasks 2, 3, and 4, using the model matching technique as described in Section 2.3. In the training phase only the second replicate in each training session was analyzed while every replicate was evaluated in the two performance sessions of the experiment. The parameters obtained were plotted versus replication (R) to determine if any correlation existed between the parameters and training.

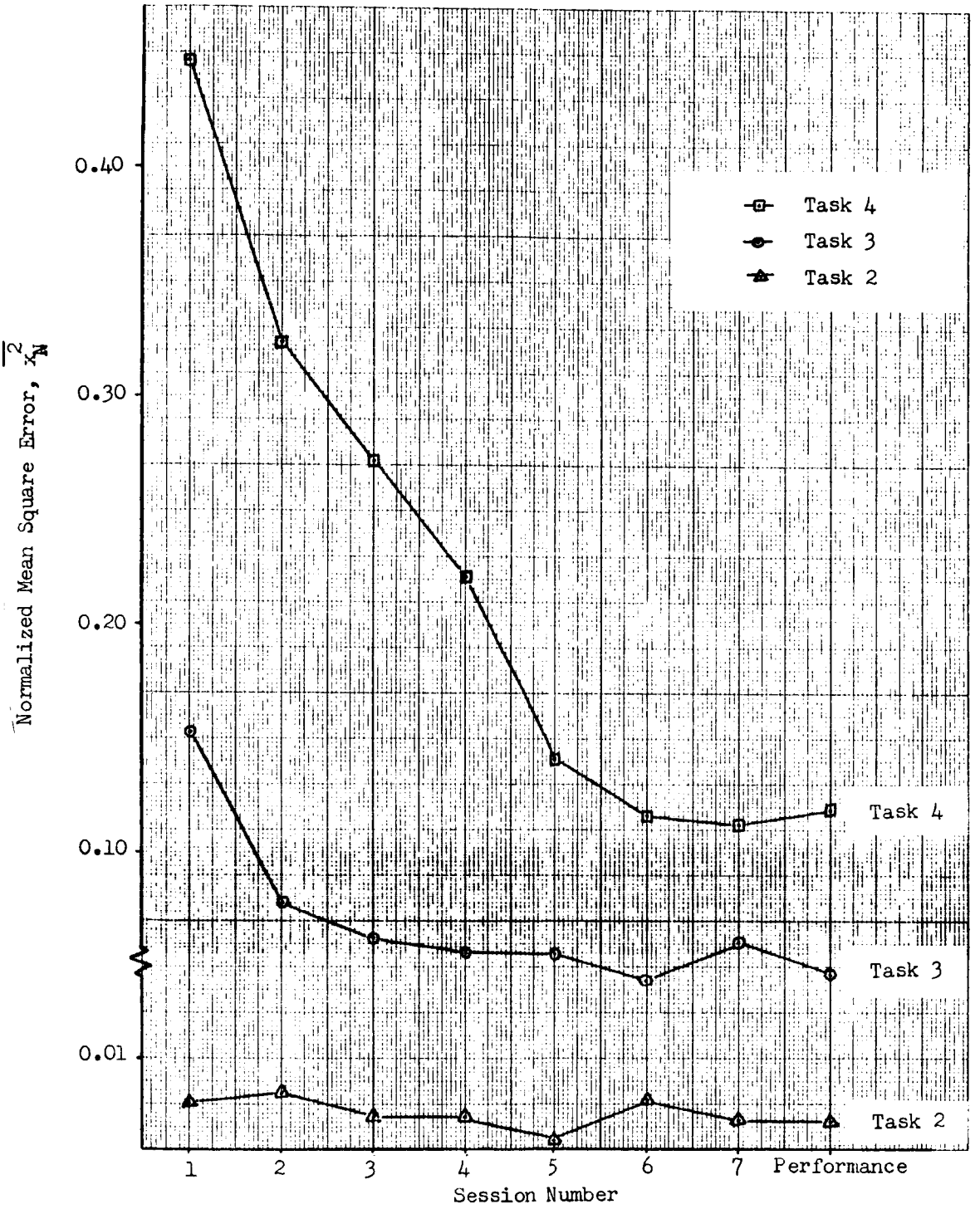

Figure 2-3 Learning Curves for Tasks 2, 3, and 4

Because the variance of the data points was large the method of least squares was used to obtain the best linear fit to the variation of the data points with replication. The linear trends obtained for each task were averaged over the three subjects to obtain the average parameter trends as a function of training and are shown in Figure 2-4.

Examination of the average trends shown in Figure 2-4 reveals an increase in the gain K for Task 3 and an increase in the time constant T_1 for Task 4. All other trends are small by comparison.

In an attempt to gain a more complete understanding of the parameter variations due to training, Bode diagrams were obtained for the untrained subject (R=4) and the trained subject (R=32). Bode diagrams were used as they give a complete picture of the describing function in the frequency domain and hence can provide an overall view of the interactions among the parameters. Figure 2-5 shows the average Bode diagram obtained for Task 4. Similar diagrams were obtained for Tasks 2 and 3. Examination of the Bode diagrams revealed that over a large frequency range, the amplitude ratio and phase lead increased with training for Tasks 2 and 4. Task 4 exhibits the greatest increase in gain and phase lead while Task 3 showed relatively little change. Task 3 did show an increase in the zero frequency gain.

The system open loop Bode diagram (human operator plus plant) for Task 4 is shown in Figure 2-6 and clearly indicates an increase in amplitude ratio and phase lead with training. As a result the open loop bandwidth (i.e., the frequency range over which the amplitude ratio is greater than 0 db) also increases with training. The phase margin γ shows little change with training and has a value of approximately 50°.

2.5.2 Two-Axis Tracking

Human describing function parameters were also evaluated for Tasks 2, 3, and 4 of the two-axis tracking system using the same analysis technique as described in Section 2.3. The parameters obtained for each axis of the two-axis system were averaged.

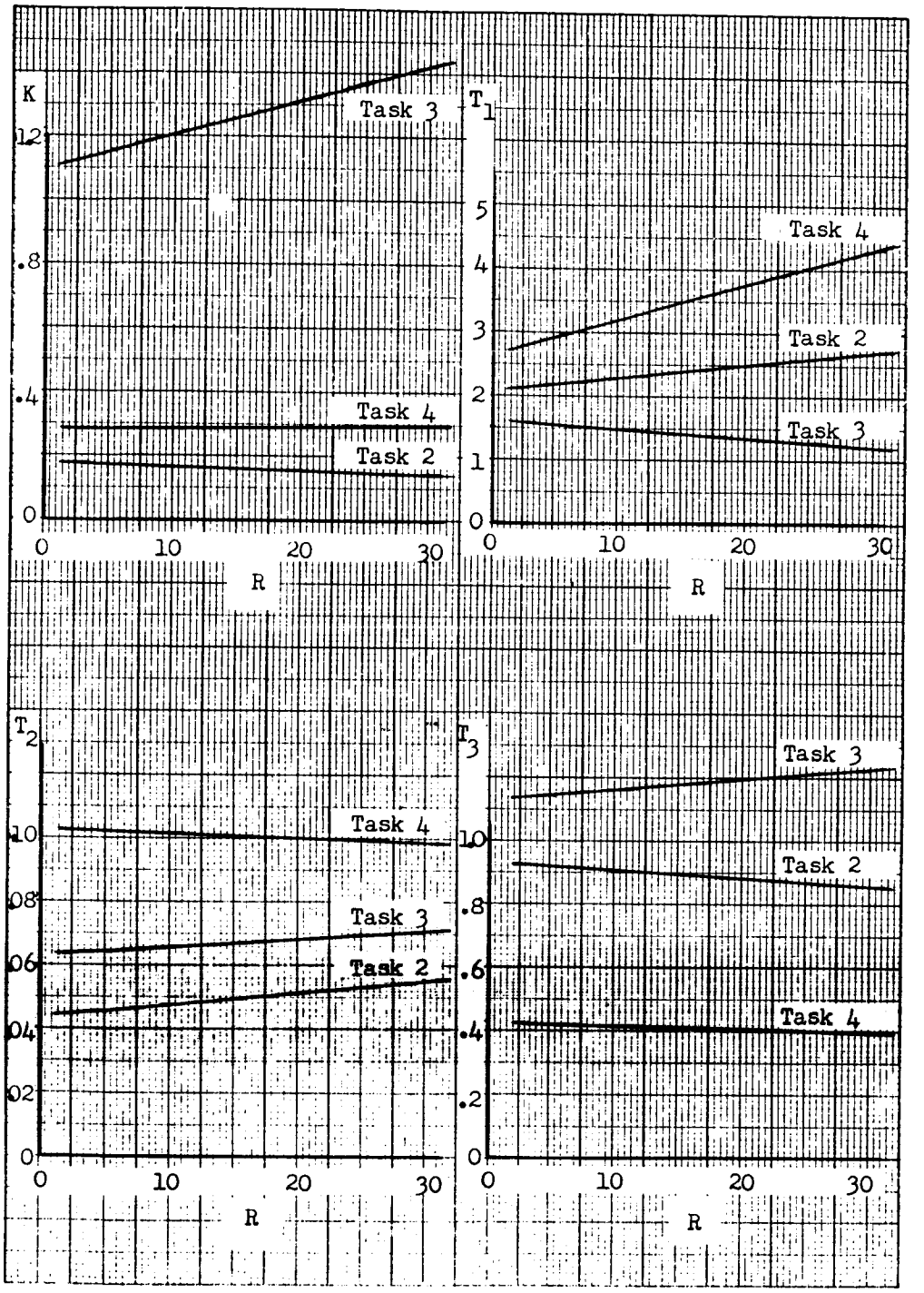

Figure 2-4

Average Parameter Trends for Single Axis Tracking

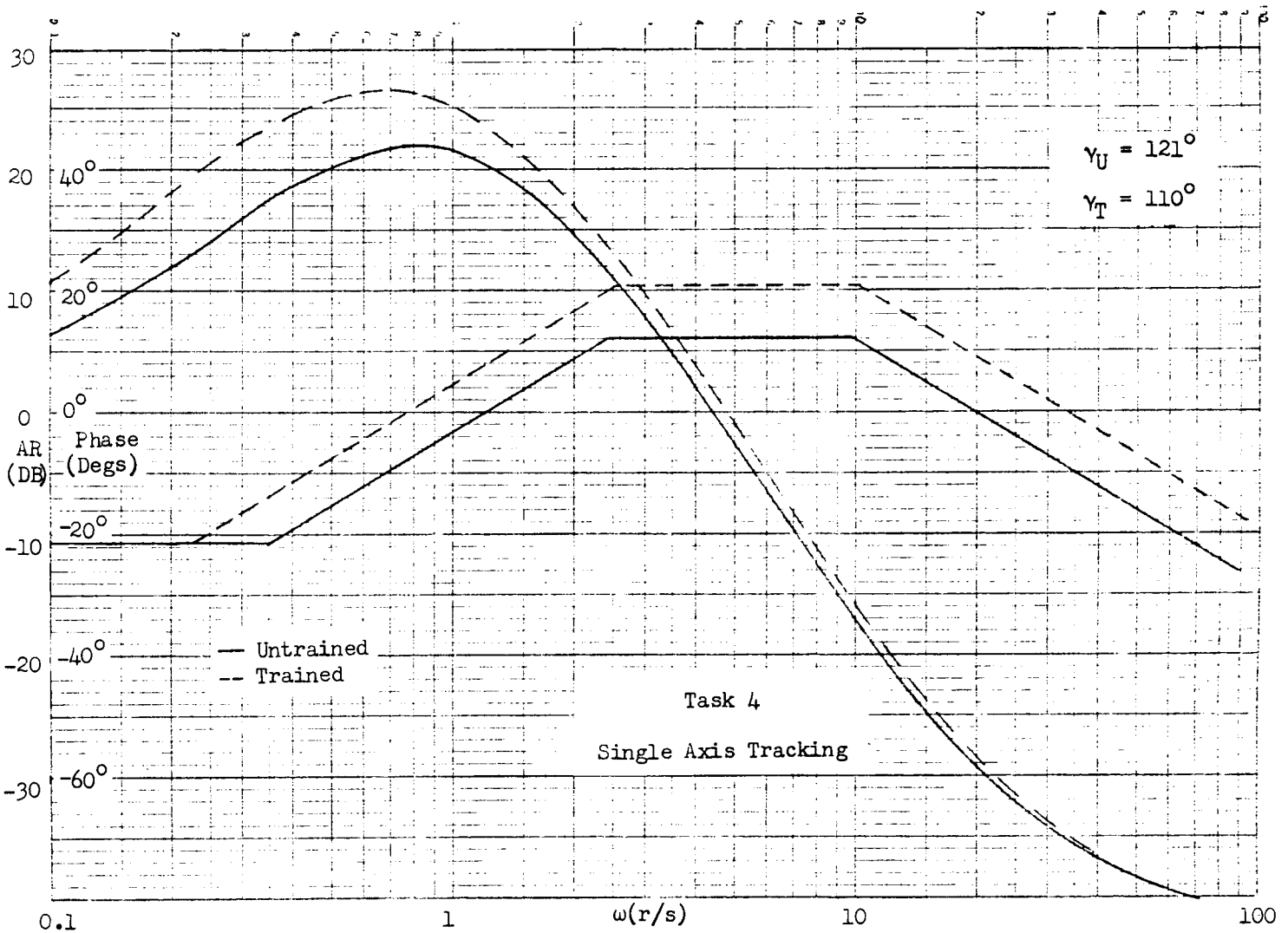

Figure 2-5 Average Bode Diagrams for Task 4 (Single-Axis)

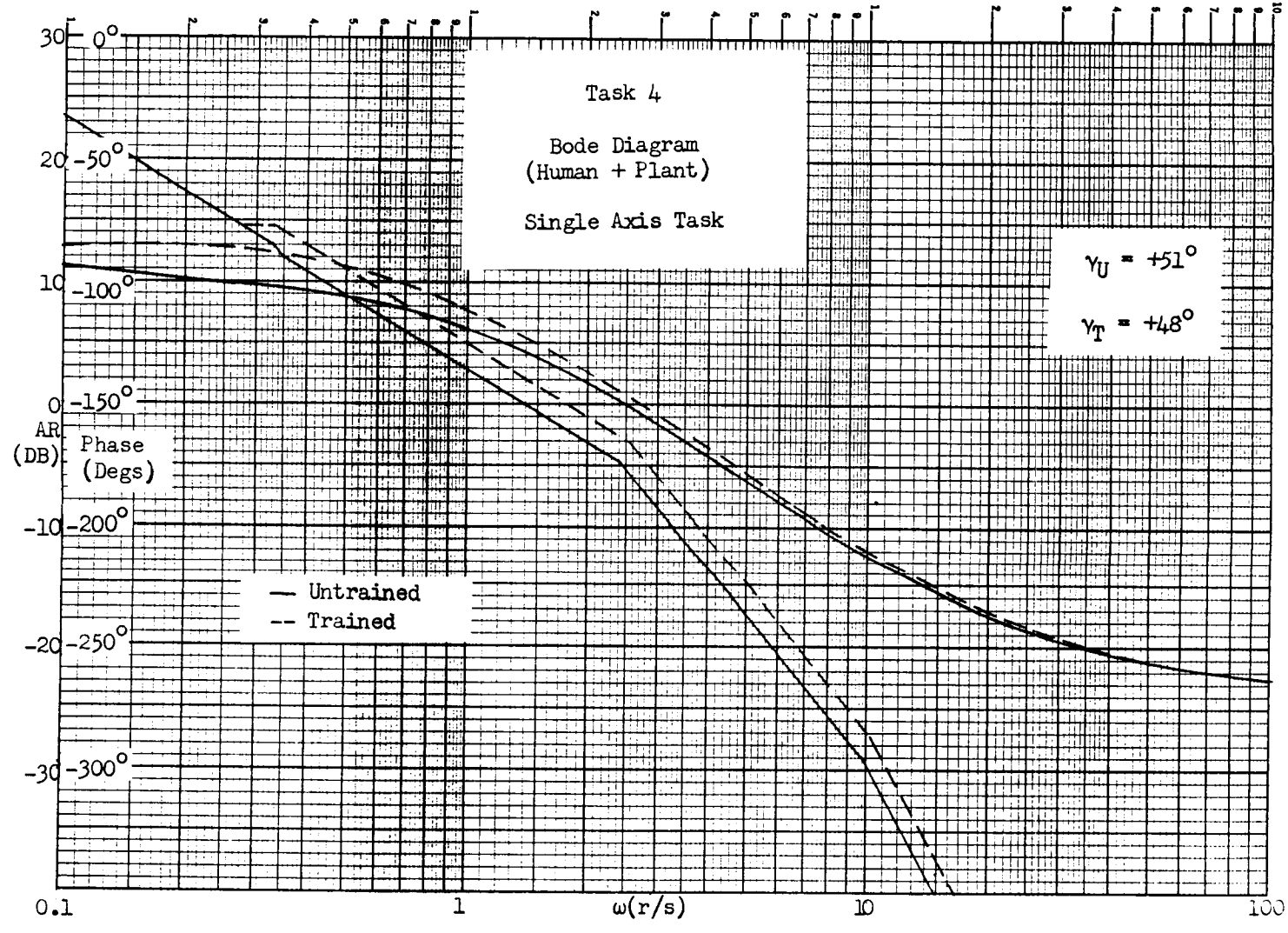

Figure 2-6 Average Open Loop Bode Diagrams for Task 4 (Single-Axis)

These parameters were now averaged over the subjects and then plotted versus replication to ascertain if any correlation existed between the parameters and training.

Figure 2-7 shows the averaged least squared linear fits obtained for the parameters in each control task analyzed. The only trends which appear are:

- K increases for Task 3
- T_1 increases for Tasks 3 and 4
- T_2 increases for Task 2
- T_3 increases for Task 3 and decreases for Task 2

Average Bode diagrams obtained for Tasks 2, 3 and 4 consistently indicate that the subjects (on the average) increased their amplitude ratio, and bandwidth with training. The Task 4 Bode diagram is shown in Figure 2-8. Phase lead increased only at low frequencies while the phase margins decreased. The system open loop Bode plot for Task 4 is shown in Figure 2-9 and indicates that an increase in amplitude ratio, phase lead and bandwidth was obtained with training. In addition the phase margin decreased from 52° to 40°.

2.6 Effect of Task Difficulty on Human Describing Function Parameters

The analysis of Section 2.4 was concerned with the relative difficulty of the four tasks of the experiment. This section deals with the correlations obtained between task difficulty and the frequency response of the human operator. Both single and two-axis performance data were analyzed. An analysis of variance was performed to determine the significance level of the results.

Bode diagrams obtained for all tasks of the performance period in the single and two-axis tracking systems were averaged over subjects. The mean amplitude and phase diagrams are shown in Figures 2-10 through 2-13. Examination of the Bode diagrams for both single and two-axis tracking reveals the following correlations between task difficulty and the frequency response parameters:

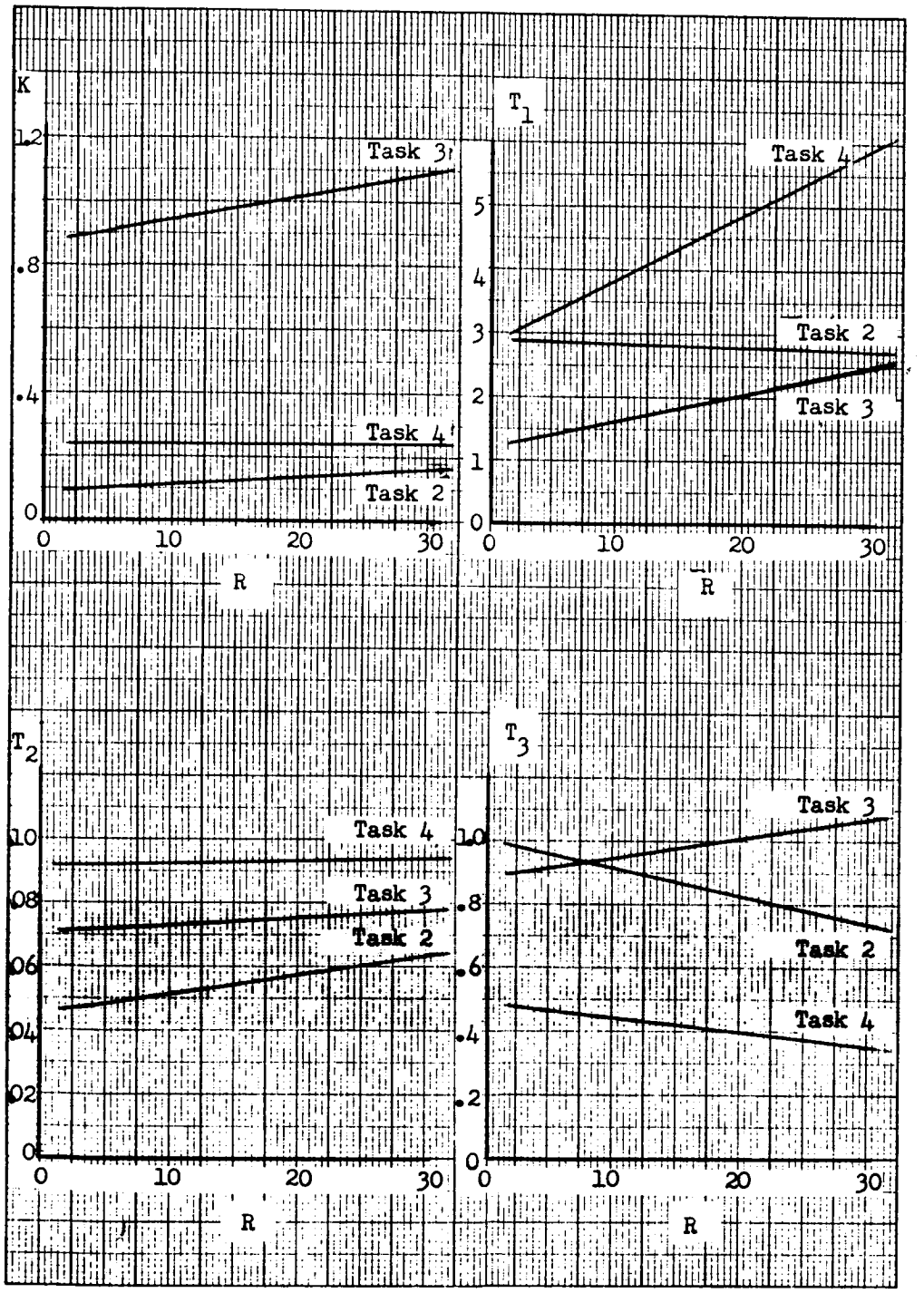

Figure 2-7 Average Parameter Trends for Two-Axis Tracking

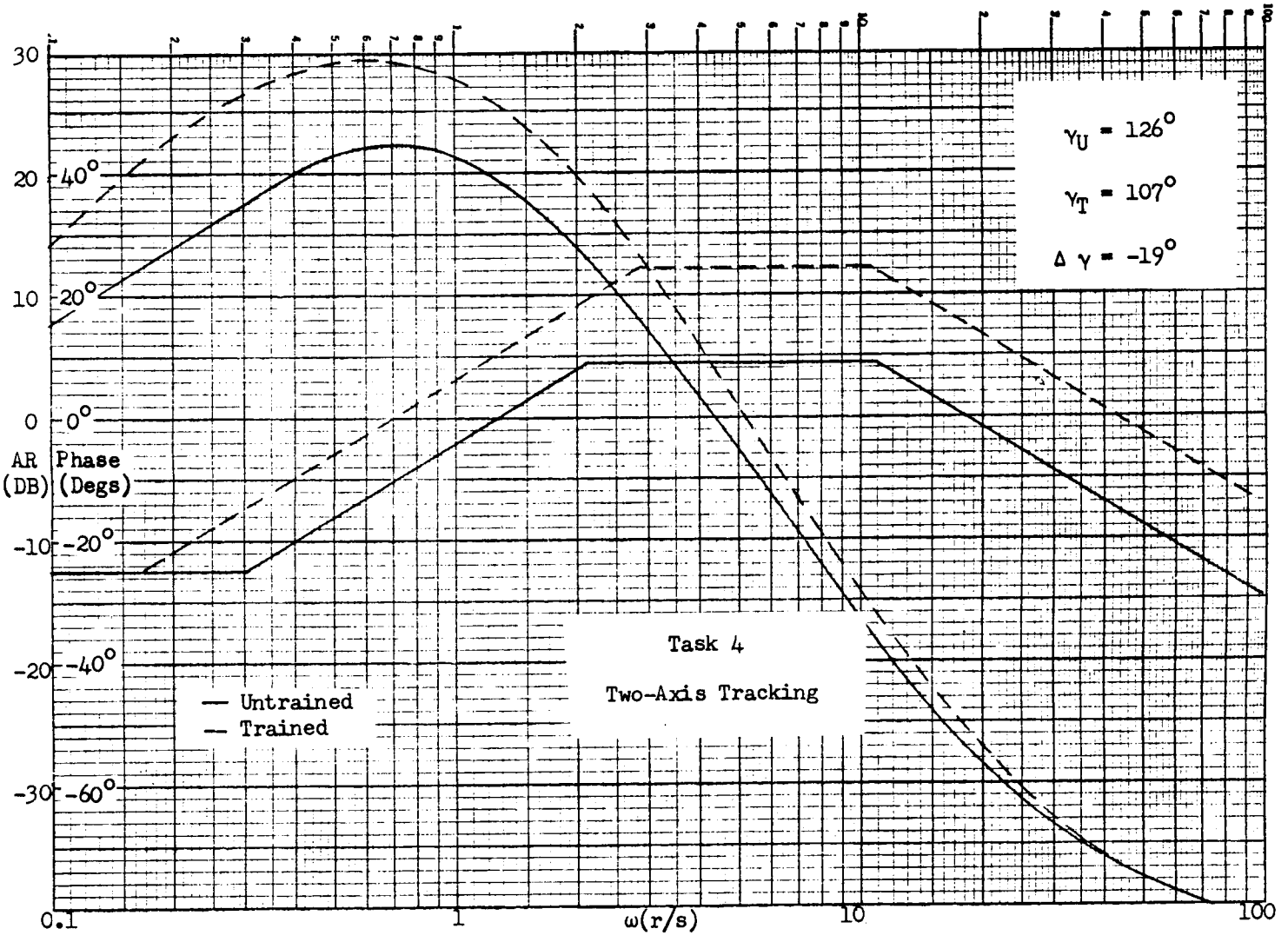

Figure 2-8 Average Bode Diagrams for Task 4 (Two-Axis)

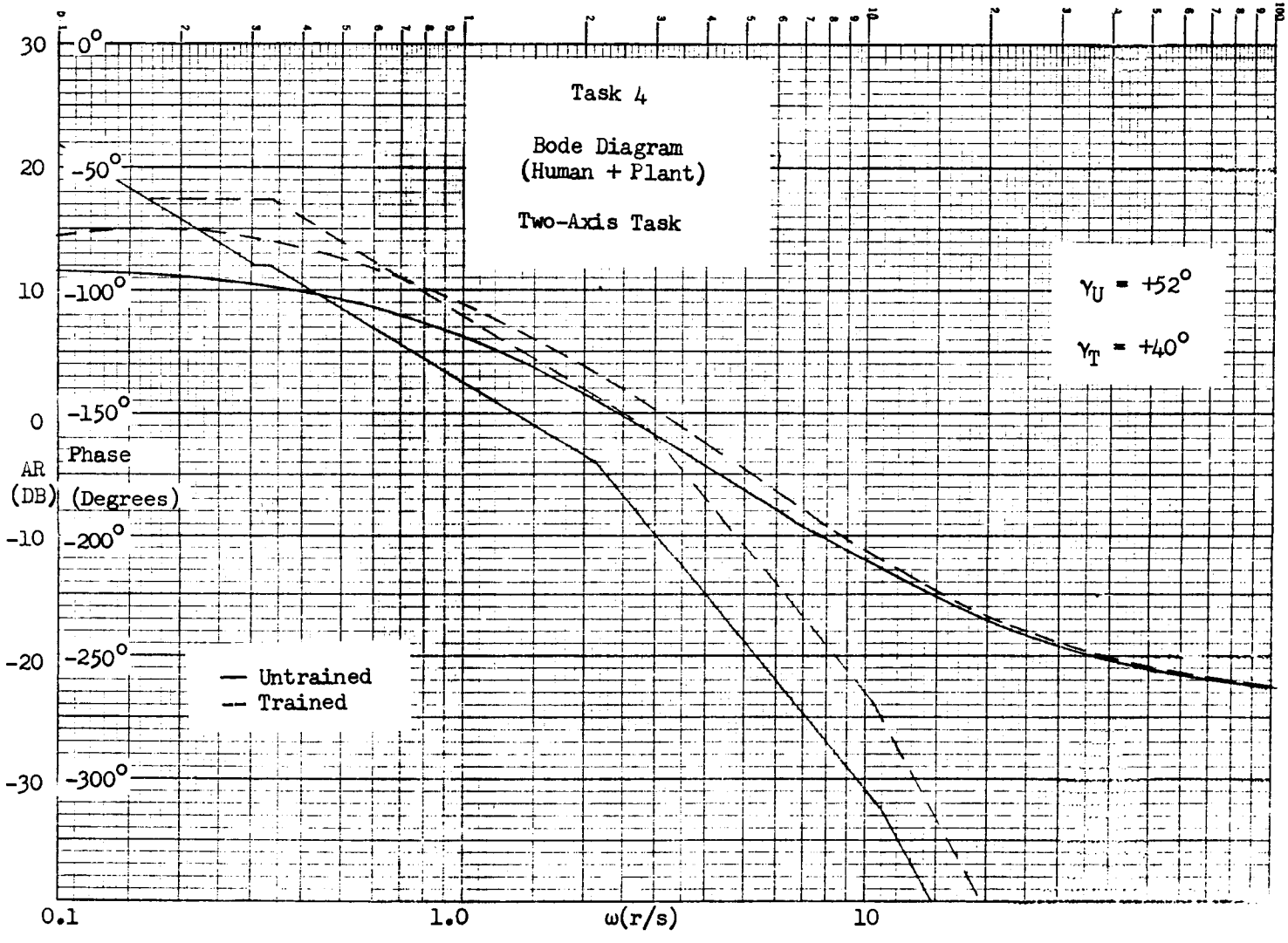

Figure 2-9 Average Open Loop Bode Diagrams for Task 4 (Two-Axis)

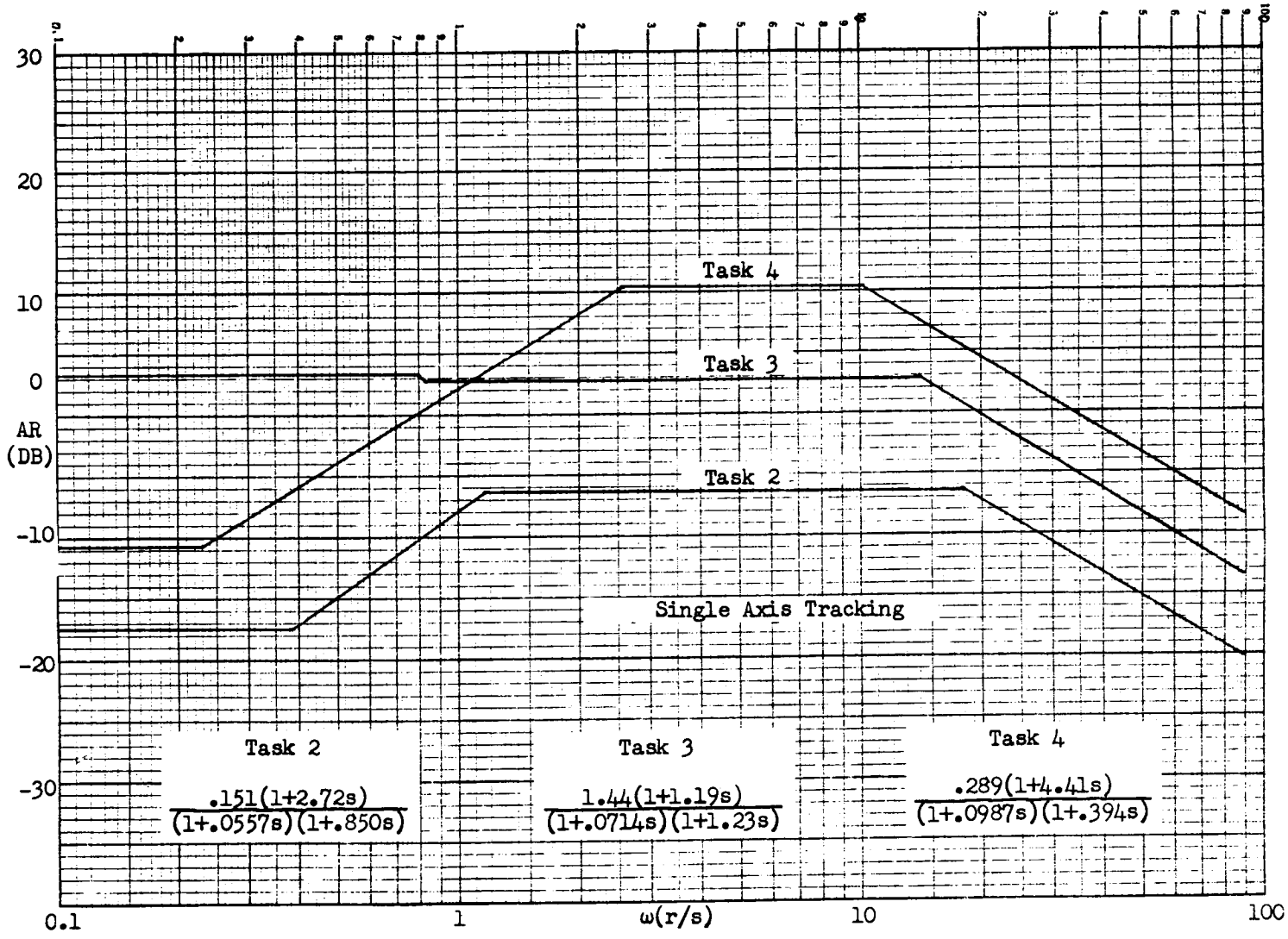

Figure 2-10 Mean Amplitude Ratio Diagrams for Single Axis Tracking

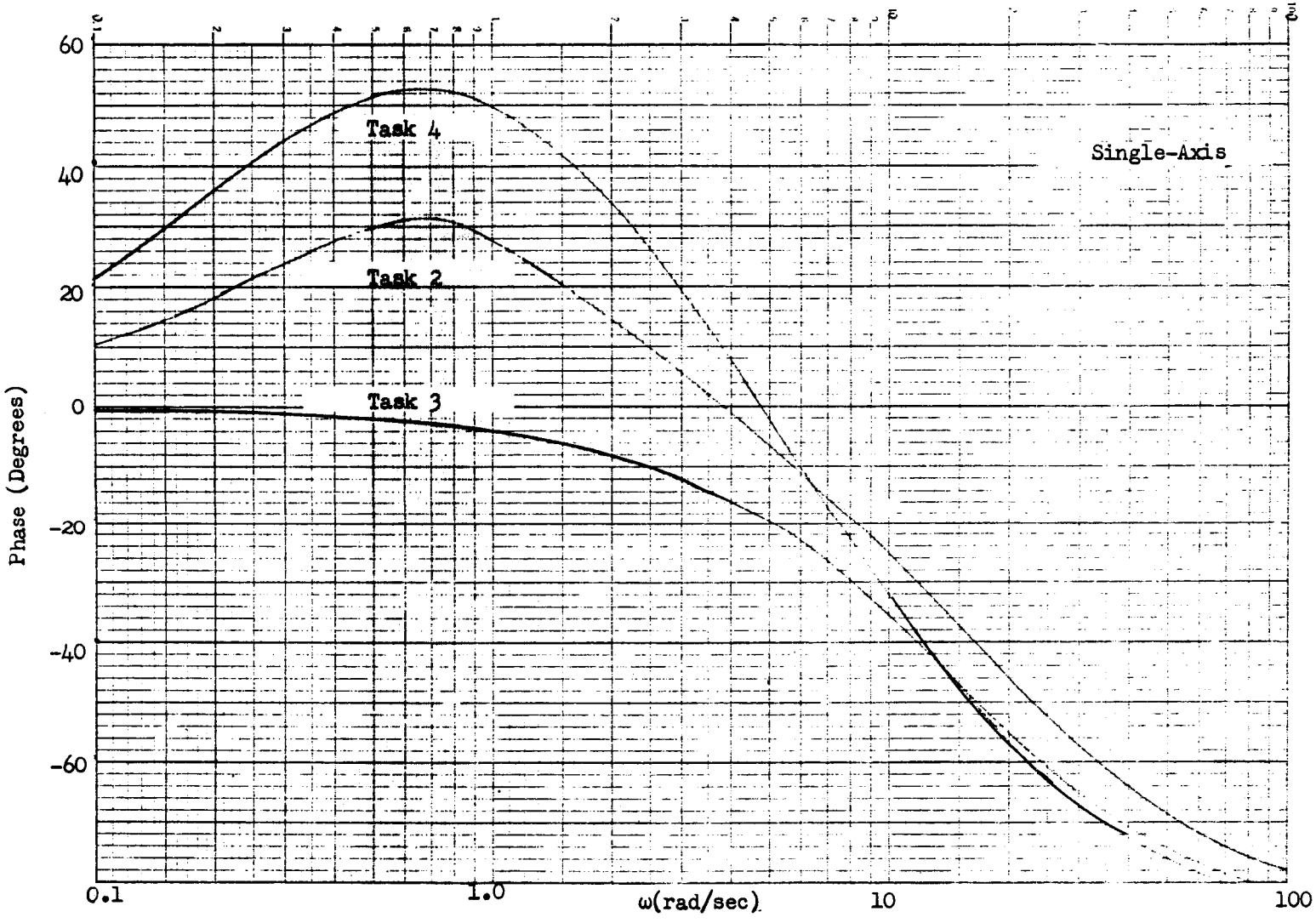

Figure 2-11 Mean Phase Diagrams for Single Axis Tracking

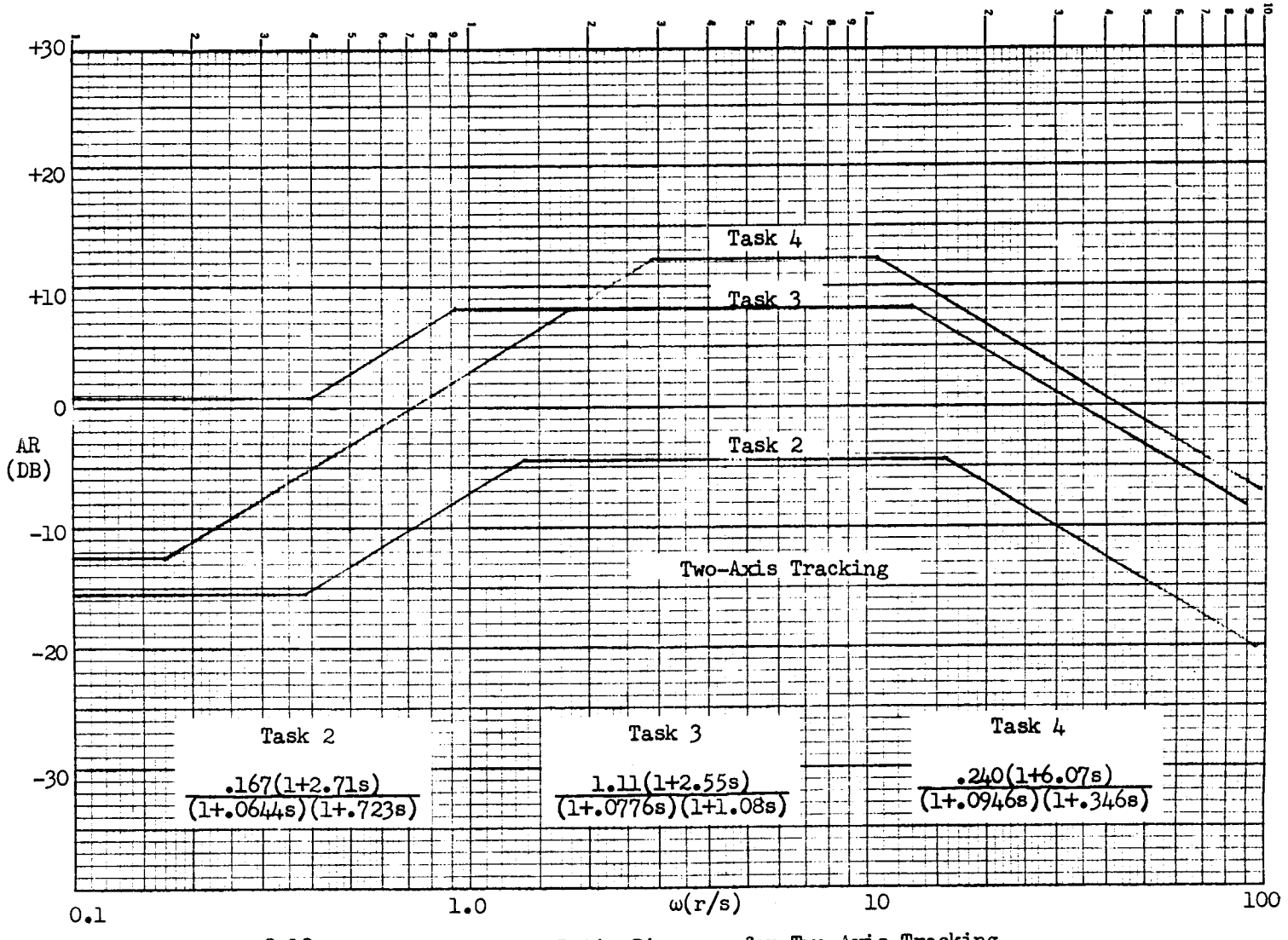

Figure 2-12 Mean Amplitude Ratio Diagrams for Two-Axis Tracking

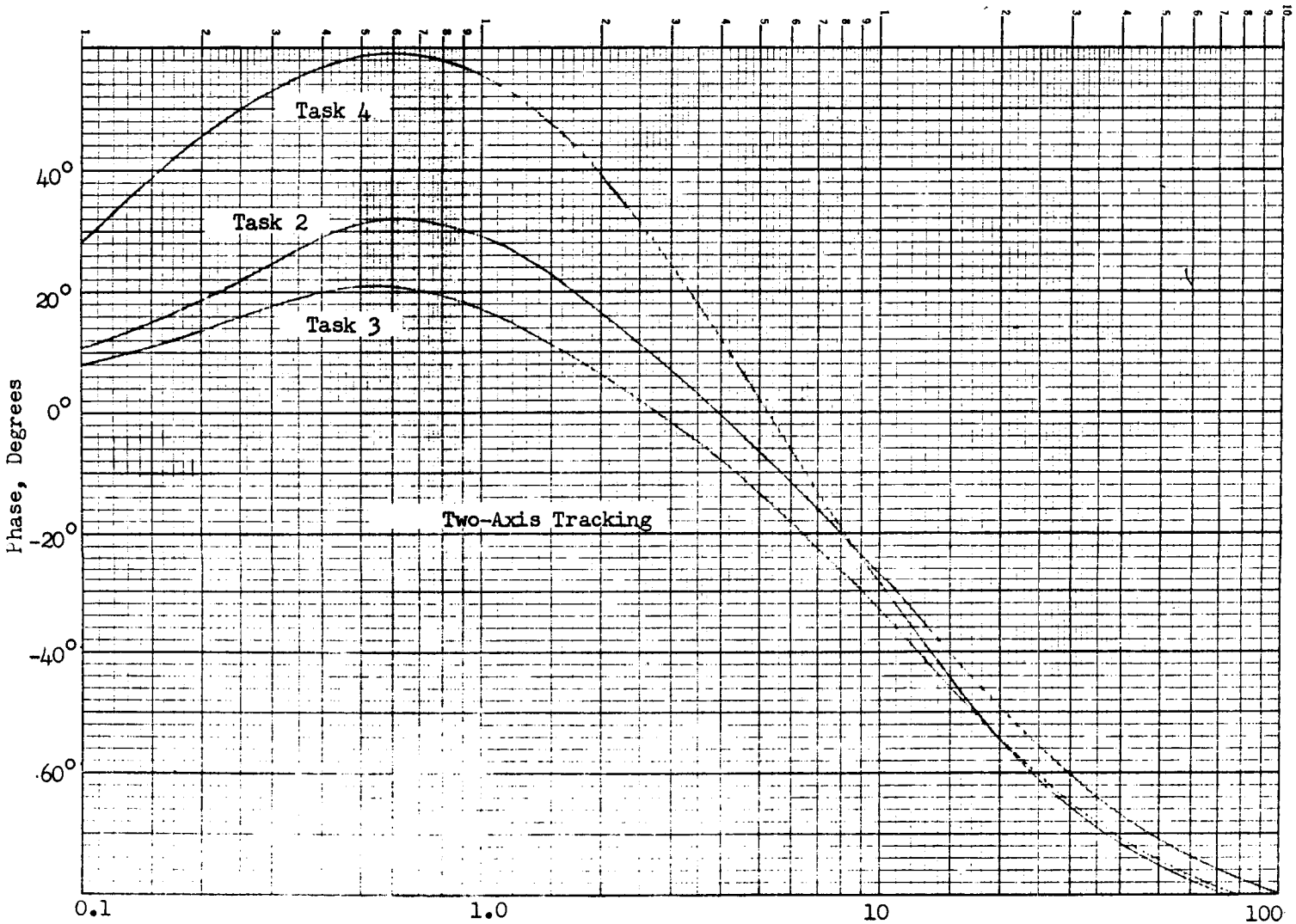

Figure 2-13 Mean Phase Diagrams for Two-Axis Tracking

1) The zero frequency gain K has a maximum value for Task 3 and a minimum value for Task 2 (see Figures 2-10 and 2-12). Since the lag time constant of the plant dynamics for Task 3 has one-tenth the value of the corresponding time constant in the plant dynamics of Tasks 2 and 4, it follows that the Task 3 dynamics are more stable than either the Task 2 or 4 dynamics. Consequently the operator can use a higher operating gain in Task 3.

2) Figures 2-11 and 2-13 indicate that the operator's phase lead at low frequencies was greater in Tasks 2 and 4 than in Task 3. Since it has been shown above that Tasks 2 and 4 are more unstable than Task 3, it is apparent that the operator compensates for the destabilizing effect of the larger lag time constant by increasing the lead time constant of his describing function.

3) The phase lead at low frequencies was less for Task 2 than Task 4 as shown in Figures 2-11 and 2-13. Since the input frequency bandwidth for Task 2 was only 0.2 r/s while the input bandwidth for Tasks 3 and 4 was 1 r/s, it follows that Task 4 is a more difficult task for which the operator will use more phase lead.

The conclusions obtained above are based on the relative magnitude of the zero frequency gain K and lead time constant T_1 obtained for Tasks 2, 3, and 4. Analysis of variance was used to test the significance of both the K and T_1 parameters obtained for each task, as shown in Tables 2-3 and 2-4 respectively. The design of the analysis was identical to that used in Section 2.4. From Tables 2-3 and 2-4 it is evident that the dependence of both K and T_1 on Tasks was significant at the 0.1% level. Thus the data used in the above discussion is significant at the 0.1% level.

Parameter variation due to learning was not significant. This factor may be due to subject differences or the small sample size. In observing the individual subjects it can be shown that they started with different parameters prior to learning. However after learning they converged to approximately the same model.

Table 2-3

Analysis of Variance for K

Source	Degrees of Freedom	Sum of Squares	Mean Square MS	F-ratio
LEARNING PERIOD				
Axis (A)	1	62	62	2.53
Subjects within Axis (S(A)	4	96	24	
Tasks (T)	2	2381	1190	79.5***
Learning (L)	6	23	4	<1
A x T	2	58	29	1.96
A x L	6	18	3	<1
T x L	12	66	6	1.50
T x S(A)	8	119	15	
L x S(A)	24	108	4	
A x T x L	12	36	3	<1
T x L x S(A)	48	231	5	
PERFORMANCE PERIOD				
Axis (A)	1	43	43	<1
Subjects within Axis (S(A))	4	202	50	
Tasks (T)	2	364	1823	38.69***
Replicates (R)	7	34	5	1.53
A x T	2	49	25	<1
A x R	7	35	5	1.44
T x R	14	73	5	1.65
T x S(A)	8	376	47	
R x S(A)	28	96	3	
A x T x R	14	67	5	1.50
T x R x S(A)	56	177	34	

*** Significant at .001 level (0.1%)

Table 2-4

Analysis of Variance for T_1

	Degrees of Freedom	Sum of Squares	Mean Square MS	F-ratio
TRAINING PERIOD				
Axis (A)	1	922	922	1.34
Subjects within Axis (S(A))	4	2740	685	
Tasks (T)	2	9520	4760	44.2***
Learning (L)	6	1265	211	1.20
A x T	2	58	29	<1
A x L	6	2313	386	2.20
T x L	12	2228	186	1.43
T x S(A)	8	862	107	
L x S(A)	24	4214	175	
A x T x L	12	1897	158	1.22
T x L x S(A)	48	6219	129	
PERFORMANCE PERIOD				
Axis (A)	1	1525	1525	2.13
Subjects within Axis (S(A))	4	2867	717	
Tasks (T)	2	20991	10496	353.4***
Replicates (R)	7	1395	199	1.09
A x T	2	405	202	6.82*
A x R	7	1143	163	<1
T x R	14	4359	311	1.42
T x S(A)	8	238	30	
R x S(A)	28	5110	182	
A x T x R	14	2283	163	4
T x R x S(A)	56	12286	219	

* Significant at .05 level (5%)
*** Significant at .001 level (0.1%)

Since subjects were treated as a random sample from a population, differences between subjects could not be tested and in this experiment there is no error term for testing the variables if subjects are treated as a fixed sample.

2.7 Comparison of Single and Two-Axis Tracking

A comparison was made between single and two-axis tracking to determine what differences existed between these two types of control tasks. An analysis of variance performed on the system tracking error for both types of control tasks showed that no significant difference existed between single and two-axis tracking for all control tasks as far as the system tracking error was concerned (cf. Section 2.4). However the analysis of variance for the T_1 data obtained in the performance period (cf. Section 2.6), showed that the interaction between tasks and single versus two-axis tracking was significant at the 5% level. This interaction is shown explicitly in the values for T_1 averaged across subjects and replicates in Table 2-5 where only Tasks 3 and 4 show a difference. For both tasks T_1 was significantly larger in the two-axis tracking system. Bode diagrams obtained from the performance data of Section 2.5 are shown in Figures 2-14 through 2-16. The Bode diagrams in general confirm the analysis of variance data in that the only large difference between single and two-axis tracking appears to be the phase angle of Tasks 3 and 4.

Table 2-5

Average T_1 for Single and Two-Axis Tracking (Seconds)

Task	2	3	4
Single Axis	2.69	1.32	4.13
Two-Axis	2.83	2.09	5.12

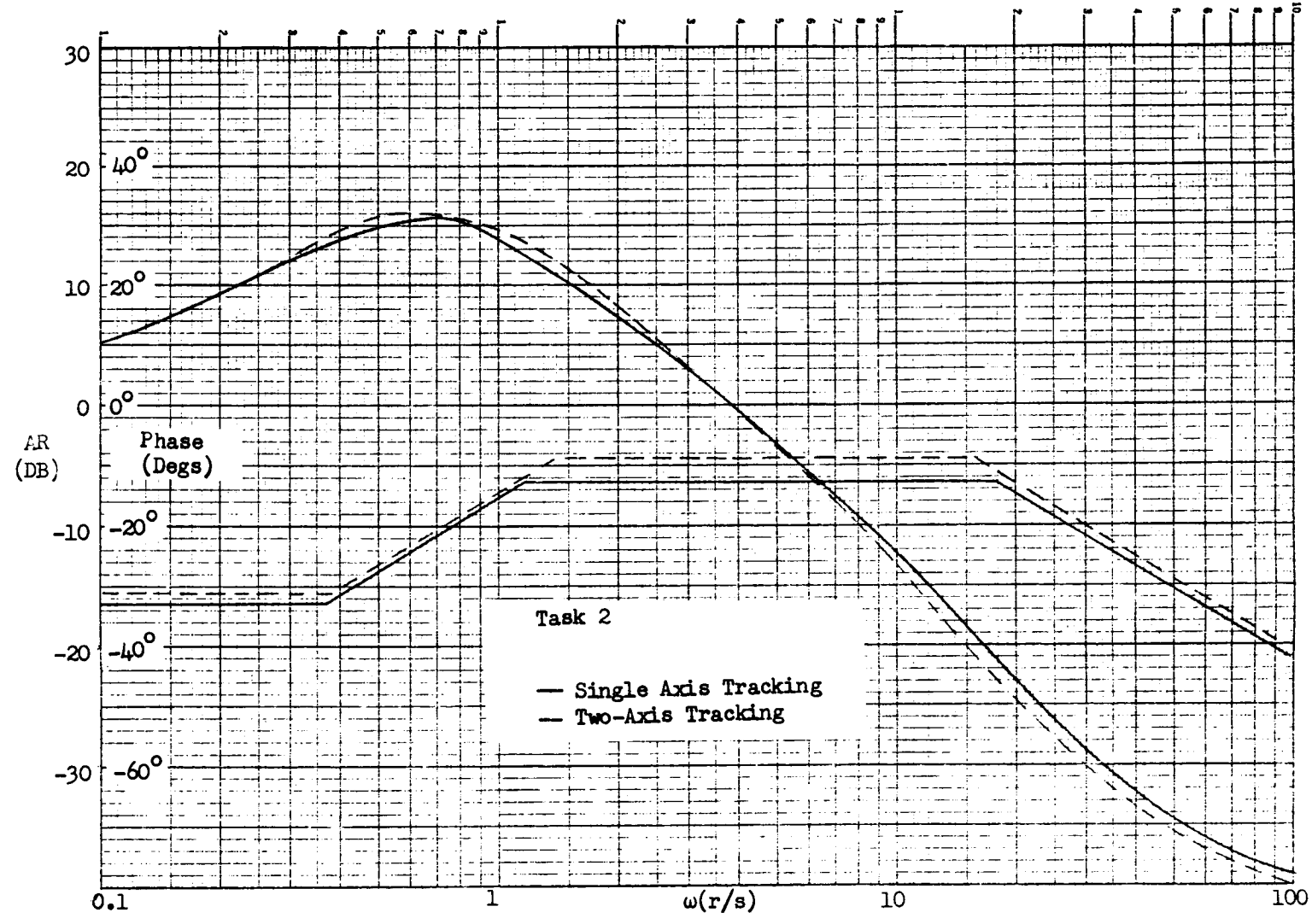

Figure 2-14 Bode Diagrams of Task 2

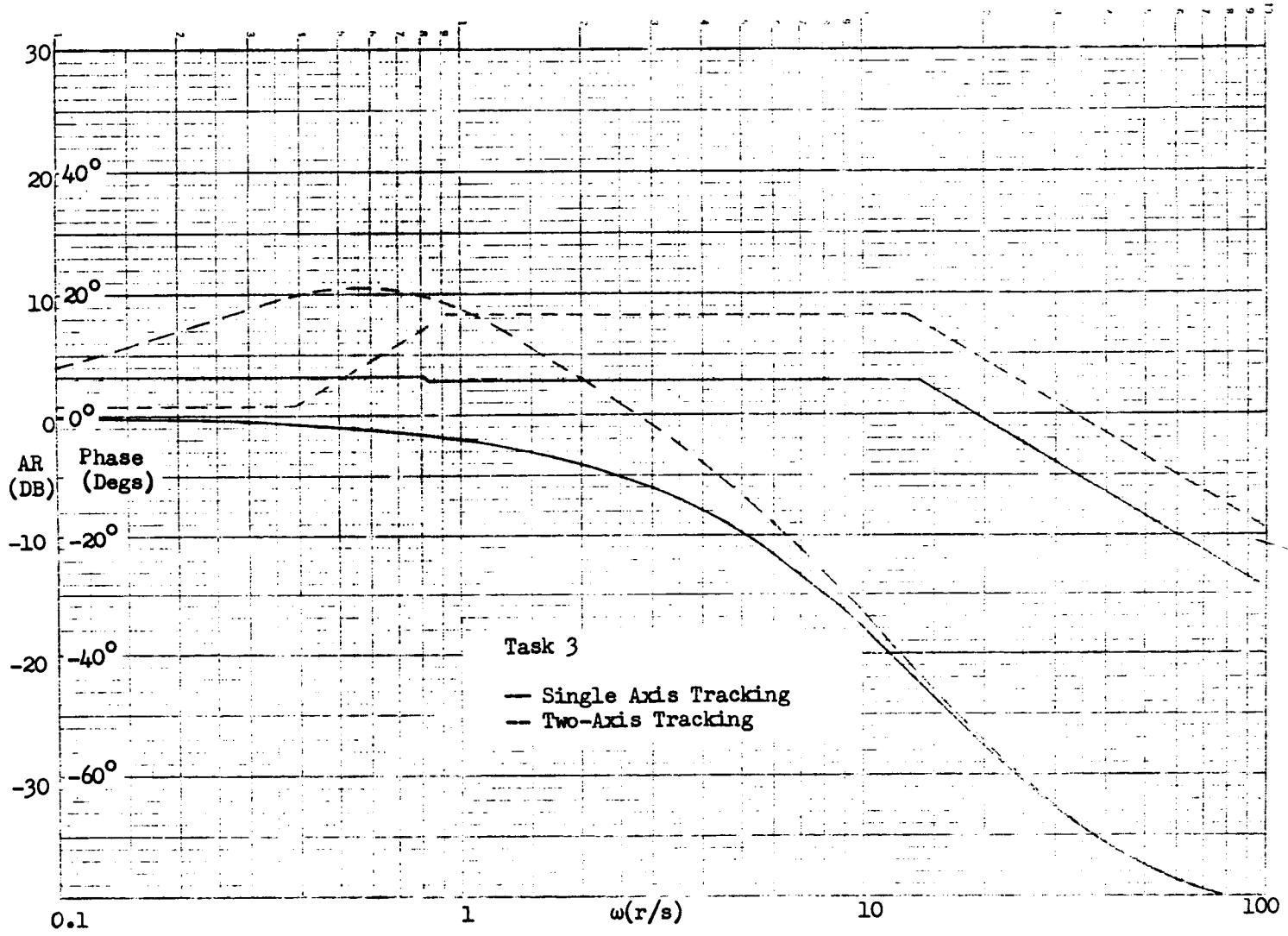

Figure 2-15 **Bode Diagrams of Task 3**

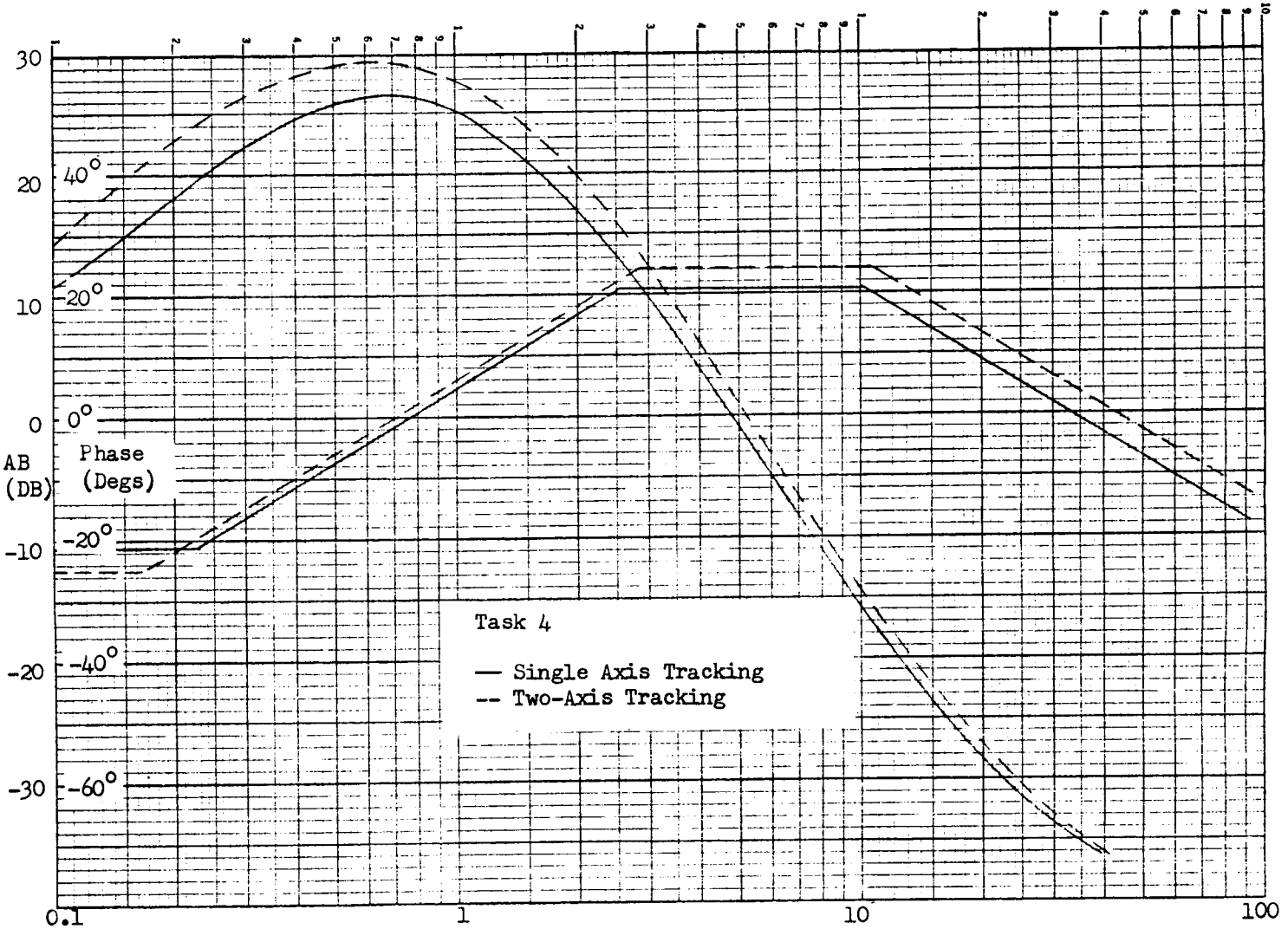

Figure 2-16 Bode Diagrams of Task 4

The fact that system tracking error in either axis of the two-axis group was no greater than that for the single axis group is not contradictory of earlier results. In reviewing the literature, very few studies have directly tested this difference. In analyzing the results of a study by Chernikoff, et al (Reference 2), there appears to be no difference between one and two-axis tracking for tasks with controlled elements of position, rate and acceleration. Recently in results from Bolt, Beranek and Newman, Inc. (Reference 3) no difference was shown between single and two-axis tracking.

2.8 Conclusions

Experimental data obtained from single and two-axis tracking experiments were analyzed using continuous matching techniques, and conventional control system theory. An analysis of variance was performed on the results obtained to determine their significance level. The analysis of the human performance data led to the following conclusions:

2.8.1 Single vs. Two-Axis Tracking Performance

1) The system tracking errors in the two-axis tasks were not significantly different from the single axis tasks. If it is assumed that the subject's information processing capability is not fully loaded the results of this experiment are plausible. The latter hypothesis could be tested by the addition of more axes with the same input function and dynamics until the subject's performance starts to degrade due to task loading.

2) For Tasks 3 and 4 only, the lead time constant T_1 was significantly larger in models of two-axis tracking than in models of single axis tracking. Since this difference did not appear in Task 2, it can be concluded that T_1 is a measure of differences in operator performance between single and two-axis tracking only when the input signal bandwidth is sufficiently high.

2.8.2 Effects of Task Difficulty

1) The task difficulty (as measured by tracking error) was found to increase significantly with the task code number.

2) The rate of decrease of system tracking error with training was dependent upon task difficulty. The more difficult tasks showed a greater degree of learning.

3) The human operator model showed a significantly higher zero frequency gain in Task 3 than either Tasks 2 or 4 because Task 3 was more stable as the lag time constant in the plant dynamics was smaller by a factor of 10. For the same reason, the human operator's model lead time constant was significantly greater in Tasks 2 and 4.

4) The operator's model lead time constant was greater in Task 4, than Task 2 because Task 4 was a more difficult task due to the input frequency bandwidth being larger.

2.8.3 Effects of Training

1) System tracking error decreased significantly for all control tasks in both single and two-axis tracking during training.

2) For both single and two-axis tracking, the average human operator increased his amplitude ratio and phase lead with training as measured from model Bode diagrams. These changes resulted in an increased open loop bandwidth and a decreased phase margin.

3) An analysis of variance showed no significant trend to exist in the variation of the parameters K and T_1 (zero frequency gain and lead time constant) with level of training. Parameters T_2 and T_3 were not tested.

The analysis of variance on the variation of the parameters K and T_1 with training showed that the variation was not significant. The significance test performed may not be a valid test in this case as only 2 parameters of the describing function were tested. Since the describing function used consisted of 4 parameters which together describe the dynamic behavior of the human operator, it appears that all parameters must be tested simultaneously to obtain an accurate significance level. Since the Bode diagram is a complete dynamic representation of the human describing function, it is probable that conclusion 2 is more valid than conclusion 3.

3. HUMAN PERFORMANCE IN TWO-AXIS SYSTEMS WITH CROSS-COUPLING

3.1 Introduction

This section presents the results of a study of human tracking performance in coupled two-axis manual control systems. In this phase of the work, the primary objective was the collection and evaluation of statistically meaningful data on the effects of training and cross-coupling. Emphasis was placed on determining whether a human operator could successfully decouple a coupled two-axis control task.

The evaluation was performed by first modeling the human operator's performance by an asymmetric lattice network and then determining the network describing functions using an iterative model matching technique. An analytical study of the coupled two-axis control system showed that the system could be manually decoupled if the network describing functions were properly related to the transfer functions of the plant dynamics. The required relations were explicitly expressed by two decoupling equations. Describing functions obtained from the experimental study were compared with the decoupling equations to determine if the human operator was able to decouple the system. Training and task difficulty were analyzed using system tracking error. The above analysis and comparison was used as the basis for describing the characteristics of human performance in the coupled two-axis systems investigated.

3.2 The Cross-Coupled Human Operator Model

Human tracking performance in a two-axis system with input cross-coupling was evaluated by modeling the human operator with an asymmetric lattice network as shown in the signal flow diagram of Figure 3-1. This system representation is identical to that given in Reference 4. The describing functions of the lattice network are designated by H_{ij} while G_{ij} represents the transfer functions of the plant dynamics. Coupling in the plant dynamics is of an input form as a control input to the plant dynamics in one axis produces a plant response in both axes. Components of the

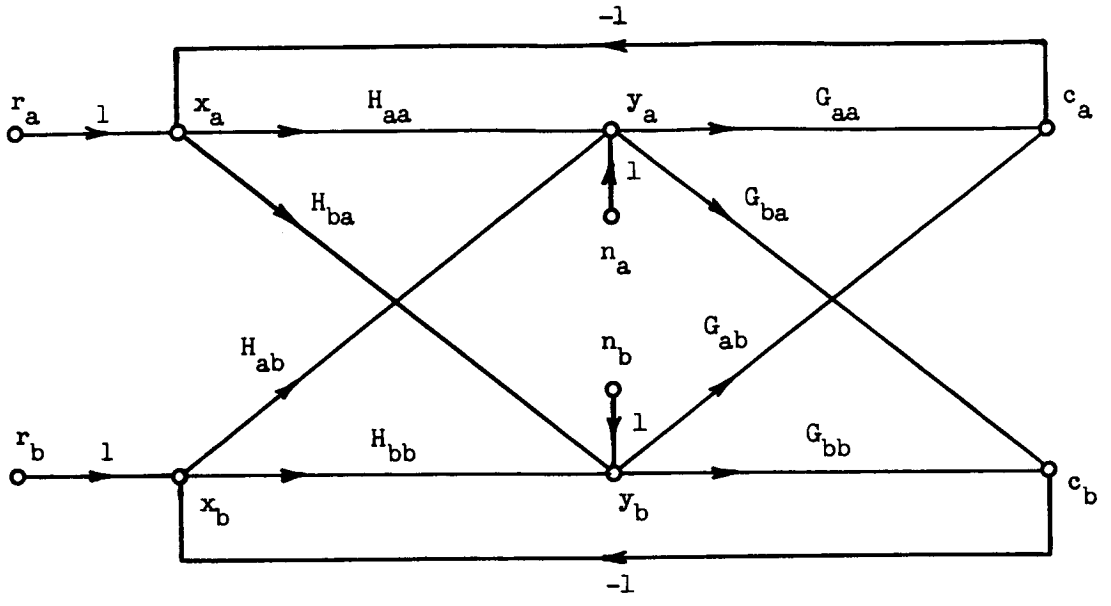

Figure 3-1: The Two-Axis Input Coupled Tracking System

r_a = a-axis reference signal

x_a = a-axis error signal

y_a = a-axis stick deflection

c_a = a-axis system output signal

n_a = human operator's response in the a-axis which is not linearly coherent with r_a or r_b

H_{aa} = linear describing function relating y_a to x_a

H_{ba} = linear describing function relating y_b to x_a

G_{aa} = a-axis plant dynamics relating c_a to y_a

G_{ba} = a-axis coupling dynamics relating c_b to y_a (i.e., input cross-coupling

The corresponding signals and transfer functions in the b axis are similarly defined.

operator outputs (y_a and y_b) which are not linearly coherent with the forcing functions (r_a and r_b) are represented by the noise signals (n_a and n_b).

The coupled two-axis system can be decoupled if the human operator is able to use the correct cross-coupled describing functions in the lattice representation of his behavior. Decoupling of the a axis from the b axis requires that the a axis output signal c_a be independent of the tracking error in the b axis x_b. For zero noise ($n_a = n_b = 0$), it may analytically be shown that c_a is related to x_a and x_b by the equation

$$c_a = (G_{aa} H_{aa} + G_{ab} H_{ba})x_a + (G_{aa} H_{ab} + G_{ab} H_{bb})x_b$$

Consequently the a axis will be decoupled from the b axis if the human operator chooses H_{ab} such that the following decoupling condition exists

$$H_{ab} = -\left(\frac{G_{ab}}{G_{aa}}\right) H_{bb} \tag{3.1}$$

Similarly it may be shown that the decoupling condition required for decoupling the b axis from the a axis is

$$H_{ba} = -\left(\frac{G_{ba}}{G_{bb}}\right) H_{aa} \tag{3.2}$$

The decoupling conditions given by Equations 3.1 and 3.2 are independent indicating that theoretically it is possible for the human operator to decouple the b axis from the a axis and not decouple the a axis from the b axis or vice versa.

In the investigation of the operator's performance in cross coupled tracking systems, the control tasks were designed to possess various degrees of cross-coupling. The control tasks are described in detail in Section 3.3.

3.3 Experimental Design

3.3.1 Experimental Outline

A training and performance experiment was performed on a two-axis manual control system with input coupling. The human operator performed a compensatory tracking task by using a finger tip controller to minimize the tracking error presented to him as a spot on a CRT display. Both asymmetrical and symmetrical input coupling was used. The experimental objectives were to obtain data for study of the following problems:

1) Evaluation of the effect of training and task difficulty on tracking performance.

2) Determination of human pilot models.

3) Evaluation of the effects of cross-coupled plant dynamics on the human pilot models.

4) Comparison of uncoupled and coupled tracking systems.

The plant dynamics were of second-order form and consisted of a pure integration plus a first-order lag with a time constant of 0.3 seconds. Four control configurations with various degrees of cross-coupling were used where the cross-coupling dynamics were of the same form as the main control dynamics.

Input signals to the two-axis compensatory tracking system were obtained by filtering the output of a Gaussian noise generator with a third-order filter operating with a cutoff frequency of 1 radian per second. The input spectrum was augmented with an additional spectrum extending to 10 radians per second with its power level 30 db below the primary spectrum. This secondary spectrum was generated from the same noise source using a first-order filter. Separate noise generators were used for generating the two input signals to guarantee zero linear coherence between the two disturbances. The magnitude of the input signal was maintained at 3.5 cms RMS deflection on the CRT display.

The experimental design was a complete factorial with the factors being subject, control task, and task replication. Three subjects with previous tracking experience were used and four control tasks were investigated. The experiment consisted of three training sessions followed by a fourth and final performance session. In a given session, each subject performed four replicates of each control task. The order of the control tasks was randomized for each subject and each session. For training purposes, performance measures were reported to the subject upon completion of each replication. Each replication was of 2.5 minutes duration and only the central 2 minutes were scored.

3.3.2 Task Definitions

Since input cross-coupling was the principal phenomenon to be examined, the tasks were designed to exhibit various degrees of cross-coupling ranging from the no-coupling level to the symmetrical coupling level. In the notation below, the subscript a refers to the horizontal channel while b refers to the vertical channel. Only the plant dynamics are shown.

Task 1 No-Coupling

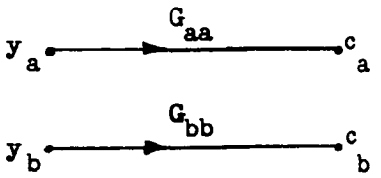

$$G_{aa}(s) = G_{bb}(s) = \frac{5.2}{s(0.3s + 1)} = G$$

Figure 3-2 Plant Dynamics for Task 1

Task 2 Asymmetrical Coupling

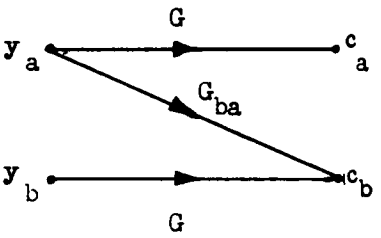

$$G_{ba} = -G = \frac{-5.2}{s(0.3s + 1)}$$

Figure 3-3 Plant Dynamics for Task 2

Task 3 Symmetrical Coupling

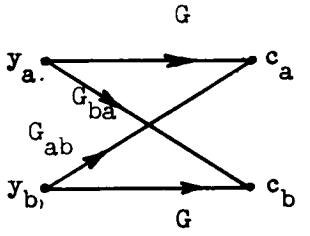

$$G_{ba} = -0.75G = \frac{-3.9}{s(0.3s + 1)}$$

$$G_{ab} = 0.75G = \frac{3.9}{s(0.3s + 1)}$$

Figure 3-4 Plant Dynamics for Task 3

Task 4 Asymmetrical Coupling

Task 4 was identical to Task 2 with the exception that the input signal r_b in the vertical axis was zero. This task was designed to determine if the human operator could decouple the b axis from the z axis when the input disturbance to the b axis was zero.

3.4 Approximate Model Determination by a Model Matching Technique

The human operator response data obtained for the cross-coupled tasks outlined in Section 3.3 was analyzed using the iterative model matching technique described in Section 4.3. For each of the four control tasks, the human operator's performance was modeled by an asymmetric lattice filter as shown for the two-axis input coupled tracking system in Figure 3-1. It was assumed that if each filter element was of linear second order form, then the lattice filter model would adequately describe the tracking behavior of the human operator provided the proper filter parameters were chosen. Specifically, each filter element was described by an equation of the form

$$\ddot{z} + \alpha_1 \dot{z} + \alpha_2 z = \alpha_3 \dot{x} + \alpha_4 x \qquad (3.3)$$

where x is the element input, z is the element output and α_i $(i = 1,2,3,4)$ are the differential equation parameters to be determined.

Equation 3.3 may be transformed to the complex frequency domain and rewritten in describing function notation as

$$\frac{Z(s)}{X(s)} = \frac{K(T_1 s + 1)}{(T_2 s + 1)(T_3 s + 1)}$$

where s is the Laplace operator, K is the zero frequency gain and T_i (i = 1,2,3) are the describing function time constants.

Individual determination of the lattice elements using closed or open loop formulations* of the model matching technique is impossible because of the coupling between the two control axes. However, approximate determinations are possible for each control task if executed in the following manner.

TASK 1

Representation of the human operator by a lattice filter leads to the following signal flow diagram for the Task 1 plant dynamics.

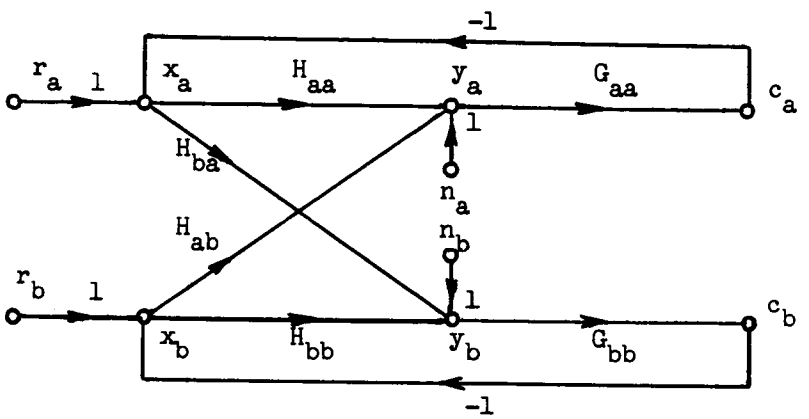

Figure 3-5 Signal Flow Diagram for Task 1

The describing functions H_{aa} and H_{bb} may be determined approximately using the closed loop formulation of the iterative model matching technique as described in Section 4.3. Signals r_a and y_a would be used to obtain H_{aa} while r_b and y_b would be required to obtain H_{bb}. In the determination of H_{aa}, the signal y_a in addition to being a function of H_{aa}, is also a function of H_{ba}, G_{bb} and H_{ab} because of the coupling functions H_{ba} and H_{ab}. Thus H_{aa} may only be approximated. However the approximation may be quite good if the combined effect of H_{ba}, G_{bb}, and H_{ab} substantially attenuates the signal x_a. Since the plant dynamics are not coupled in Task 1, it is probable that the human operator will not introduce appreciable cross-coupling and consequently accurate determination of H_{aa} and H_{bb} could be made.

*The relative merits of open and closed formulations are discussed in Section 4.3.

Describing function H_{ab} and H_{ba} may be determined in an open loop manner using the signals x_b, y_a and x_a, y_b. Again the determinations are approximate because of the cross-coupling.

TASK 2

Figure 3-6 shows the signal flow diagram for Task 2. Again the elements H_{aa} and H_{bb} may be determined approximately using a closed loop formulation. However, the element H_{ab} may be determined in a closed loop manner by closing the loop through the plant coupling function G_{ba} and the b axis feedback path. Note that the zero frequency gain of H_{ab} must be negative for stable operation.* An open loop formulation was used to obtain H_{ba}.

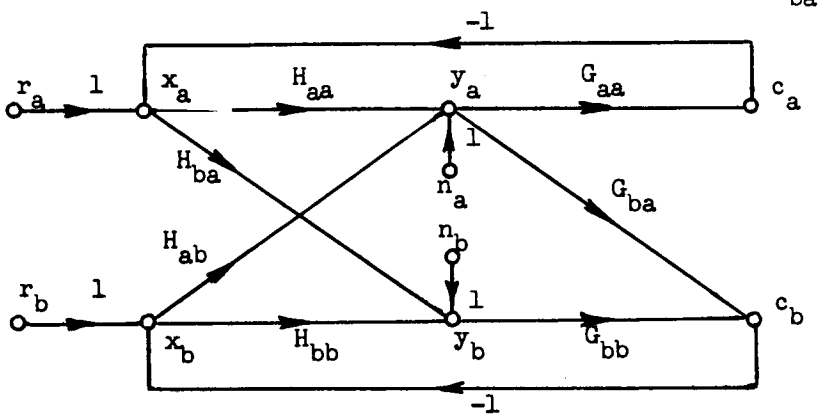

Figure 3-6 Signal Flow Diagram for Task 2

TASK 3

For this task, the elements H_{aa} and H_{bb} were determined using the closed loop formulation as for Task 1, while the elements H_{ab} and H_{ba} were obtained using the closed loop technique as for Task 2. No stability problem arose in the determination of H_{ba} as G_{ab} had a positive zero frequency gain.

TASK 4

The elements were determined in the same manner as outlined for Task 2 except that H_{bb} and H_{ab} could not be determined since the excitation signal $r_b(t)$ was zero.

---

* In this task $G_{ba} = \dfrac{-5.2}{s(0.3s+1)}$.

Approximate determinations of the describing functions were obtained by using the iterative model matching technique described in Section 4.3. The iterative technique employing a finite difference calculation for the sensitivity coefficient was used. Table 3-1 shows the operational constants used in the analog computer implementation of the technique. In all determinations the iteration interval was 1.5 seconds. A comparison between the approximate models and the correct models was made for one subject (Section 4.8) and yielded close agreement, thus indicating that the approximate models obtained were satisfactory. Typical time histories of the human operator's parameters for Tasks 2 and 3 are given in Appendix C.

Table 3-1

Operational Constants for the Iterative Model Matching Technique

Task and Describing Function		All Tasks H_{aa} & H_{bb}	Task 2 H_{ab} Task 3 H_{ab} & H_{ba}	Task 1 H_{ab}	Task 1 H_{ba}	Tasks 2 & 4 H_{ba}
Parameter Adjustment Gains	k_1	20	50	25	10	10
	k_2	120	300	150	60	60
	k_3	20	25	12.5	5	5
	k_4	60	150	75	30	30
Parameter Offset	$\Delta\alpha_1$	1	1	1	1	1
	$\Delta\alpha_2$	3	3	3	3	3
	$\Delta\alpha_3$	0.5	0.5	0.5	0.5	0.5
	$\Delta\alpha_4$	3	3	3	3	3
Maximum Parameter Correction Per Iteration	α_1	1	1	1	1	1
	α_2	2	2	2	2	2
	α_3	1	1	1	1	1
	α_4	1	1	1	1	1
Initial Parameter Values	α_{10}	8	12	10	4	10
	α_{20}	16	22	20	32	16
	α_{30}	10	7	4	10	6
	α_{40}	15	2	4	4	18

3.5 Prediction of Human Tracking Performance

Using the decoupling equations derived in Section 3.2 it is possible to express the coupling describing functions H_{ij} in terms of the coupling functions H_{ii} for the case when the human operator is able to decouple the system and not generate appreciable noise signals (n_a, n_b) in the process. Since the operator will neither be able to decouple the system completely nor generate zero noise signals, the relations between H_{ij} and H_{ii} will at best be approximations. However an a priori knowledge of human performance in cross-coupled systems would be valuable in design of such systems even though the prediction would be an approximation.

The following predictions of human performance may be made for the control tasks specified in Section 3.3.

Task 1

$$G_{ab} = G_{ba} = 0, \quad G_{aa} = G_{bb} = G$$

$$H_{ab} = -\left(\frac{G_{ab}}{G_{aa}}\right) H_{bb} = 0$$

$$H_{ba} = -\left(\frac{G_{ba}}{G_{bb}}\right) H_{aa} = 0$$

Task 2, 4

$$G_{ab} = 0, \quad G_{ba} = -G, \quad G_{aa} = G_{bb} = G$$

$$H_{ab} = 0$$

$$H_{ba} = H_{aa}$$

Task 3

$$G_{ab} = 0.75G, \quad G_{ba} = -0.75G, \quad G_{aa} = G_{bb} = G$$

$$H_{ab} = -0.75\, H_{bb}$$

$$H_{ba} = 0.75\, H_{aa}$$

Examination of the human coupling describing functions H_{ij} indicates that they are simply related to the uncoupled describing functions H_{ii}. Since the relations are simple for all tasks except Task 3, the human operator could be expected to decouple the system. Task 3 is difficult to decouple since the operator must introduce a 180 degree phase shift in generating H_{ab}. The discussion in Section 3.7 will in fact show that the human operator's performance in coupled two-axis tracking can be predicted with a fair degree of accuracy.

In order to visualize the manner in which the operator should ideally decouple the system, the control problem may be treated as a transformation of coordinate axes. For the control tasks investigated, the coupling transfer functions of the plant dynamics differed from the uncoupled functions by multiplicative constants. Ideal decoupling required that the coupling describing functions of the human operator be similarly related to the uncoupled describing functions. Consequently the ideally decoupled system may be represented by the signal flow diagram shown in Figure 3-7. In this diagram K_{Hi} represents the multiplicative constant of the human operator and K_{Gi} represents the corresponding constant in the plant dynamics. If matrix notation is used, then the system block diagram may be represented as shown in Figure 3-8 where

$$r = \begin{bmatrix} r_a \\ r_b \end{bmatrix} \quad x = \begin{bmatrix} x_a \\ x_b \end{bmatrix} \quad H = \begin{bmatrix} H_{aa} & 0 \\ 0 & H_{bb} \end{bmatrix} \quad G' = \begin{bmatrix} G_{aa} & 0 \\ 0 & G_{bb} \end{bmatrix} \quad H_C = \begin{bmatrix} 1 & K_{Hb} \\ K_{Ha} & 1 \end{bmatrix}$$

$$G_C = \begin{cases} \begin{bmatrix} 1 & 0 \\ 0 & 1 \end{bmatrix} & \text{for Task 1} \\ \begin{bmatrix} 1 & 0 \\ -1 & 1 \end{bmatrix} & \text{for Tasks 2 and 4} \\ \begin{bmatrix} 1 & .75 \\ -.75 & 1 \end{bmatrix} & \text{for Task 3} \end{cases}$$

Decoupling requires that the matrix product $G_C H_C$ be diagonal. Thus the elements of H_C have the following values:

$$H_C = \begin{bmatrix} 1 & 0 \\ 0 & 1 \end{bmatrix} \qquad \text{Task 1}$$

$$H_C = \begin{bmatrix} 1 & 0 \\ 1 & 1 \end{bmatrix} \qquad \text{Tasks 2 and 4}$$

$$H_C = \begin{bmatrix} 1 & -.75 \\ .75 & 1 \end{bmatrix} \qquad \text{Task 3}$$

Physically the decoupling process may be considered as a transformation of axes. Assume the system is decoupled and use the unit vectors $\vec{a}$ and $\vec{b}$ to specify the error signal x. In generating the signal y, the human operator must transform these vectors to a new coordinate system whose unit vectors are $\vec{a}'$ and $\vec{b}'$. The new vectors must be related to the a and b vectors such that the signal y is transformed back to the original coordinate system when operated on by the coupling matrix G_C.

Since Task 1 possesses no cross-coupling, the transformation between the unit vectors is one to one, i.e.;

$$\vec{a}' = \vec{a} \qquad \text{and} \qquad \vec{b}' = \vec{b}$$

For Tasks 2 and 4, the transformation may be derived by considering the matrix operations on the vector $\vec{y}$. Specifically

$$\vec{y} = y_a \vec{a} + y_b \vec{b} = y_{a'} \vec{a}' + y_{b'} \vec{b}'$$

or

$$\begin{bmatrix} y_a & y_b \end{bmatrix} \begin{bmatrix} \vec{a} \\ \vec{b} \end{bmatrix} = \begin{bmatrix} y_{a'} & y_{b'} \end{bmatrix} \begin{bmatrix} \vec{a}' \\ \vec{b}' \end{bmatrix}$$

But

$$\begin{bmatrix} y_a \\ y_b \end{bmatrix} = H_C \begin{bmatrix} y_{a'} \\ y_{b'} \end{bmatrix}$$

Thus for Tasks 2 and 4

$$\begin{bmatrix} y_a & y_b \end{bmatrix} \begin{bmatrix} \vec{a} \\ \vec{b} \end{bmatrix} = \begin{bmatrix} y'_a & y'_b \end{bmatrix} \begin{bmatrix} 1 & 1 \\ 0 & 1 \end{bmatrix} \begin{bmatrix} \vec{a} \\ \vec{b} \end{bmatrix}$$

or

$$\begin{bmatrix} \vec{a}' \\ \vec{b}' \end{bmatrix} = \begin{bmatrix} \vec{a} + \vec{b} \\ \vec{b} \end{bmatrix}$$

Consequently the transformation equations are

$$\vec{a}' = \vec{a} + \vec{b}$$

$$\vec{b}' = \vec{b}$$

Similarly the transformation equations for Task 3 are found to be

$$\vec{a}' = \vec{a} + 0.75\,\vec{b}$$

$$\vec{b}' = -0.75\,\vec{a} + \vec{b}$$

Figure 3-9 illustrates the transformation equations for Tasks 1 through 4. If, for example, the operator observes the displayed error stationary at position A, he ideally would move the control stick to position B to null the error. If the human performs in this manner, he will be able to decouple the system.

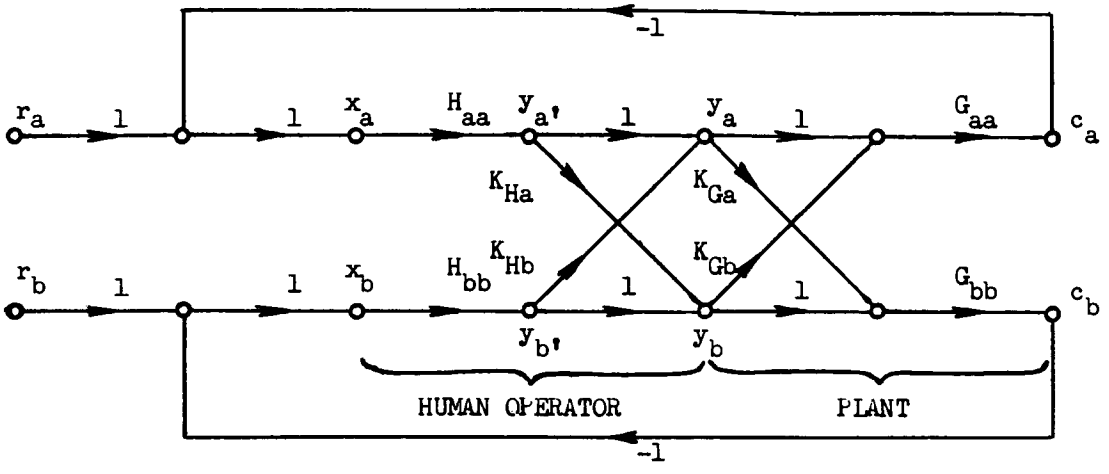

Figure 3-7 Signal Flow Diagram of Decoupled System

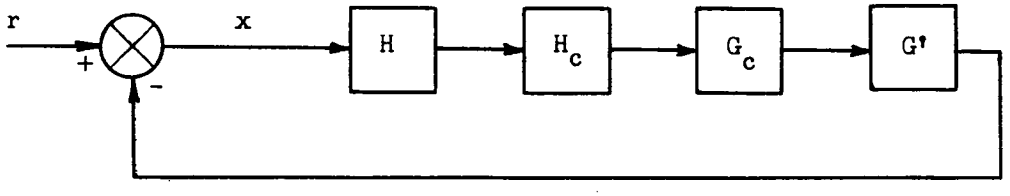

Figure 3-8 Matrix Block Diagram of Decoupled System

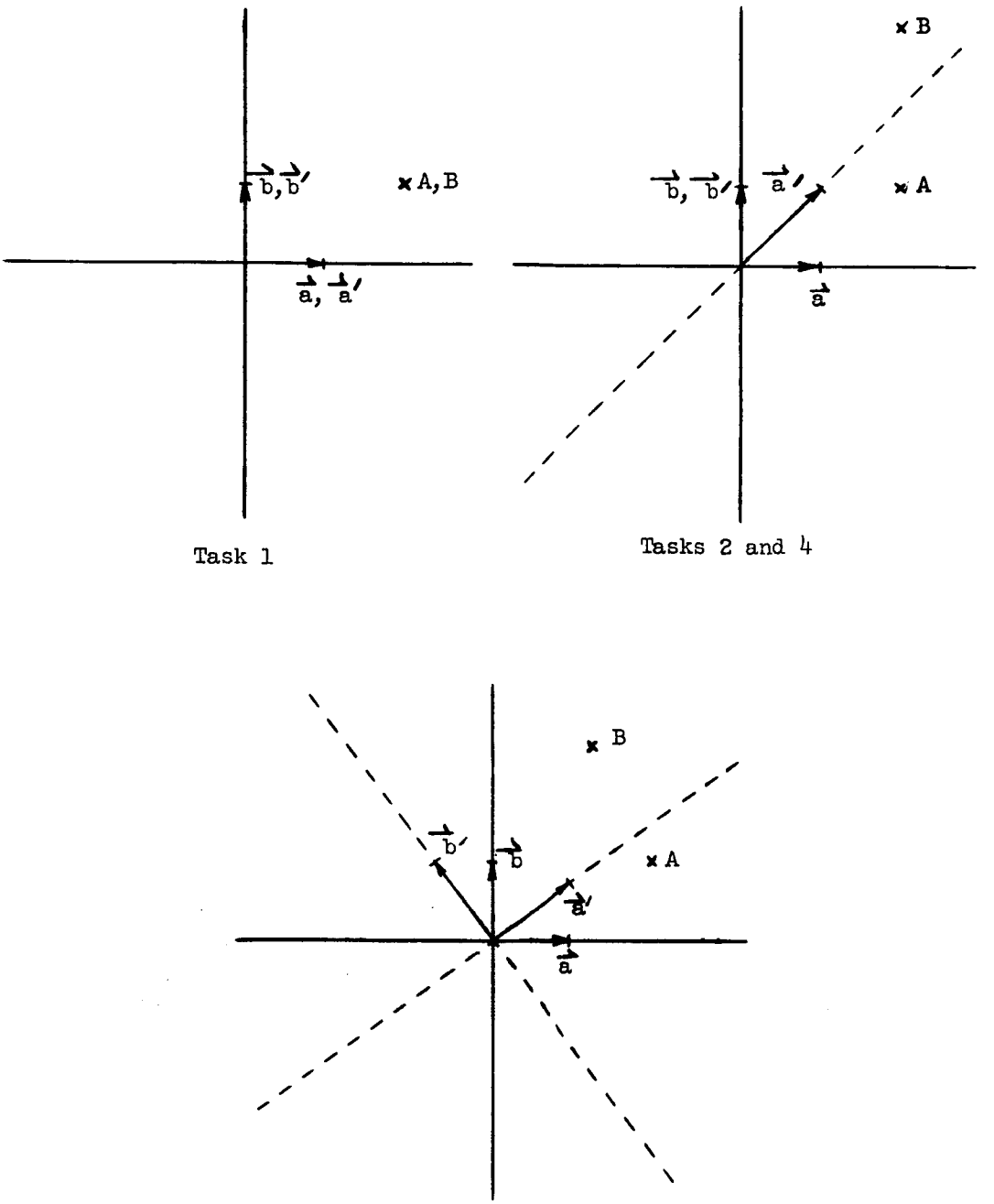

Figure 3-9 Transformation of Coordinate Axes

3.6 Effect of Training and Task Difficulty on System Tracking Error

The root mean square value of the system tracking error was used as a criterion to evaluate training and task difficulty. Normalization with respect to the input signal was not done since the input signal was held approximately constant. Specifically an RMS error score was calculated for each axis in each of the task replications. Each score was obtained from the integral of the square of the error signal over the $2\frac{1}{2}$ minute run:

$$x_{RMS} = \left[\frac{1}{T} \int_0^T x^2 dt \right]^{\frac{1}{2}}$$

The RMS errors were averaged over the three subjects and plotted as a function of replication number in Figures 3-10 and 3-11. Training is evidenced by the downward trend of the scores with increasing replication number. Examination of the learning curves shown in Figures 3-10 and 3-11 yields the following observations on the effect of training and task difficulty on system tracking error.

1) In the first few replications, the lower error scores are found in Task 1 in both axes and Task 2 in the a axis. These are the axes in which cross-coupling has no effect. Since the subjects had been previously trained in two-axis uncoupled tasks, they were initially able to perform these better than the new cross-coupled tasks.

2) Task 3, a symmetrical task, has error scores of approximately equal magnitude in each axis, whereas Task 2, an asymmetrical task, results in markedly different errors. In fact, the error score for Task 2 in the b axis is greater than any other score, indicating that this was the most difficult task.

3) Task 4 is one in which there is no input signal to the b axis. The only input to the b axis error was cross-coupling from the a axis. The low RMS error score in the b axis indicates the ability of the subject to learn to remove the effect of the cross-coupling

and reduce the error signal in that axis. Note that training was most pronounced for this case. The error in the a axis is about that of the a axis of Task 2, the task with the same configuration but inputs in both axes.

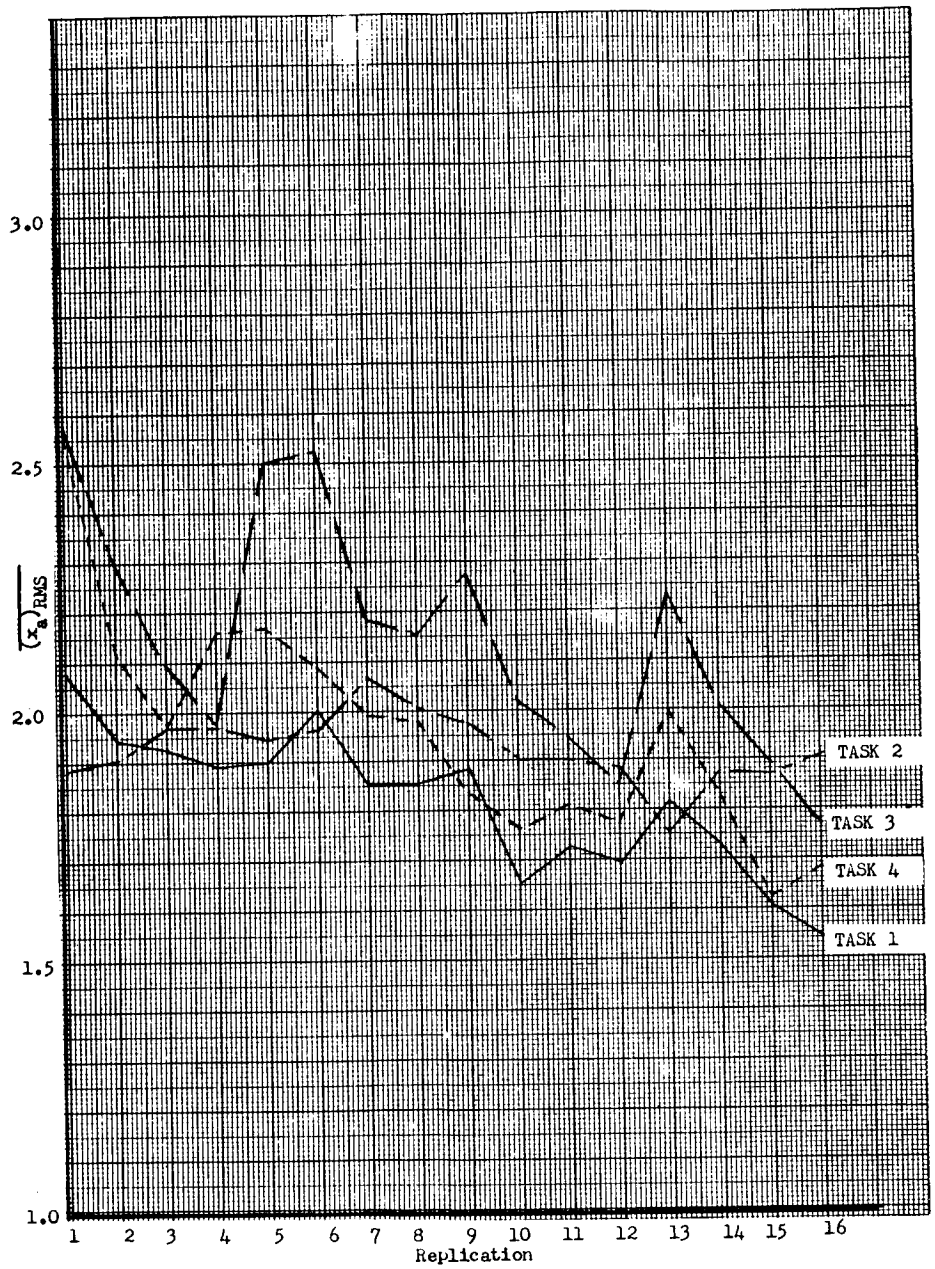

Figure 3-10 Learning Curves for the a Axis

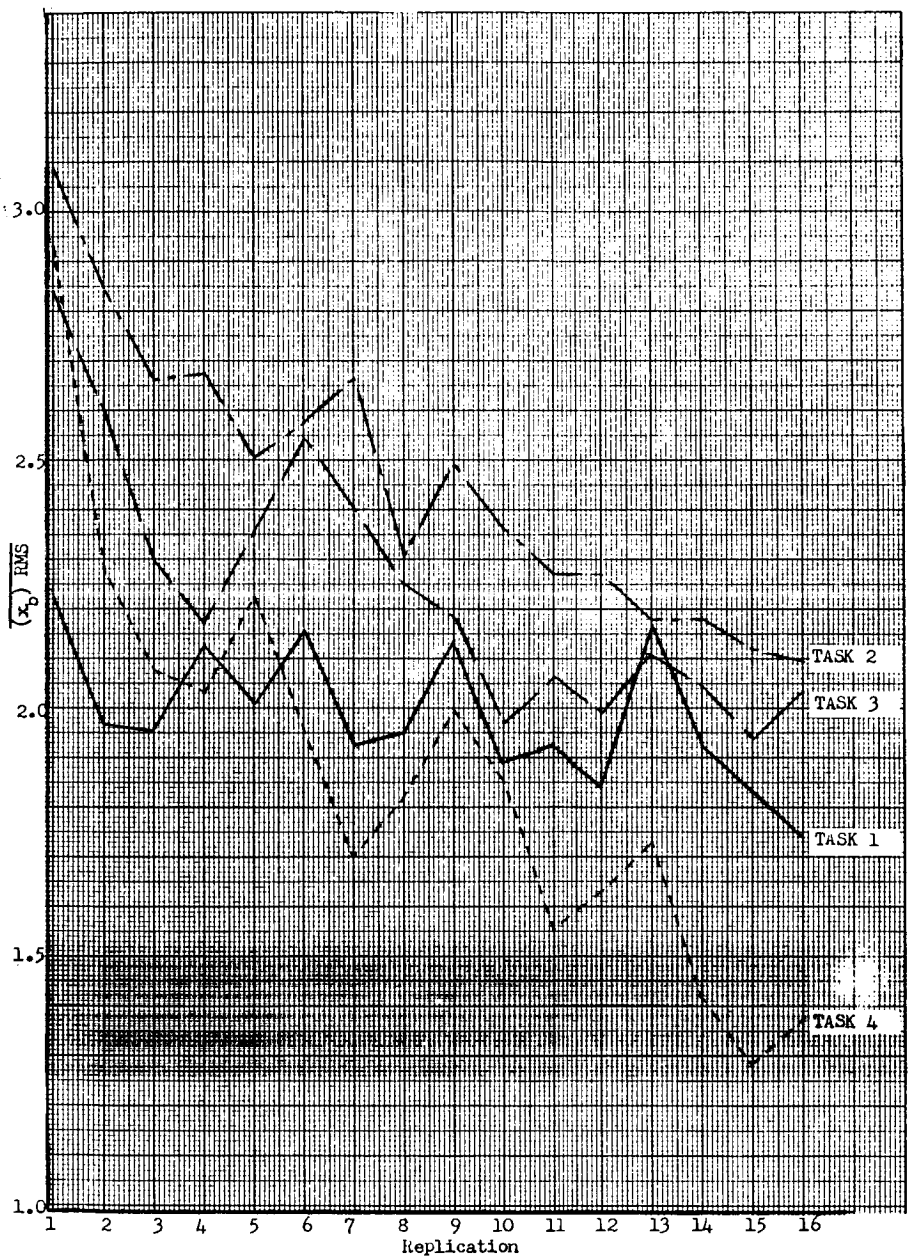

Figure 3-11 Learning Curves for the b Axis

3.7 Effect of Cross-Coupling on Human Performance

3.7.1 Introduction

Approximate human operator models were obtained for the final performance session of the cross-coupled experiment using the iterative model matching technique. The average second-order describing functions determined are tabulated in Table 3-2 as a function of control task. Figures 3-12 through 3-15 show the corresponding Bode diagrams for these tasks. Comparison of the frequency response data with the prediction of human performance made in Section 3.5 leads to the following results.

3.7.2 Results

Figures 3-12 and 3-13 indicate clearly that the average describing functions H_{aa} and H_{bb} were essentially identical for all control tasks investigated. It may be concluded that various degrees of cross-coupling in the plant dynamics do not affect the human's major describing functions H_{aa} and H_{bb}. However the describing functions H_{ab} and H_{ba} are related to the degree of cross-coupling. Specifically the following relations were found.

Task 1

The control dynamics in Task 1 were uncoupled and theoretically the human operator should not introduce any cross-coupling (i.e., ideally, $H_{ab} = H_{ba} = 0$). Figure 3-14 indicates that $|H_{ab}|$ is down 10 db from $|H_{bb}|$ (Figure 3-13). The zero frequency gain of H_{ba} (Figure 3-15) is down 19 db from $|H_{aa}|$ (Figure 3-12) while the response around 6 r/s is of the same order as $|H_{aa}|$. This latter result indicates that the operator did not perform as predicted.

Task 2

To decouple this asymmetrically coupled control task, the human operator must adjust H_{ab} and H_{ba} such that

$$H_{ab} = 0$$

$$H_{ba} = H_{aa}$$

Figure 3-14 shows that $|H_{ab}|$ is 25 db down with respect to $|H_{bb}|$ and thus $|H_{ab}|$ may be considered zero for all practical purposes. The comparison of $|H_{ba}|$ and $|H_{aa}|$ shown in Figure 3-16 indicates that $|H_{ba}|$ closely resembles $|H_{aa}|$ and consequently the operator was essentially able to decouple the system. Since the magnitude of the frequency response for $|H_{ba}|$ was consistently greater than the response for $|H_{aa}|$ (Figure 3-16), it was concluded that the operator overcompensated for the decoupling required.

Task 3

Decoupling of the symmetrically coupled task requires that the human operator choose H_{ab} and H_{ba} such that

$$H_{ab} = -0.75\ H_{bb}$$

$$H_{ba} = 0.75\ H_{aa}$$

Since the amplitude ratio of H_{ab} (Figure 3-14) is down 21 db from $|H_{bb}|$, H_{ab} may be considered zero for all practical purposes. The amplitude ratio of H_{ba} (Figure 3-15) does closely resemble $|H_{aa}|$ between 1.5 and 10 r/s, but at frequencies below 1.5 r/s the resemblance no longer exists. Thus the human operator chooses $|H_{ba}|$ as predicted over the frequency bandwidth indicated but is unable to properly choose $|H_{ab}|$.

Task 4

The decoupling equations for Task 4 are identical with those for Task 2 since the plant dynamics of the two tasks are equal. Comparison of H_{ba} and H_{aa} (Figure 3-16) indicates that the two Bode diagrams closely resemble each other and consequently the operator behaves as predicted. The difference in zero frequency gains for Task 4 is only 3.8 db while for Task 2 this difference was 7.4 db. Note that the phase curves for Task 4 are also more identical than in Task 2. Thus the prediction was much better for Task 4 than Task 2. This was attributed to the fact that r_b was made zero for Task 4 and consequently the task was less difficult than Task 2. Reference to the RMS tracking error scores in

Figures 3-10 and 3-11 indicates that Task 4 was indeed less difficult than Task 2. Since H_{ab} was not determined, no information was available for comparison purposes. However it is believed that H_{ab} is essentially zero as was found in Task 2 since the two tasks are so closely related.

3.7.3 Statistical Analysis of Zero Frequency Gain (K)

An analysis of variance test was applied to the obtained values of the zero frequency gain (K) for the describing functions H_{aa}, H_{bb}, H_{ab} and H_{ba}. This analysis was performed to determine if the differences obtained in these terms were due to differences in the task or intra- and/or inter-subject variability. The analysis of variance design was a full factorial using the scores from the last session of the experiment (Section 3.3). The variables were the four cross-coupling tasks, the four replicates of the last session and the three subjects. The subjects were treated as a random sample from a group of previously trained subjects and the other variables were treated as fixed populations.

The results of the analysis are shown in Table 3-3 for the four describing functions. Using the 1% level as the a priori significance level because of the small sample size, H_{ba} was the only function showing significant differences between the tasks. This agrees with the previous analysis of the Bode diagrams in Section 3.7.2. It should also be noted that H_{bb} and H_{ab} showed significant task differences at the 5% level and H_{ba} and H_{ab} showed significant replicate differences at the 5% level. These differences are probably due to the small subject variability as reflected in the subject mean square terms and the subject interaction mean square terms of Table 3-3. This indicates that the three subjects utilized in this task had similar describing functions for the various tasks. If the subject sample had been larger it is expected that the 5% level differences would disappear.

Duncan's Multiple Range Test was applied to the mean values of K for H_{ba}. This analysis showed no differences between Tasks 1 and 3 or 2 and 4 but significant differences at the 2% level existed between these two groupings.

Table 3-2

Average Describing Functions

	Task 1	Task 2	Task 3	Task 4
H_{aa}	$\frac{1.11(1+.580s)}{(1+.147s)(1+.634s)}$	$\frac{.952(1+.614s)}{(1+.113s)(1+.598s)}$	$\frac{.714(1+.657s)}{(1+.128s)(1+.464s)}$	$\frac{1.07(1+.518s)}{(1+.119s)(1+.646s)}$
H_{bb}	$\frac{1.02(1+.582s)}{(1+.133s)(1+.733s)}$	$\frac{1.26(1+.541s)}{(1+.0946s)(1+1.01s)}$	$\frac{.847(1+.600s)}{(1+.124s)(1+.564s)}$	
H_{ba}	$\frac{.140(1+2.44s)}{1+.163s+.0286s^2}$	$\frac{2.25(1+.278s)}{(1+.138s)(1+.811s)}$	$\frac{.203(1+3.35s)}{(1+.100s)(1+.633s)}$	$\frac{1.64(1+.312s)}{1+.485s+.0770s^2}$
H_{ab}	$\frac{.315(1-.238s)}{(1+.104s)(1+.514s)}$	$\frac{.0749(1-.005s)}{(1+.111s)(1+.342s)}$	$\frac{.0750(1-.345s)}{(1+.101s)(1+.407s)}$	

Table 3-3

Analysis of Variance of Zero Frequency Gain (K)

Source	Degrees of Freedom	Sum of Squares	Mean Square	F Ratio
H_{aa}				
Task	3	167	55.6	2.40
Replicates	3	158	52.7	3.22
Subjects	2	269	134.5	
T x R	9	67	7.4	< 1
T x S	6	139	23.2	
R x S	6	98	16.3	
T x R x S	18	157	8.7	
H_{bb}				
Task	2	134	67	16.7*
Replicates	3	75	25	2.53
Subjects	2	75	37.5	
T x R	6	33	5.5	< 1
T x S	4	16	4	
R x S	6	59	9.9	
T x R x S	12	109	8.4	
H_{ba}				
Task	3	3885	1295	48.87**
Replicates	3	35	11.7	5.03*
Subjects	2	58	29	
T x R	9	49	5.4	1.56
T x S	6	159	26.5	
R x S	6	14	2.33	
T x R x S	18	62	3.45	
H_{ab}				
Task	2	514	257	11.81*
Replicates	3	158	52.7	5.85*
Subjects	2	3	1.5	
T x R	6	134	22.3	1.89
T x S	4	87	21.8	
R x S	6	54	9	
T x R x S	12	142	11.8	

* Significant at 0.05 level (5%)
** Significant at 0.01 level (1%)

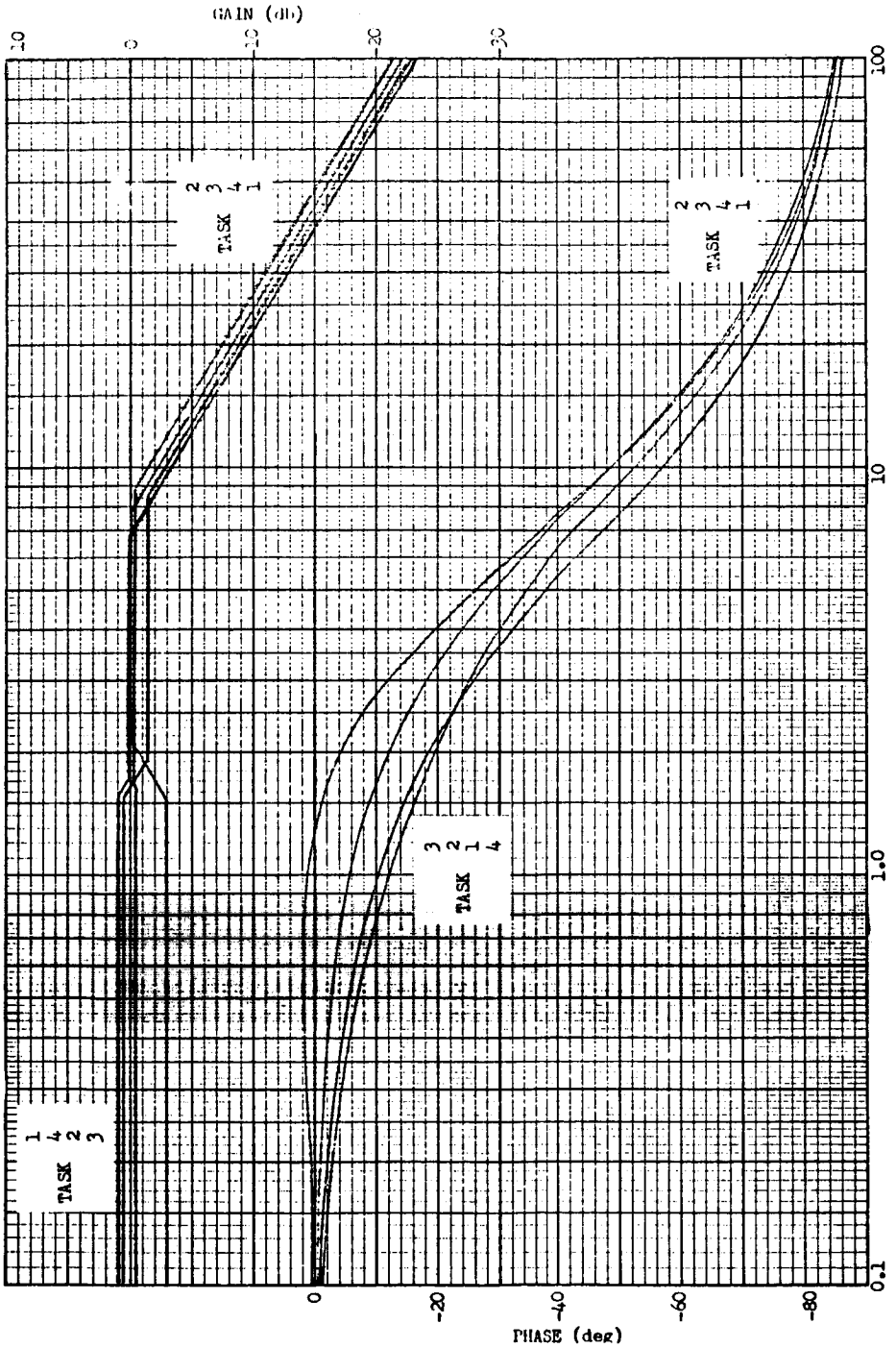

Figure 3-12 Bode Diagrams for H_{aa}

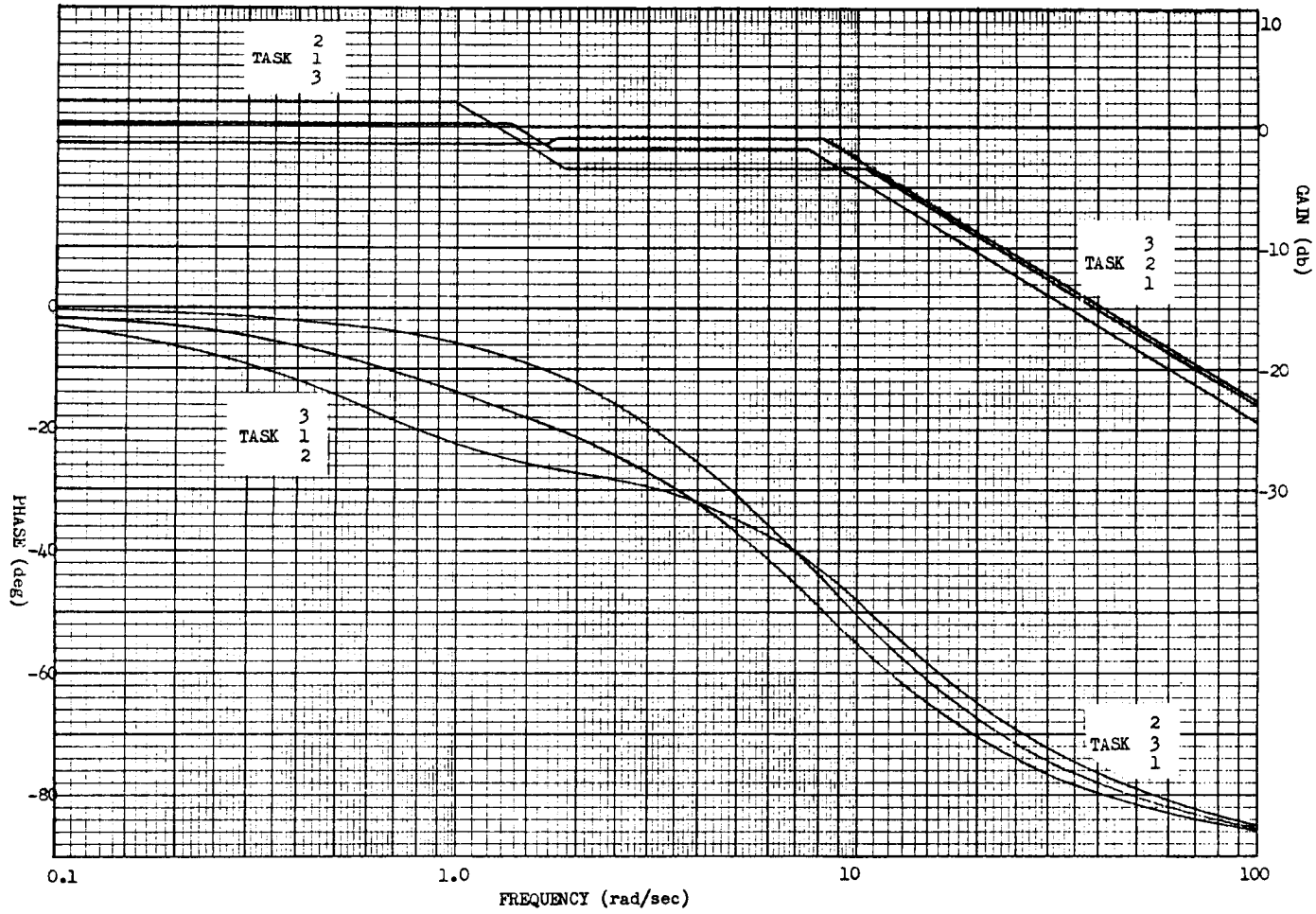

Figure 3-13 Bode Diagrams for H_{bb}

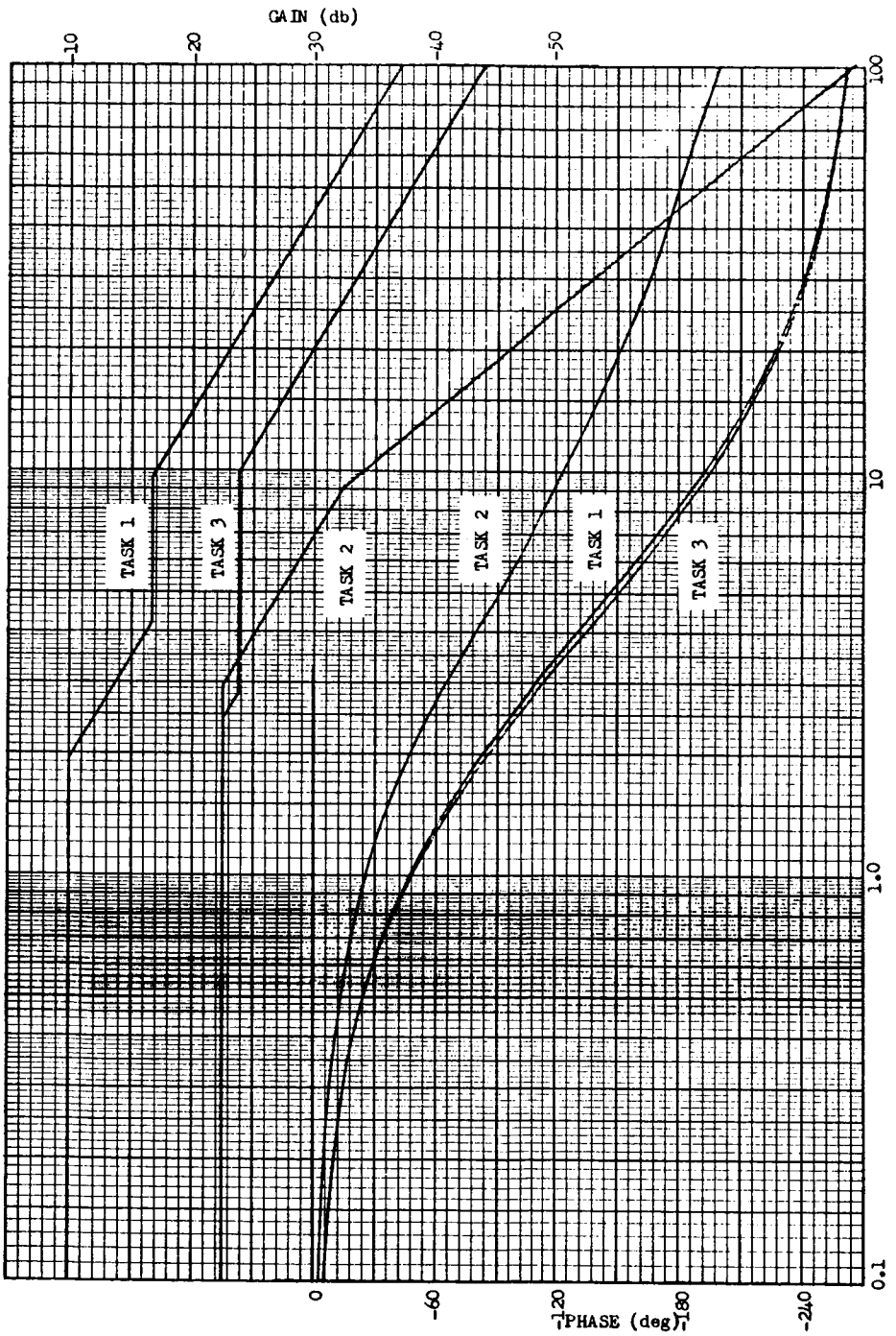

Figure 3-14 Bode Diagrams for H_{ab}

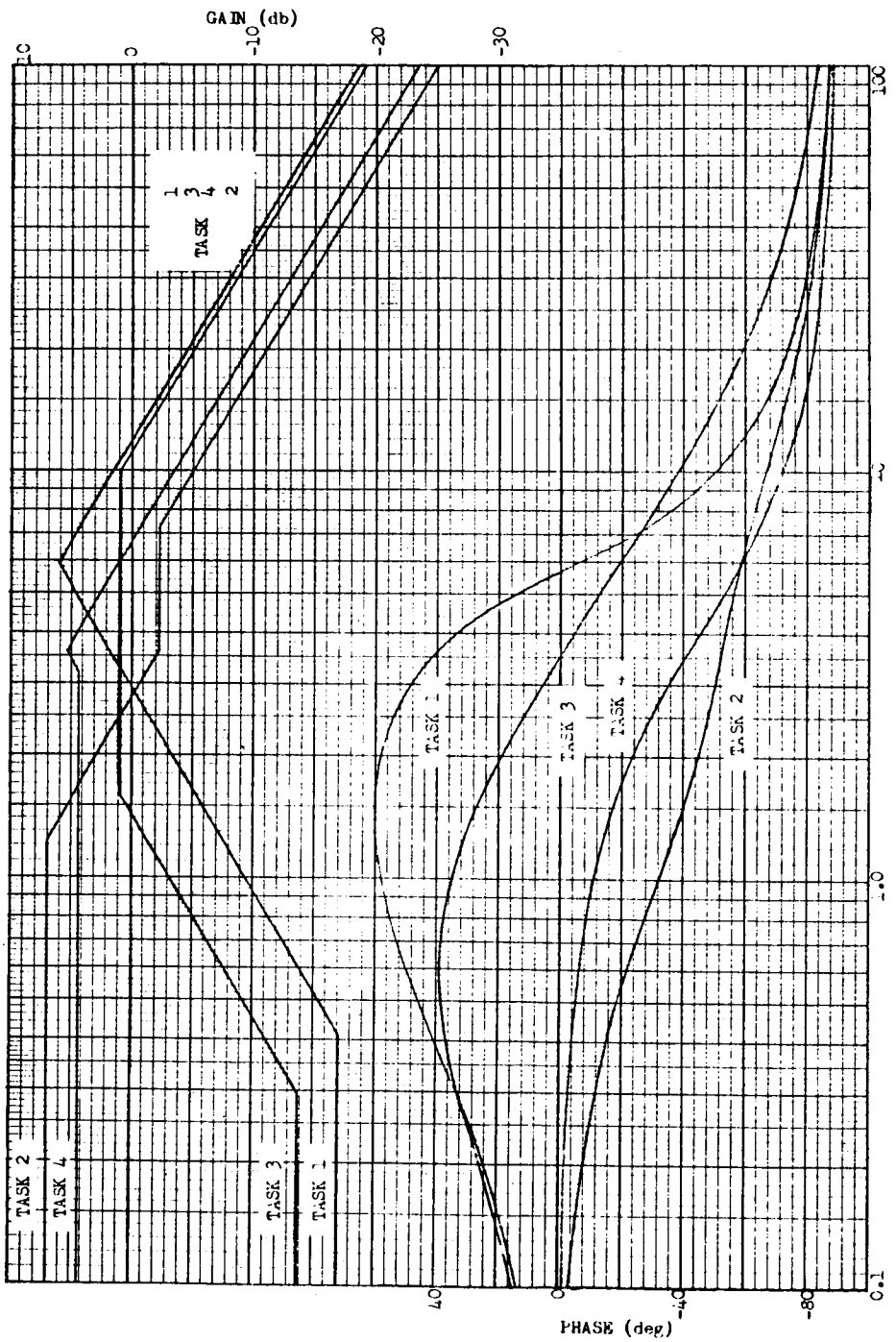

Figure 3-15 Bode Diagrams for H_{ba}

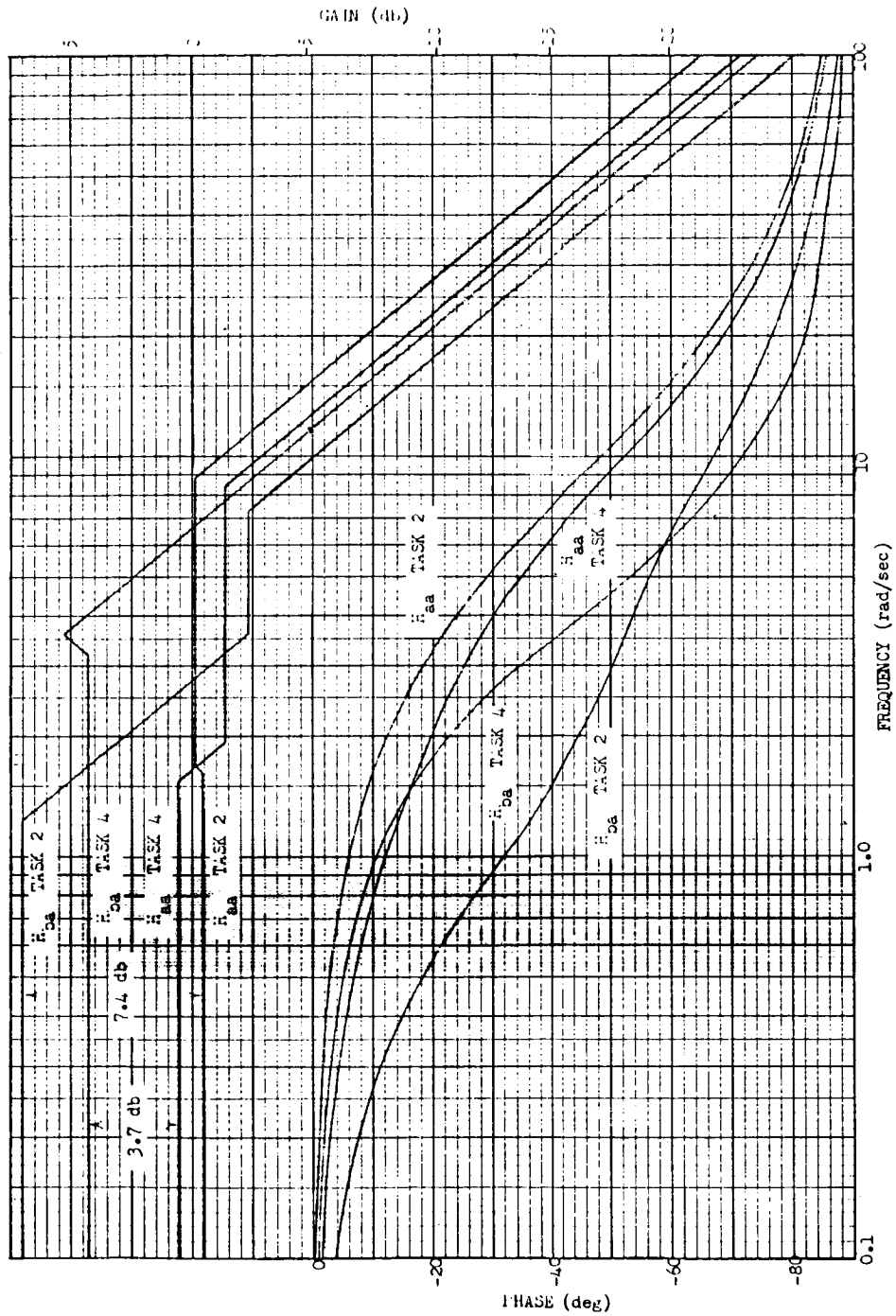

Figure 3-16 Comparison of Tasks 2 and 4

3.8 Conclusions

Experimental data obtained from a coupled two-axis tracking experiment was analyzed by mathematical modeling of the human operator's performance. The models were used to determine if the operator could decouple the system. An analysis of variance was performed to determine the significance level of the zero frequency gain. Task difficulty and learning were evaluated using the RMS tracking error. The analysis of human performance in coupled two-axis systems with cross-coupling led to the following conclusions:

1) The human operator can essentially decouple the system for Tasks 2 and 4 according to prediction from decoupling equations which were analytically derived. The decoupling performance was better in Task 4 than Task 2 due to the excitation signal r_b being zero in Task 4.

2) The human operator was not able to decouple the symmetrically coupled system for Task 3. Decoupling in Task 3 is difficult since the operator must introduce a 180 degree phase shift in generating H_{ab}.

3) In Task 1, the human operator introduces some coupling in the form of H_{ba} around a frequency of 6 r/s. This was considered a transfer effect due to the full factorial design in which H_{ba} was transferred from Tasks 2, 3 and 4 to Task 1.

4. For all tasks, the describing functions H_{aa} and H_{bb} were essentially identical, indicating that various degrees of cross-coupling in the plant dynamics do not affect the human's major describing functions H_{aa} and H_{bb}.

5. Learning was evident for all tasks with Task 2, an asymmetrical task, being the most difficult.

4. METHODOLOGY STUDY

4.1 Introduction

The objective of this study was to develop refined model matching techniques which would be capable of precise mathematical modeling of human tracking performance. Three basic modeling techniques of the output error category were evaluated where the primary consideration was identification accuracy of model parameters. The three techniques (continuous, iterative, and extrapolation) were experimentally studied by determining their identification accuracy using second-order systems with known parameters.

In the continuous technique, a modified square law criterion function was investigated to determine if identification accuracy could be increased by utilizing a high parameter adjustment gain when the model matching error was small. To increase the modeling accuracy of the iterative technique, precise methods of calculating the influence coefficients were evaluated. First-order extrapolation was used in the extrapolation technique to determine the effect of first-order prediction on parameter convergence. Modeling of higher order model terms by extrapolation was also investigated. Conventional spectral analysis techniques of determining transfer functions were extended to permit exact estimates of human describing functions in coupled two-axis tracking systems.

4.2 The Continuous Model Matching Technique

In general the model matching concept of system parameter identification is based on determining a model which will operationally match the performance of an unknown system when both the system and model are excited by the same input signal. In using model matching techniques, the functional form of the unknown system equations must be specified or assumed in advance. The model form is then selected to approximate as closely as possible the assumed form of the unknown system. To permit precise parameter identification, the excitation signal should have a bandwidth which covers the dynamic range of the unknown system. Theoretically the signal input bandwidth must be infinite to obtain exact identification but in practice this is neither possible nor necessary. For human operator identification, either random or random appearing signals are used.

Consider the system identification problem shown in Figure 4-1 where H represents the unknown system and M the model. Assume that the functional form H is of second order and can be described by

$$\ddot{y} + a_1\dot{y} + a_2 y = a_3\dot{x} + a_4 x \qquad (4.1)$$

where

x is the system input

y is the system output

a_i (i = 1, 2, 3, 4) are constant coefficients.

Rewriting Equation (4.1) in operator form yields

$$y = \left(\frac{a_3 p + a_4}{p^2 + a_1 p + a_2} \right) x = H(p)x$$

where p is the differential operator $\frac{d}{dt}$.

Since M and H are assumed to have the same form, then z is related to x by the equation

$$z = \left(\frac{\alpha_3 p + \alpha_4}{p^2 + \alpha_1 p + \alpha_2} \right) x = M(p,\bar{\alpha})x$$

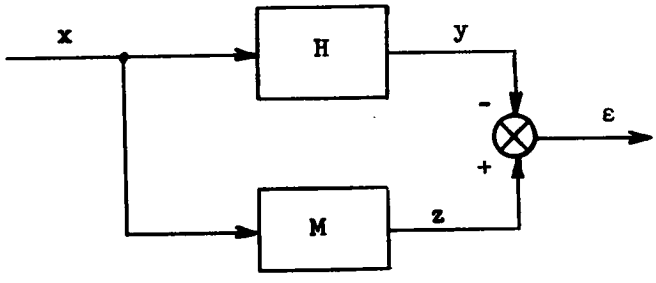

Figure 4-1 The Model Matching Concept

where x is the model input

z is the model output

$\bar{\alpha}$ is the variable parameter vector

If the model matching error ε is defined by

$$\varepsilon = z - y$$

then the model parameters will be identical to the system coefficients when the model matching error is zero over the whole frequency bandwidth of the system being identified. In the continuous model matching technique (Reference 5), a criterion function f which depends on the error ε is minimized by an approximate steepest descent method. The criterion function must be positively definite with a unique minimum at $\epsilon = 0$ and with $\partial f/\partial \varepsilon > 0$ for $\varepsilon > 0$ and $\partial f/\partial \varepsilon < 0$ for $\varepsilon < 0$. A square law criterion function satisfies these requirements and may be used in model matching, i.e.

$$f = \tfrac{1}{2}\varepsilon^2 \qquad (4.2)$$

The method of steepest descent can be described by the vector equation

$$\frac{d}{dt}(\bar{\alpha}) = -k\ \overline{\nabla f}(\varepsilon)$$

where $\overline{\nabla f}$ is the gradient of f and

k is a positive proportionality constant.

Considering only the i'th component of the equation yields

$$\frac{d}{dt}(\alpha_i) = -k\frac{\partial f}{\partial \alpha_i} \qquad (4.3)$$

Implementation of the technique on an analog computer requires the generation of the partial derivatives shown in Equation (4.3). Performing the differentiation indicated in Equation (4.3) yields the result

$$\frac{\partial f}{\partial \alpha_i} = \varepsilon\ u_i \qquad (4.4)$$

where the sensitivity coefficient u_i is defined by

$$\frac{\partial z}{\partial \alpha_i} \triangleq u_i$$

Strictly speaking u_i is defined only when the α_i are constant. This restriction leads to a contradiction since, by Equation (4.3) the product $\epsilon\, u_i$ is made proportional to a rate of change of α_i. In this discussion the rules of differentiation will be applied formally and the method will be termed "approximate steepest descent". A more thorough discussion of this problem is given in References 6 and 7. Substituting for the i'th gradient component in Equation (4.3) and integrating over time yields the value of the i'th parameter at time t_1 as indicated by the equation

$$\alpha_i(t_1) = -k \int_0^{t_1} \varepsilon u_i dt$$

The sensitivity coefficients are obtained by solving sensitivity equations. For the i'th parameter the sensitivity equation is obtained by formally computing the partial derivative of the model equation with respect to the i'th parameter. The differentiation takes the following form for the α_1 parameter

$$\frac{\partial}{\partial \alpha_1}\left[\dddot{z} + \alpha_1\ddot{z} + \alpha_2\dot{z}\right] = \frac{\partial}{\partial \alpha_1}\left[\alpha_3\dot{x} + \alpha_4\right]$$

Assuming that parameter cross coupling is negligible yields

$$\ddot{u}_1 + \alpha_1\dot{u}_1 + \alpha_2 u_1 = -\dot{z}$$

Solving the sensitivity equation obtained yields the sensitivity coefficient,

$$u_1 = \frac{-p}{(p^2 + \alpha_1 p + \alpha_2)}\, z = -Jpz$$

where J is an operator defined by:

$$J = \frac{1}{p_2 + \alpha_1 p + \alpha_2}$$

Similarly it may be shown that

$$u_2 = -Jz$$

$$u_3 = Jpx$$

$$u_4 = Jx$$

Observing that the influence coefficients are interdependent gives the following interdependence relations

$$u_1 = pu_2$$

$$u_3 = pu_4$$

Since it has been shown that the sensitivity coefficients may be obtained by solving the sensitivity equations, the continuous method may readily be implemented on a conventional analog computer according to the block diagram given in Figure 4-2. Note that the model matching method is continuous in that the parameters are continually being updated.

In practical applications of the technique it has been found advantageous for stability reasons to introduce a rate term into the criterion function in the manner shown below

$$f_1 = \tfrac{1}{2} (\varepsilon + q\dot{\varepsilon})^2$$

The error rate coefficient q may be varied from zero to unity to yield the proper amount of lead required. Use of a lead term permits more rapid convergence and hence a shorter identification time. However, like all quadratic functions, this criterion function has the disadvantage of a shallow minimum. This causes a relatively large uncertainty in the final parameter values, since the error criterion in practice does not register small deviations of the parameters from the theoretical optimum. An increase of the adjustment gain constant k tends to reduce the uncertainty level but also tends to cause instability of the adjustment process if the error and hence the slope of the error criterion is large.

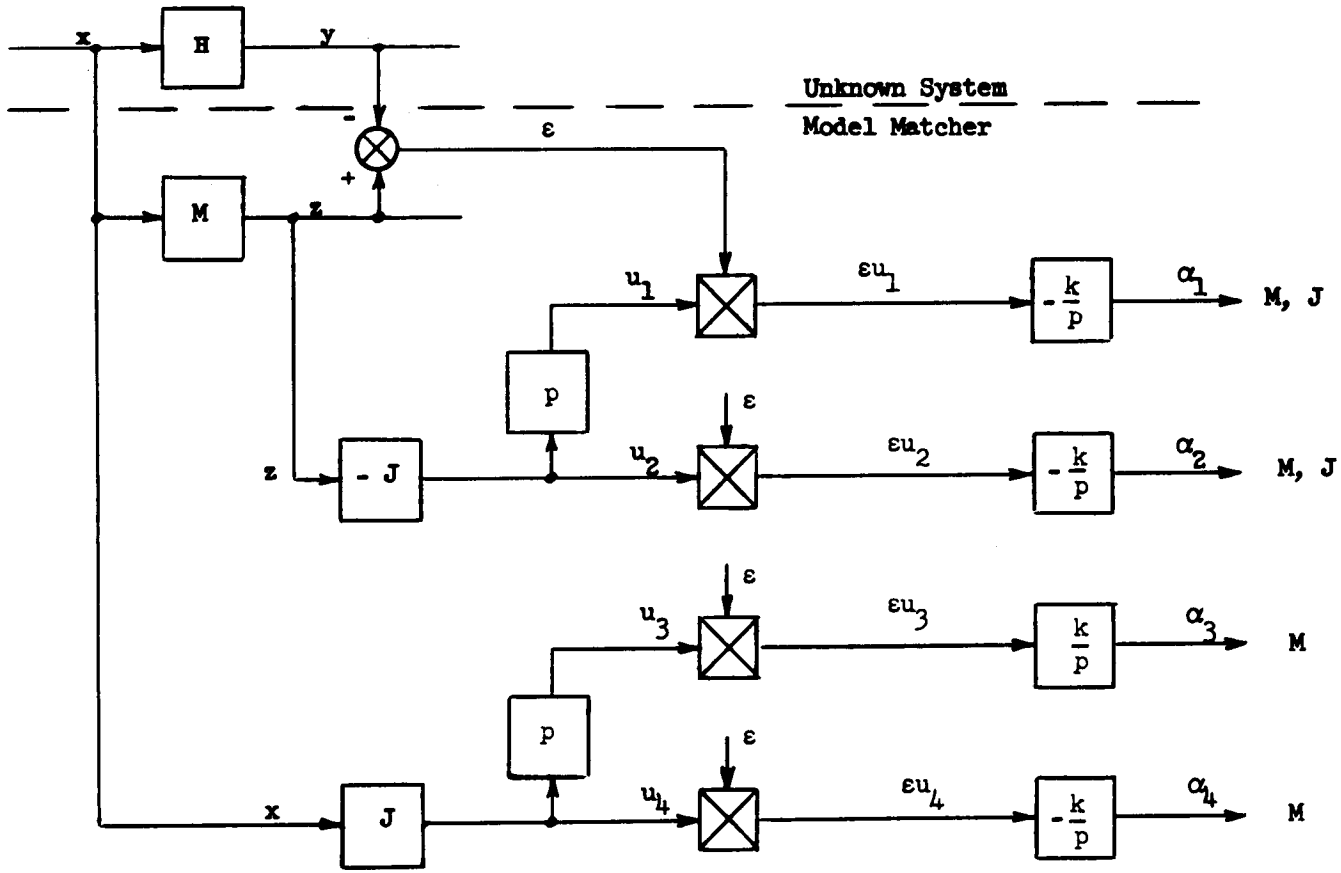

$$M = \frac{\alpha_3 p + \alpha_4}{p^2 + \alpha_1 p + \alpha_2} \qquad J = \frac{1}{p^2 + \alpha_1 p + \alpha_2}$$

Figure 4-2 The Continuous Open Loop Model Matcher

A modified error criterion having a limited slope for large deviations from the minimum was adopted to overcome this difficulty. This criterion function f_2 and its slope is shown in Figure 4-3. It can be expressed mathematically by

$$f_2 = \begin{cases} \frac{1}{2}(\varepsilon+q\dot{\varepsilon})^2 & \text{if} \quad -L \leq \varepsilon+q\dot{\varepsilon} \leq L \\ L\,|\varepsilon+q\dot{\varepsilon}| - \frac{L^2}{2} & \text{if} \quad |\varepsilon+q\dot{\varepsilon}| \geq L \end{cases}$$

Independent choice of the breakpoint L, and the rate coefficient q permits adaptation of the error criterion for optimum model matching performance. For a given adjustment gain k in Equation (4.3) and breakpoint L, the limit of $kdf_2/d(\varepsilon+q\dot{\varepsilon})$ is determined from $M = k\,L$. If the adjustment gain is increased and the breakpoint L is decreased such that M is constant, it follows the criterion function f_2 approximates the absolute value criterion

$$|f_3 = |\varepsilon+q\dot{\varepsilon}|$$

without the attendant problems of switching transients at $\varepsilon+q\dot{\varepsilon} = 0$ and of limit cycles occurring in the adjustment loops.

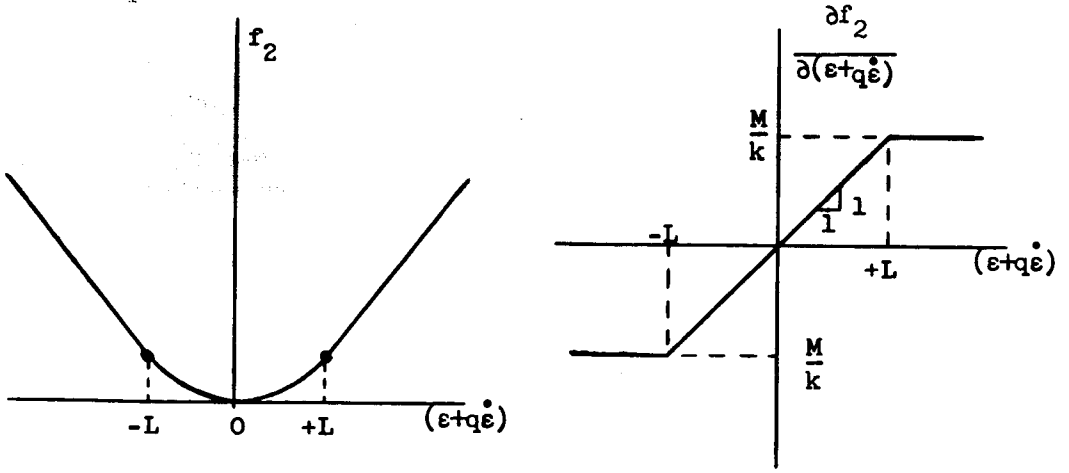

Figure 4-3 Modified Error Criterion f_2 and Derivative

4.3 The Iterative Model Matching Technique

4.3.1 Introduction

The continuous model matching technique is mathematically not precise, since the solutions of the sensitivity equations (u_i) are equal to the partial derivatives $\partial z/\partial \alpha_i$ only when the α_i are constant. Iterative techniques overcome this difficulty by holding the model parameters constant during the computation of the influence coefficients. Following such a computation, the parameters are adjusted incrementally.

The time interval (T) during which the parameter influence coefficients are being computed is one of the variables of the iterative method. Early formulations of the iterative technique at TRW Systems (Reference 8) required repetitive processing of the entire data record, as the computation interval was made equal to the record length. During the present study, computation intervals of only a few seconds were used, thus making possible parameter identification during a single processing of a human tracking record. The formulation of the iterative model matching technique is described in the following paragraphs.

4.3.2 The Iterative Model Matching Technique

In general the output error form of model matching may be formulated in either an open or closed loop manner to identify the describing function of a human operator performing a compensatory tracking task. In open loop model matching (Figure 4-4), the model input is identical to the human operator input, while in closed loop model matching (Figure 4-5), the model input is generated by differencing the reference input and the task dynamics response of the model. It may be shown analytically (Reference 9) that the human operator describing function will be inaccurate if determined by the open loop technique for the case where the human operator output contains an appreciable amount of noise which is not linearly correlated with the reference input. In such situations, the closed loop model matching technique should be used.

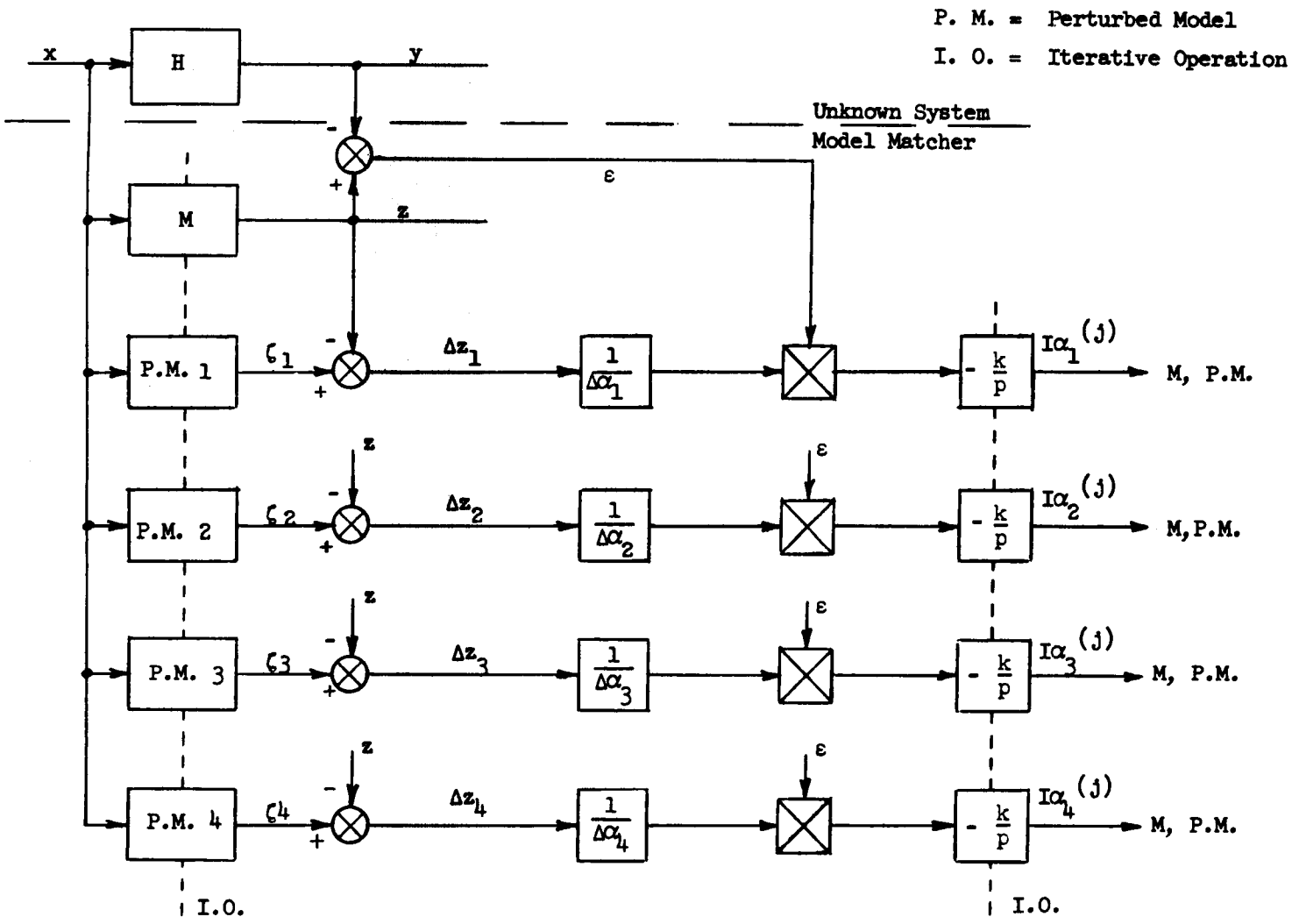

Figure 4-4 The Iterative Open Loop Model Matcher $\left(u_i \simeq \frac{\Delta z}{\Delta \alpha_i}\right)$

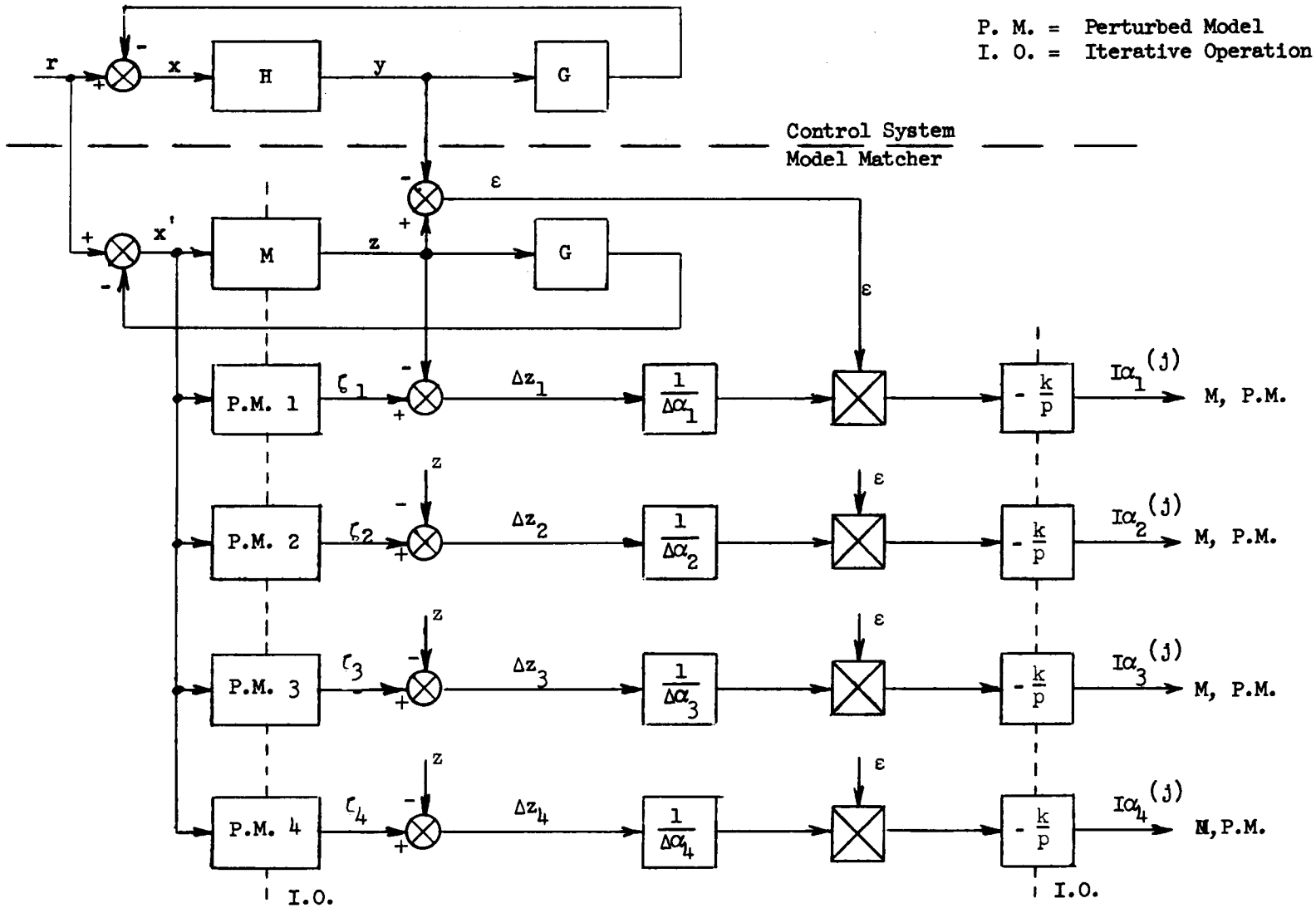

Figure 4-5 The Iterative Closed Loop Model Matcher $\left(u_i \cong \frac{\Delta z}{\Delta \alpha_i}\right)$

In using the closed loop technique, the human operator is assumed to behave as a linear second order system describable by

$$\ddot{y} + a_1\dot{y} + a_2 y = a_3\dot{x} + a_4 x \qquad \dot{y}(0) = y(0) = 0$$

where x is the human operator input

y is the human operator output

a_i (i = 1,2,3,4) are constant coefficients

On the basis of this assumption, the model is constructed to have an identical form given by

$$\ddot{z} + \alpha_1\dot{z} + \alpha_2 z = \alpha_3\dot{x}' + \alpha_4 x' \qquad \dot{z}(0) = z(0) = 0$$

where x' is the model input

z is the model output

α_i (i = 1,2,3,4) are variable coefficients

The model and human operator outputs are then differenced to form the model matching error. A steepest descent method is used to reduce the model matching error to zero and thus identify the parameters of the human operator.

In the iterative technique, the parameters are updated at the end of each computation interval by an incremental correction calculated during the iteration period as shown in the following equation

$$\alpha_i(j+1) = \alpha_i(j) + I\alpha_i(j)$$

where j = j'th iteration interval

$I\alpha_i(j)$ = incremental correction in the α_i parameter

The incremental corrections for each parameter is calculated using a steepest descent method which requires that the incremental change be made proportional to the negative of the local gradient of a criterion function f. If only the i'th parameter is considered, then the steepest descent method requires that

$$I\alpha_i(j) = -k \frac{\partial F(j)}{\partial \alpha_i} \tag{4.5}$$

where k is a positive proportionality constant.

For the iterative technique, the criterion function has the form

$$F = \int_{jT}^{(j+1)T} \tfrac{1}{2} \varepsilon^2 dt$$

where T is the length of the iteration interval. The rate term ($q\dot{e}$) used for stabilization in continuous model matching is not needed here since the parameter adjustment loop is not closed during computation of the incremental correction.

If the partial differentiation indicated in **Equation** (4.5) is performed, then the following integral equation is obtained for the calculation of the incremental parameter correction

$$I\alpha_i(j) = -k \int_{jT}^{(j+1)T} \varepsilon \frac{\partial z}{\partial \alpha_i} dt$$

The influence coefficient $\frac{\partial z}{\partial \alpha_i} = u_i$ is implemented directly on an analog computer by the finite difference approximation,

$$u_i \cong \frac{\Delta z_i}{\Delta \alpha_i} = \frac{z(\alpha_i + \Delta\alpha_i) - z(\alpha_i)}{\Delta \alpha_i} = \frac{\zeta_i - z_i}{\Delta \alpha_i}$$

The term ζ_i is generated by using a perturbed model. For the α_1 parameter, ζ_1 is given by

$$\zeta_1 = \frac{\alpha_3 p + \alpha_4}{p^2 + (\alpha_1 + \Delta\alpha_1) p + \alpha_2}$$

Similar perturbed models are used to generate the perturbed model outputs ζ for the other parameters.

The closed loop iterative model matching technique was implemented on an analog computer as shown in Figure 4-5. An open loop formulation of the iterative technique is shown in Figure 4-4 for comparison purposes. An experimental study of

the iterative technique was performed on systems with known parameters and the results are presented in Section 4.5.2.

It is also possible to calculate the influence coefficients in the iterative technique by solving sensitivity equations. These equations were derived in Section 4.2 for the open loop formulation and are repeated here for convenience;

$$u_1 = -Jpz$$
$$u_2 = -Jz$$
$$u_3 = Jpx$$
$$u_4 = Jx$$

where $J = \dfrac{1}{p^2 + \alpha_1 p + \alpha_2}$

Since the α parameters are held constant during the computation interval, it follows that J now becomes only a function of time and consequently the influence coefficients may be determined exactly. In theory this method of influence coefficient determination is superior to the finite difference method as the latter method approximates the true partial derivative by a finite difference approximation. Hence the iterative technique employing this type of influence coefficient determination should provide better system identification accuracy. A block diagram of the open loop formulation is shown in Figure 4-6. The experimental study performed on this method is described in Section 4.5.2.

The iterative technique utilizing sensitivity equations for influence coefficient computation may also be formulated in a closed loop manner. Figure 4-7 illustrates the closed loop model matching concept where H is the unknown system element and M is the model of that element. The influence coefficients are determined by solving the influence equations of the element M. If the model M is describable by

$$\ddot{z} + \alpha_1 \dot{z} + \alpha_2 z = \alpha_3 \dot{x}' + \alpha_4 x'$$

then it may be shown that the influence coefficients are

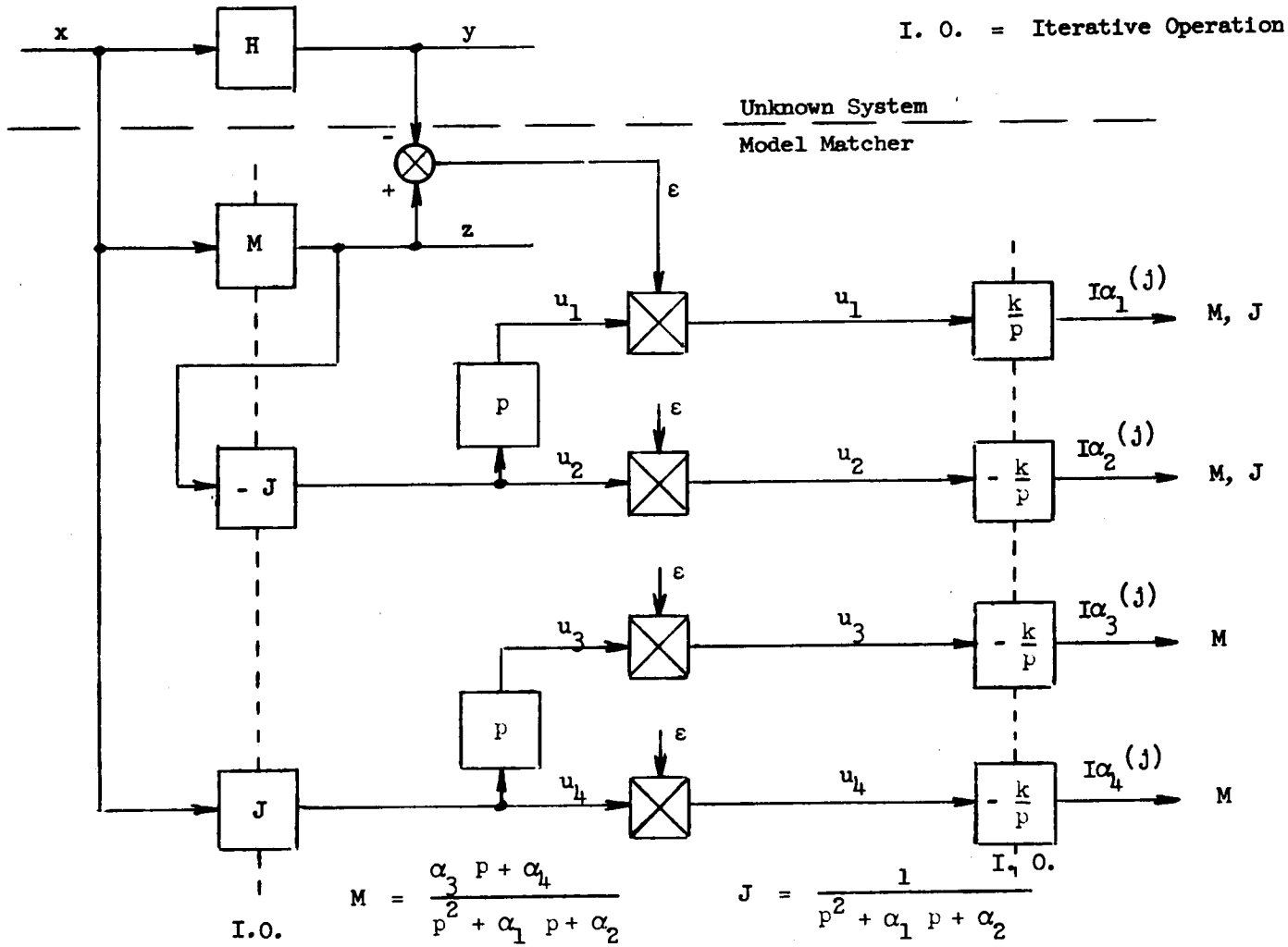

Figure 4-6 The Iterative Open Loop Model Matcher $\left(u_i = \frac{\partial z}{\partial \alpha_i}\right)$

$$u_1 = -Jpz + M\frac{\partial x'}{\partial \alpha_1}$$

$$u_2 = -Jz + M\frac{\partial x'}{\partial \alpha_2}$$

$$u_3 = Jpx + M\frac{\partial x'}{\partial \alpha_3}$$

$$u_4 = Jx + M\frac{\partial x'}{\partial \alpha_4}$$

where $$u_i = \frac{\partial z}{\partial \alpha_i} \qquad (i = 1,2,3,4)$$

$$J = \frac{1}{p^2 + \alpha_1 p + \alpha_2}$$

The partial derivatives of x' with respect to α_i may be related to the influence coefficients in the following manner.

Since the signal x' is defined by the equation

$$x' = r - c'$$

it follows that

$$\frac{\partial x'}{\partial \alpha_i} = -\frac{\partial c'}{\partial \alpha_i} \qquad (i = 1,2,3,4)$$

as r is independent of α_i. Because c' is defined by the equation

$$c' = Gz$$

then

$$\frac{\partial c'}{\partial \alpha_i} = G\frac{\partial z}{\partial \alpha_i} = Gu_i \qquad (i = 1,2,3,4)$$

Consequently the required relation is given by

$$\frac{\partial x'}{\partial \alpha_i} = -Gu_i \qquad (i = 1,2,3,4)$$

The influence coefficients can now be written in the following simplified form,

$$u_1 = \frac{-Jp}{1 + MG} \quad z$$

$$u_2 = \frac{-J}{1 + MG} \quad z$$

$$u_3 = \frac{Jp}{1 + MG} \quad x'$$

$$u_4 = \frac{J}{1 + MG} \quad x'$$

As in the open loop case, the influence coefficients are interrelated by the equations

$$u_1 = pu_2$$

$$u_3 = pu_4$$

The closed loop iterative technique may now be readily implemented on an analog as shown in Figure 4-8.

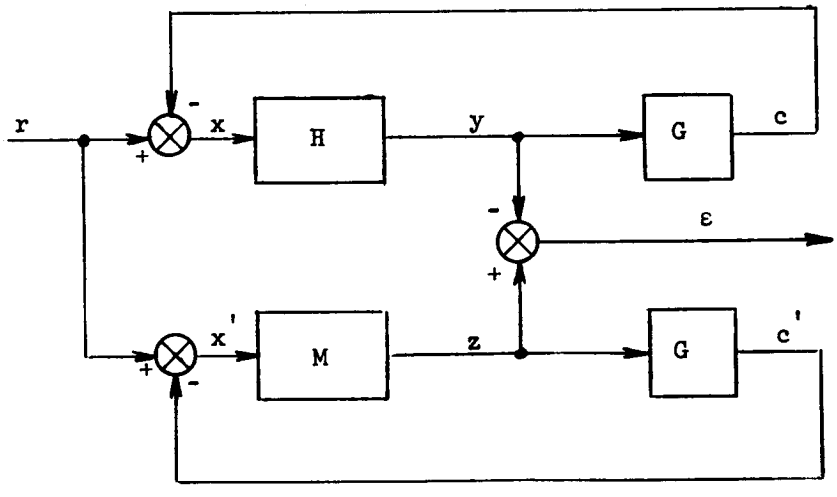

Figure 4-7 The Closed Loop Model Matching Concept

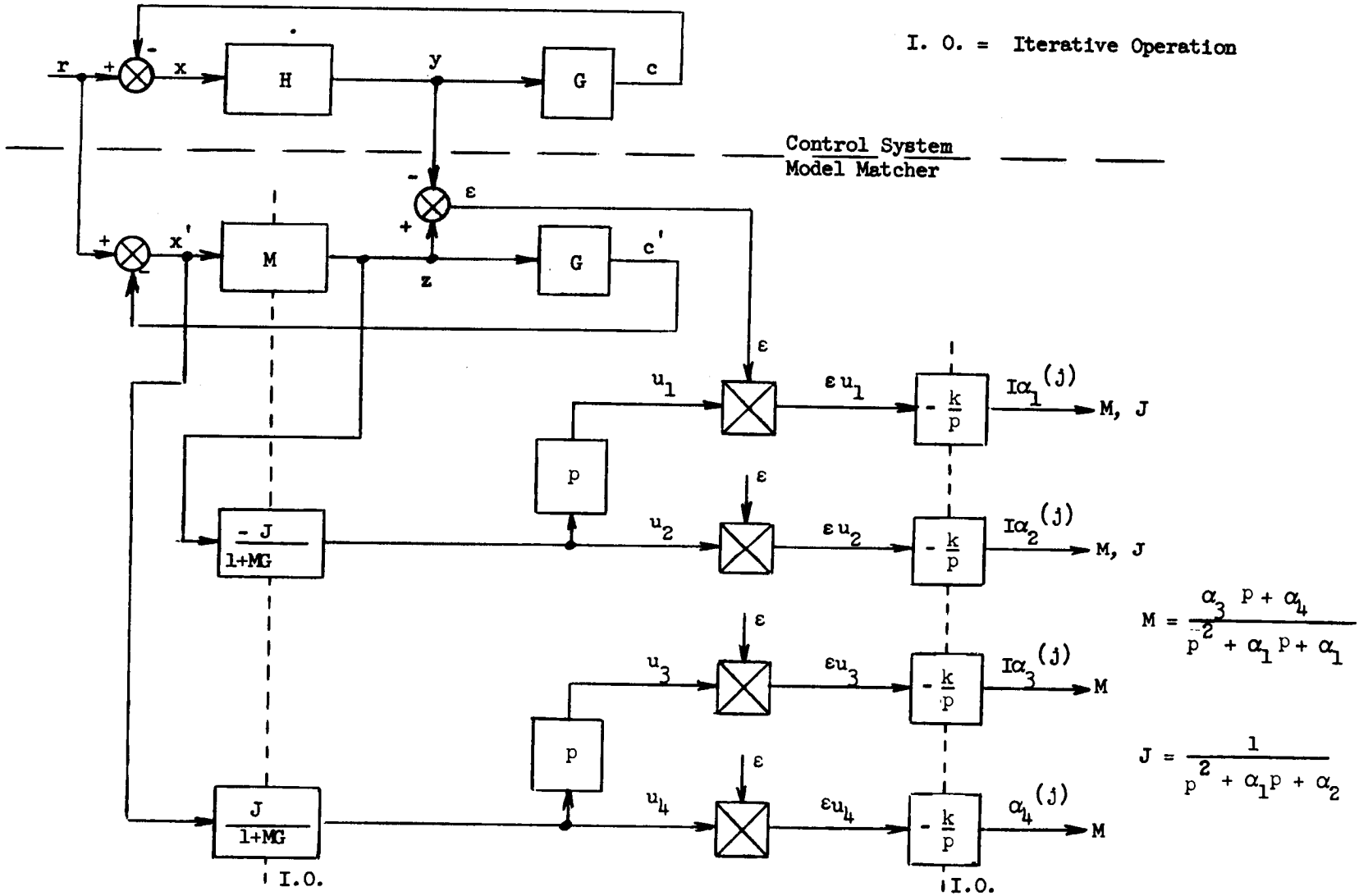

Figure 4-8 The Iterative Closed Loop Model Matcher ($u_i = \frac{\partial z}{\partial \alpha_i}$)

4.4 The Extrapolation Technique

4.4.1 Introduction

One of the difficulties of the continuous model matching technique is that the gradient cannot be defined in a rigorous manner unless the parameters are constant. This problem is not present in the iterative technique, where the parameters are held fixed during each iteration interval and thus the solution of the sensitivity equations yields well defined gradient components. In contrast with the instantaneous criterion function of the form $f = \frac{1}{2} [\varepsilon(t)]^2$ used in the continuous method, the iterative technique uses an integrated criterion function of the form

$$F = \int_{t_i}^{t_i + T} \frac{1}{2} [\varepsilon(t)]^2 \, dt$$

Evidently, while f depends on the time history of the parameters, F depends only on their value during the i-th iteration interval.

The extrapolation technique presented in this section is based on a first-order extrapolation of the matching error. As a result, the criterion function becomes an ordinary, algebraic function of the parameters (i.e., f depends only on the instantaneous values of the α_i and not on their entire history), and the gradient vector $\overline{\nabla f}$ can be rigorously defined. The resulting strategy is again iterative, even though an instantaneous criterion function is used.

4.4.2 The Extrapolation Technique

Consider the parameter identification problem shown in Figure 4-1 where H represents the unknown system and M the model. The model output z may be expanded in a Taylor's series about the initial conditions α_{io} as

$$z(\alpha_i, t) = z_o(t) + \sum_i u_{io}(t) \quad \delta\alpha_i(t) + \text{higher order terms}$$

where $$z_o(t) \triangleq z(\alpha_i,t)\Big|_{\alpha_i = \alpha_{io}}$$

$$u_{io}(t) \triangleq \frac{\partial z(\alpha_i,t)}{\partial \alpha_i(t)}\Big|_{\alpha_i = \alpha_{io}}$$

The extrapolated parameter values are obtained from

$$\alpha_i(t) = \alpha_{io} + \delta\alpha_i(t)$$

where the increments $\delta\alpha_i(t)$ are calculated using a steepest descent method. Note that the computation of u_{io} is theoretically exact since the model parameters are held fixed at their initial values.

Using the first two terms of the expansion for z yields the first-order extrapolation

$$z_1 = z_o + \sum_i u_{io}\,\delta\alpha_i$$

The corresponding first-order extrapolation for the model matching error is

$$\varepsilon_1 = z_1 - y = \varepsilon_o + \sum_i u_{io}\,\delta\alpha_i$$

where $\varepsilon_o = z_o - y$

If the square law criterion function

$$f = \tfrac{1}{2}\varepsilon_1^{\,2}$$

is used, then the method of steepest descent can be used to compute the parameter increments $\delta\alpha_i$ which minimize f. The required equations are

$$\frac{d}{dt}(\delta\alpha_i) = -k\frac{\partial f}{\partial(\delta\alpha_i)} \quad , \quad i = 1,2,\ldots n.$$

The gradient components may be evaluated as

$$\frac{\partial f}{\partial(\delta\alpha_i)} = \varepsilon_1 \frac{\partial \varepsilon_1}{\partial(\delta\alpha_i)} = \varepsilon_1 u_{io}$$

assuming that cross-coupling terms are zero. Consequently the quantity $\delta\alpha_i(t)$ may be evaluated from the integral equation

$$\delta\alpha_i(t) = -k\int_{t_o}^{t_o+t} \varepsilon_1 u_{io} d\tau \qquad (4.6)$$

The integration shown in Equation 4.6 may be performed until $\delta\alpha_i$ reaches a steady state value at which time the initial conditions α_{io} may be updated by the amount $\delta\alpha_i$. Another integration is then performed and the process is repeated iteratively until the steady state value of $\delta\alpha_i$ approaches zero. Figure 4-9 illustrates the analog computation implementation for the case where the system H may be represented by a second-order equation of the same form as discussed in Section 4.2.

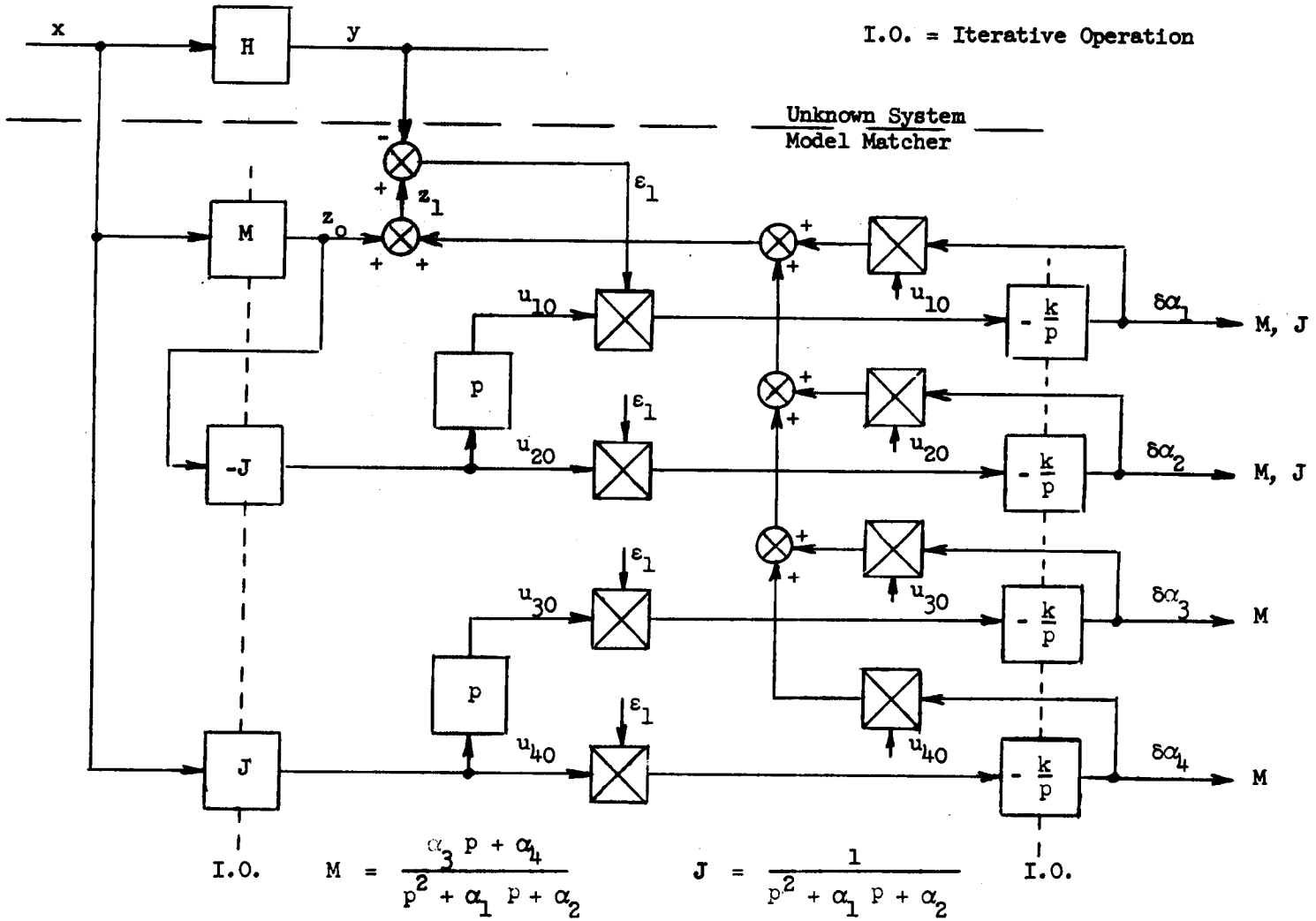

Figure 4-9 The Extrapolation Open Loop Model Matcher $\left(u_i = \frac{\partial z}{\partial \alpha_i}\right)$

4.5 Effect of Excitation Bandwidth on Parameter Identification Accuracy

4.5.1 Introduction

The accuracy of parameter identification of unknown systems by a model matching technique is primarily determined by the frequency bandwidth of the excitation signal. Inadequate excitation bandwidth generally results in poor parameter identification accuracy. A bandwidth study was performed on the model matching techniques described in Sections 4.2 through 4.4 to obtain a quantitative measure of the degradation in system identification accuracy due to insufficient excitation bandwidth. The secondary consideration in the study was a comparison of the different model matching techniques with the ultimate goal being the selection of an optimum technique.

4.5.2 Procedure

The study was performed by identifying the parameters of a second-order linear system with known parameters. Band-limited white noise was used as the excitation signal to the system. This signal was obtained by filtering the output of a gaussian noise generator with a third-order filter of the form

$$F(s) = \frac{K_1 \omega_f^3}{(s + \omega_f)(s^2 + 0.8\ \omega_f s + \omega_f^2)}$$

Filter cutoff frequencies, ω_f, of 20, 3 and 0.4 rad/sec were used in the study. The study was conducted using the the systems A and B whose transfer functions and Bode diagrams are shown in Figure 4-10. The transfer functions of system A and B were chosen to approximate typical human describing functions obtained in modeling human tracking response. Continuous, iterative and extrapolation model matching techniques were evaluated. Both open and closed loop formulations were used in evaluating the iterative technique. Open loop formulations only were used in investigating the continuous and extrapolation techniques.

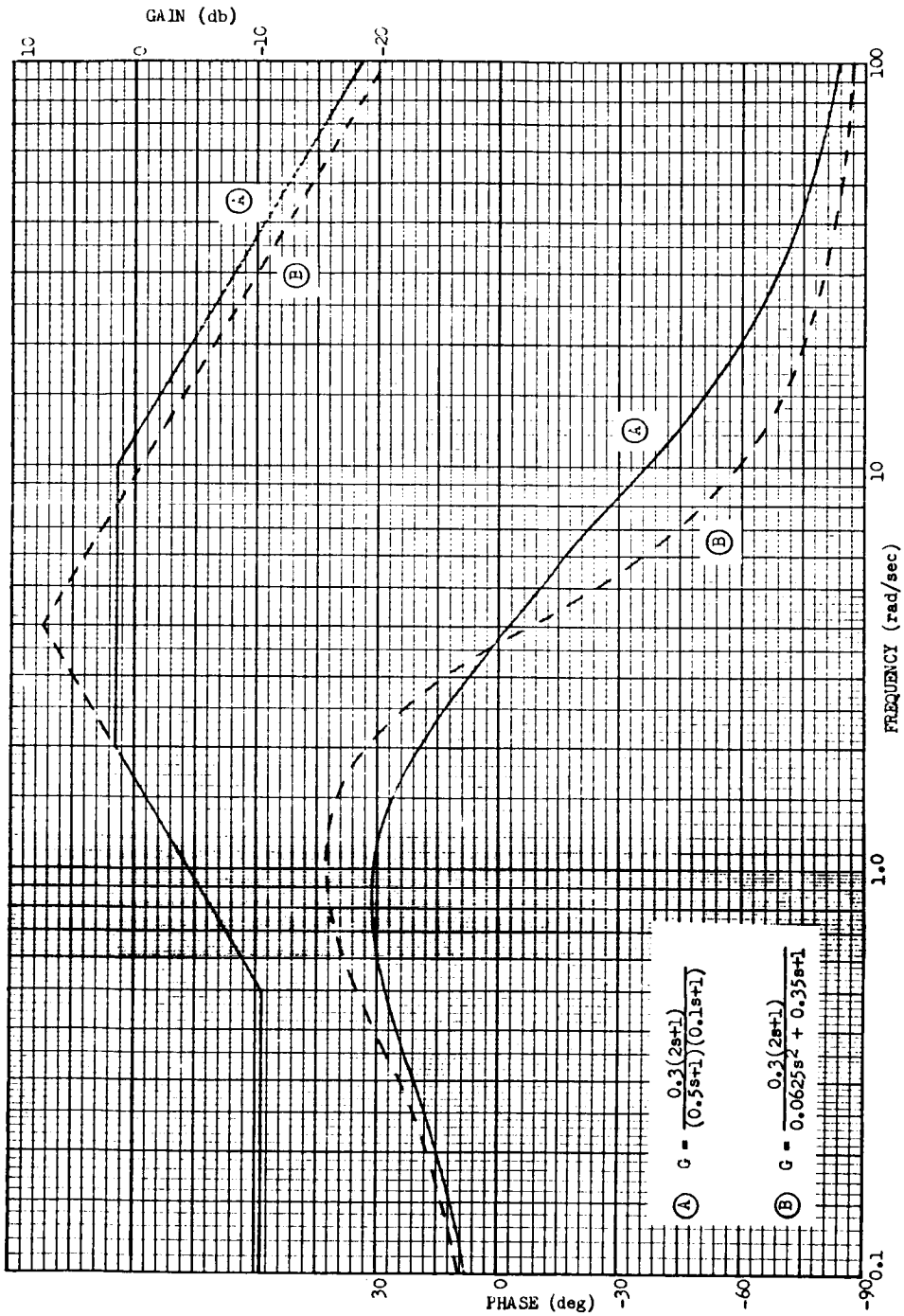

Figure 4-10 Bode Diagrams for Systems A and B

4.5.3 The Continuous Technique

The continuous technique described in Section 4.2 was implemented on an analog computer in an open loop formulation and used to model the known systems A and B. The modified error criterion function was used. Use of unequal parameter adjustment gains k_i substantially decreased the convergence time. That is, the parameter adjustment rates were equalized by increasing the adjustment gain of the less sensitive parameters. Parameter convergence rates are analytically treated in Reference 12. Table 4-1 lists the operational constants used for the continuous technique where these constants were chosen to yield the optimum convergence time. Initial conditions for the parameters α_1 through α_4 were 10, 20, 4 and 4 respectively.

Table 4-1

Operational Constants for the Continuous Technique

		System A			System B		
Input Bandwidth (rad/sec)		20	3	0.4	20	3	0.4
Adjustment Gains	k_1	8	2	4	2	0.5	4
	k_2	40	4	8	10	1.0	8
	k_3	20	40	10	5	10	20
	k_4	100	40	10	25	10	20
Limit on Error Term $\dot{\varepsilon} + q\varepsilon$		10					
Error Rate Gain	q	0.5 sec					

Each system was identified twice for each excitation frequency and the model parameters measured at the end of the model matching run. The α parameters were then averaged and converted to transfer function form. Percentage errors were calculated and these are tabulated in Table 4-2. In general the overall identification accuracy increased as the excitation bandwidth increased. The accuracy of the zero frequency gain parameter K was least affected

Table 4-2 Percentage Modeling Errors for the Continuous, Iterative and Extrapolation Techniques

	System	ω_f	%K	$\%T_1$	$\%\omega_n$	$\%\zeta$	$\mathcal{F}$	Run Length (Minutes)
Continuous Open Loop	A	20	+1.3	-1.5	+0.9	+3.0	3.7	5
		3	-0.3	-1.0	-0.7	-5.2	5.4	5
		0.4	+0.7	-11.5	-11.6	-40.3	43.5	5
	B	20	+0.7	+1.5	-0.8	-3.0	3.5	5
		3	0.0	0.0	+0.3	-5.6	5.6	5
		0.4	-1.0	-0.5	+1.3	-10.7	10.8	5
Iterative Finite Difference Open Loop	A	20	+4.0	-8.5	+1.1	-4.5	10.5	4
		3	-3.3	+8.5	+7.8	+14.9	19.1	3.5
	B	20	-2.3	+1.5	+2.5	-1.1	3.9	4
		3	-1.3	+23.0	+15.0	+38.2	47.1	4
Iterative Finite Difference Closed Loop	A	20	+10.7	-16.5	+4.3	-3.0	20.3	4
		3	-40.2	+95.0	-1.6	+30.6	104	6
	B	20	+15.3	+3.0	-0.5	+11.1	19.2	6
		3	parameters would not converge					-
Iterative Influence Coefficient Open Loop	A	20	+0.0	-0.4	+0.3	-0.1	0.5	2
		3	+3.0	-7.0	+0.1	-5.7	9.5	2
	B	20	+8.9	-10.2	+1.3	-0.6	13.6	5
		3	+12.9	+0.2	+1.4	+13.0	18.4	2
Extrapolation Open Loop	A	20	-6.9	+11.5	-1.5	+2.2	13.7	2
		3	+4.6	-5.4	+2.2	+0.5	7.4	2
	B	20	+6.0	-7.6	+1.0	-0.1	9.7	2
		3	+18.8	-29.3	+4.3	-12.5	37.2	2

$$\mathcal{F} = \sqrt{\sum (\text{errors})^2} \text{ in } \%$$

by the change in bandwidth. However the error in the damping ratio parameter ζ increased sharply as the excitation bandwidth was decreased, indicating that there was insufficient energy at the vicinity of the poles to adequately define the damping ratio for low excitation bandwidths. It was concluded that excellent identification accuracy could be obtained if the excitation bandwidth was 20 rad/sec. This bandwidth is beyond the highest break point frequency in the Bode diagrams for systems A and B shown in Figure 4-10.

4.5.4 The Iterative Technique

The iterative technique described in Section 4.3 was experimentally studied by modeling the known systems A and B in both open and closed loop formulations. For this study of the iterative technique, the influence coefficients were computed by a finite difference approximation as discussed in Section 4.3. Unequal parameter adjustment gains k_i were again used to equalize the adjustment rate of the parameters. In addition the maximum parameter correction per iteration was limited to reduce cross-coupling during parameter convergence. Specifically the maximum parameter corrections per iteration were limited to 1, 2, 1, 1 for parameters α_1 through α_4 respectively. Table 4-3 lists the operational constants used for the iterative technique where the constants were chosen to give an optimum convergence time.

An identical experimental procedure to the one described in Section 4.5.1 was used to obtain the identification accuracy of the technique. The identification accuracy of the open loop formulation is comparable to the open loop formulation of the continuous technique as shown in Table 4-2. However, the iterative technique possessed a shorter convergence time.

Table 4-3

Operational Constants for the Iterative Technique

		Open Loop				Closed Loop			
System		A		B		A		B	
Input Bandwidth (rad/sec)		20	3	20	3	20	3	20	3
Parameter Adjustment Gains	k_1	8	8	8	8	28	28	28	10
	k_2	96	48	48	48	168	168	168	60
	k_3	4	4	4	4	14	14	14	4
	k_4	24	24	24	24	84	84	84	30
Parameter Offset	$\Delta\alpha_1$	0.4	0.4	0.4	0.4	0.4	0.4	0.4	0.4
	$\Delta\alpha_2$	2.4	1.2	1.2	1.2	1.2	1.2	1.2	1.2
	$\Delta\alpha_3$	0.2	0.2	0.2	0.2	0.2	0.2	0.2	0.2
	$\Delta\alpha_4$	1.2	1.2	1.2	1.2	1.2	1.2	1.2	1.2
Initial Parameter Values	α_{10}	10	10	10	10	16	16	16	16
	α_{20}	20	20	20	20	32	32	32	32
	α_{30}	4	4	4	4	4	4	4	4
	α_{40}	4	4	4	4	4	4	4	4
Iteration Interval T		1.5 secs				1.5 secs			

In the closed loop formulation, the identification accuracy was much poorer than for the open loop case as shown in Table 4-2. The cause of this inaccuracy may be explained by comparing the system transfer functions of an open and a closed loop system (Figure 4-7). For an open loop system, the system function is

$$\frac{y}{x} = H$$

while for the corresponding closed loop system, the system function is

$$\frac{y}{r} = \frac{H}{1 + GH}$$

In considering the frequency response for those frequencies for which the magnitude of GH is significantly less than unity, the transfer function will be approximately

$$\frac{y}{r} = H$$

which is the open loop transfer function. For those frequencies for which the magnitude of GH is significantly greater than unity, however, the transfer function will be approximated by

$$\frac{y}{r} = \frac{H}{GH} = \frac{1}{G}$$

This function gives no information about the nature of H, the system which is to be determined. Consequently H may only be determined accurately when the magnitude of GH is significantly less than unity.

For the closed loop system studied, the plant system function was

$$G(s) = \frac{5.2}{s(0.3s + 1)}$$

Thus, for low frequencies the magnitude of GH will be greater than unity, and for high frequencies, less than unity. For typical human responses the crossover frequency is about 4 rad/sec. It is to be concluded that the low frequency parameters, K and T_1, cannot be accurately determined by the closed loop method. The computer results in Table 4-2 indicate that this is the case.

In addition to the accuracy problem discussed above, the closed loop method also has the disadvantage of producing instability in the closed loop of the model and plant dynamics. Instability will result if during the adjustment process the model parameters assume values such that the phase margin becomes negative. This form of instability has frequently been observed in modeling of human data.

The iterative technique utilizing sensitivity equations for true influence coefficient computation was also experimentally studied. This technique is described in Section 4.3 and in this study the open loop formulation was used. Unequal parameter adjustment gains and limiting of the maximum parameter correction per iteration were again employed to optimize the performance of the technique. Operational constants used for this technique are shown in Table 4-4. For the parameters α_1 through α_4 respectively, the initial conditions were 16, 32, 4, 4 and the maximum corrections per iteration were 1, 2, 1, and 1.

Table 4-4

Operational Constants for the Iterative Technique Using True Influence Coefficients

		System A		System B	
Bandwidth Cutoff Frequency (rad/sec)		20	3	20	3
Adjustment Gains	k_1	10	10	5	5
	k_2	200	40	40	20
	k_3	10	10	5	5
	k_4	10	10	10	5
Iteration Interval		1.5 sec			

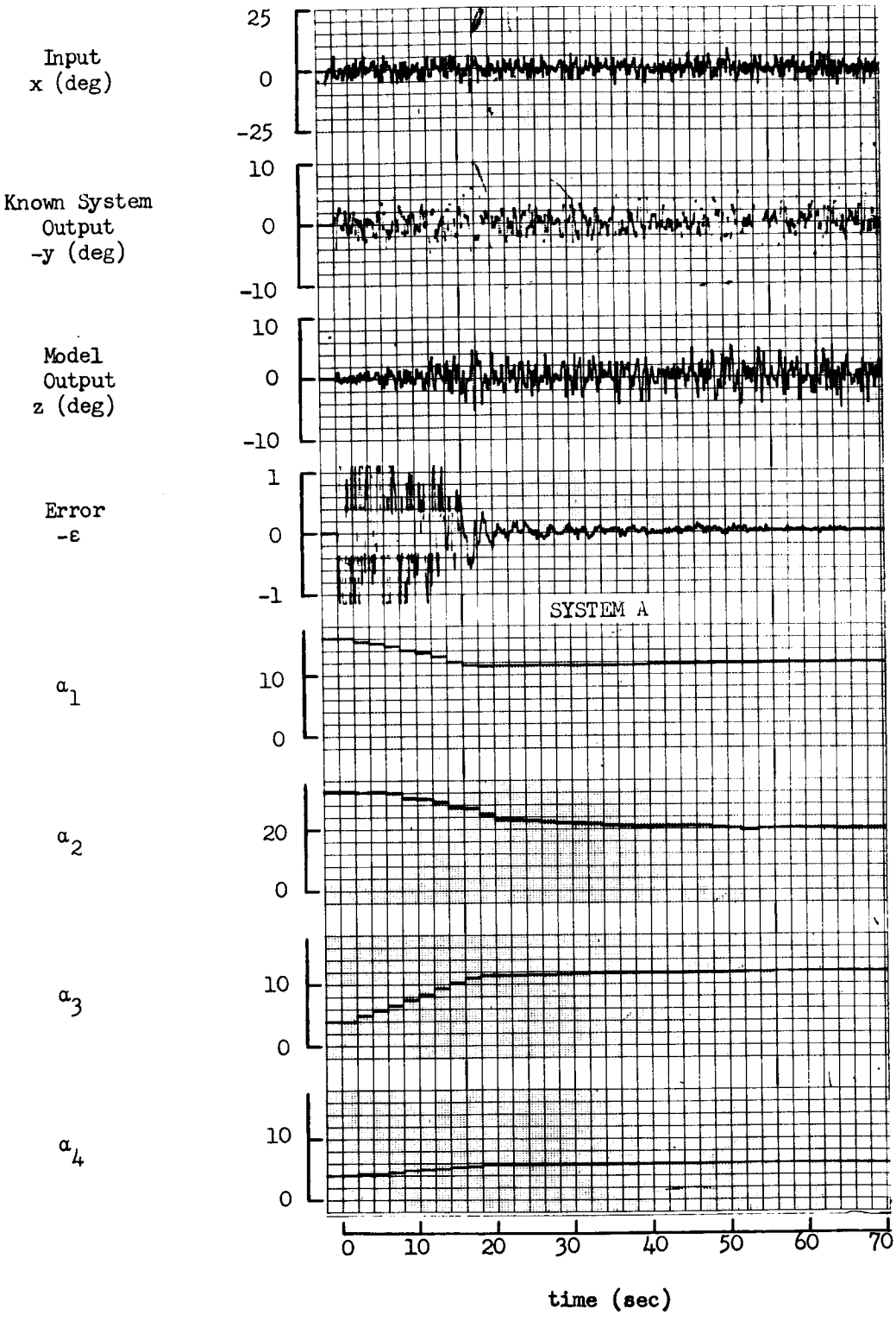

Figure 4-11 Typical Parameter Time History for the Open Loop Iterative Technique Using True Influence Coefficients

The identification accuracy of the technique was determined using the experimental procedure described in Section 4.5.1. Table 4-2 shows that the identification accuracy obtained was excellent. The convergence time was in the order of 30 seconds. A typical parameter time history is shown in Figure 4-11.

4.5.5 The Extrapolation Technique

The extrapolation technique as described in Section 4.4 was formulated in an open loop manner and experimentally studied using the known systems A and B. Unequal parameter adjustment gains were used to equalize the adjustment rates of the parameters. Using the same initial conditions as in the tests of the iterative technique resulted in an unstable set of parameter corrections $\delta\alpha_i$. However if the initial conditions were sufficiently close to the true parameter values such that an accurate extrapolation could be performed, then stable parameter corrections $\delta\alpha_i$ were obtained. Consequently the technique was studied by using the same initial conditions as for the iterative technique but limiting the computation interval to 5 seconds to maintain stability. Operational constants used in studying the technique are shown in Table 4-5. The initial conditions of the parameters α_1 through α_4 were 16, 32, 4 and 4 respectively.

Table 4-5

Operational Constants for the Extrapolation Technique

		System A		System B	
Bandwidth Cutoff Frequency (rad/sec)		20	3	20	3
Adjustment Gains	k_1	50	40	50	20
	k_2	400	400	400	80
	k_3	50	40	50	10
	k_4	50	40	50	10
Iteration Interval		5 sec.			

The identification accuracy of the technique was determined using the experimental procedure described in Section 4.5.1. Table 4-2 indicated that the identification accuracy was good. A convergence time comparable to the iterative technique using the theoretically exact influence coefficients was obtained.

4.5.6 Closed Loop Model Matching With Prefiltering

In Sections 4.5.3 through 4.5.5 it was shown that the accuracy of system identification was poor if the excitation bandwidth was insufficient. Manual tracking systems are commonly analyzed using disturbance functions consisting of a very narrow primary spectrum whose level is much greater than the level of a much wider secondary spectrum. Since the narrow primary spectrum is dominant, then the accuracy of system identification will suffer due to insufficient excitation bandwidth. This inaccuracy was measured for a known system using the same excitation signal as was used in the experimental design described in Section 3.3.

The excitation signal shown in Figure 4-12 was generated using a gaussian noise generator and appropriate filters. A known system (System A) with a transfer function similar to that of a human operator was implemented on an analog computer. Using the iterative technique with the finite difference influence coefficient calculation and the excitation signal shown in Figure 4-12, the parameters of System A were identified with the accuracy shown in Table 4-6. These accuracies are unacceptable for model matching. To overcome this dilemma, the excitation bandwidth to the model matcher was increased by prefiltering.

Figure 4-7 of Section 4.3.2 illustrates the basic closed loop concept of model matching. If the input signals to the model matcher are prefiltered by a filter F to increase their bandwidth, then the model matching scheme illustrated in Figure 4-13 results. All operations shown in Figure 4-13 are functions of the differential operator p and all signals indicated are functions of time. The signals y' and z' are related to the disturbance signal r by the following equations

$$y' = Fy = \left(\frac{HF}{1 + HG}\right) r$$

$$z' = \left(\frac{M}{1 + MG}\right) r' = \left(\frac{MF}{1 + MG}\right) r$$

Consequently the model matching error is given by

$$\varepsilon' = z' - y' = \left(\frac{M}{1 + MG} - \frac{H}{1 + HG}\right) Fr$$

Thus model matching may be performed as before since the error ε' approaches zero uniquely as M approaches H, provided of course that the signal Fr is non-zero.

The effect of prefiltering on the system identification accuracy of System A was measured by using the input disturbance r as before. Acceptable identification accuracy was obtained as shown in Table 4-6. Note again that the parameters K and T_1 are the least accurate for the same reasons as given in Section 4.5.4.

Table 4-6

Effect of Prefiltering on Model Matching Accuracy

		Unfiltered Percentage Error	Prefiltered Percentage Error
System Parameters	K	- 104	+ 11.3
	T_1	-1560	- 10.5
	ω_n	- 21	+ 0.7
	ζ	+ 94	- 3

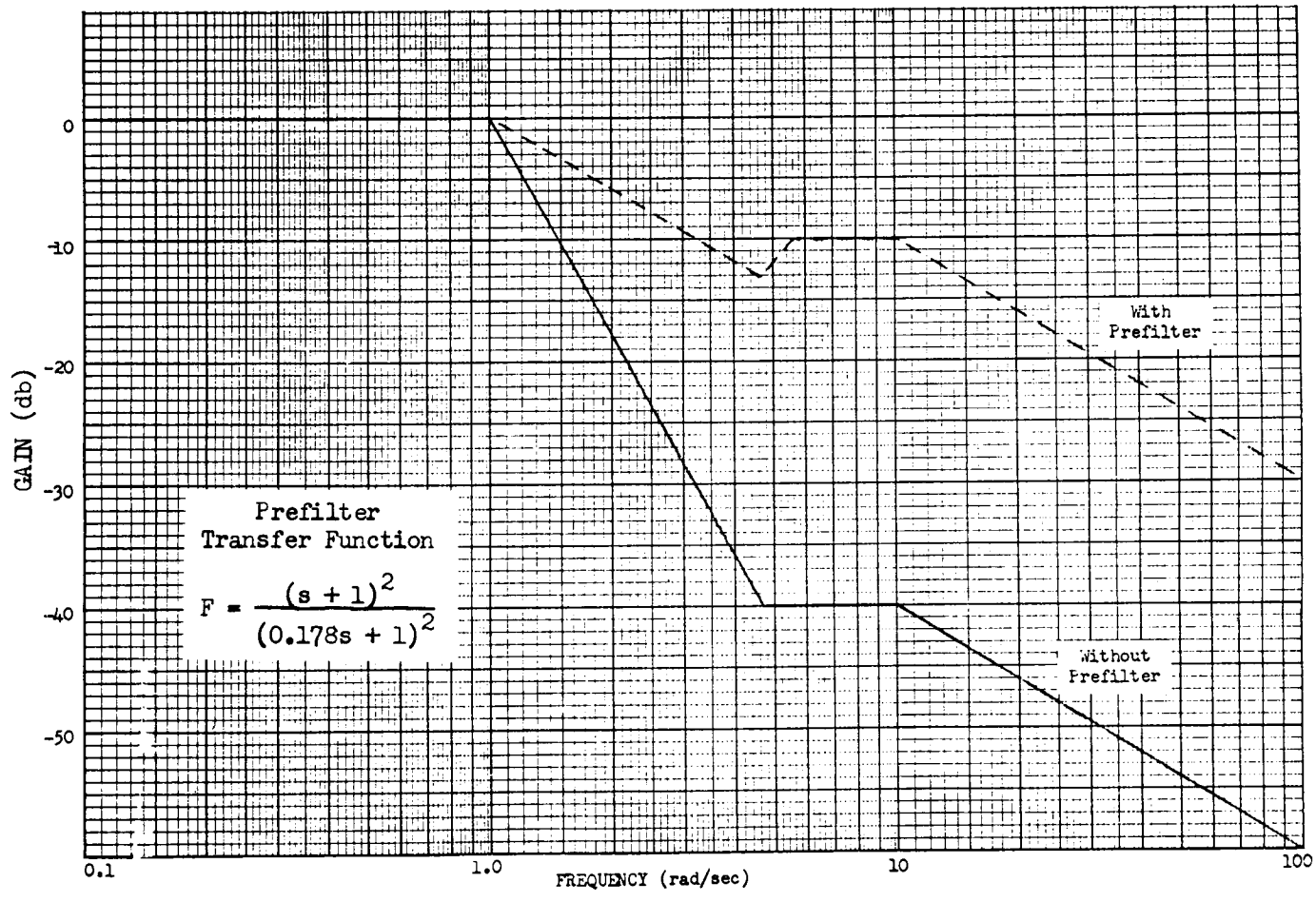

Figure 4-12 Excitation Signal With and Without Prefilter

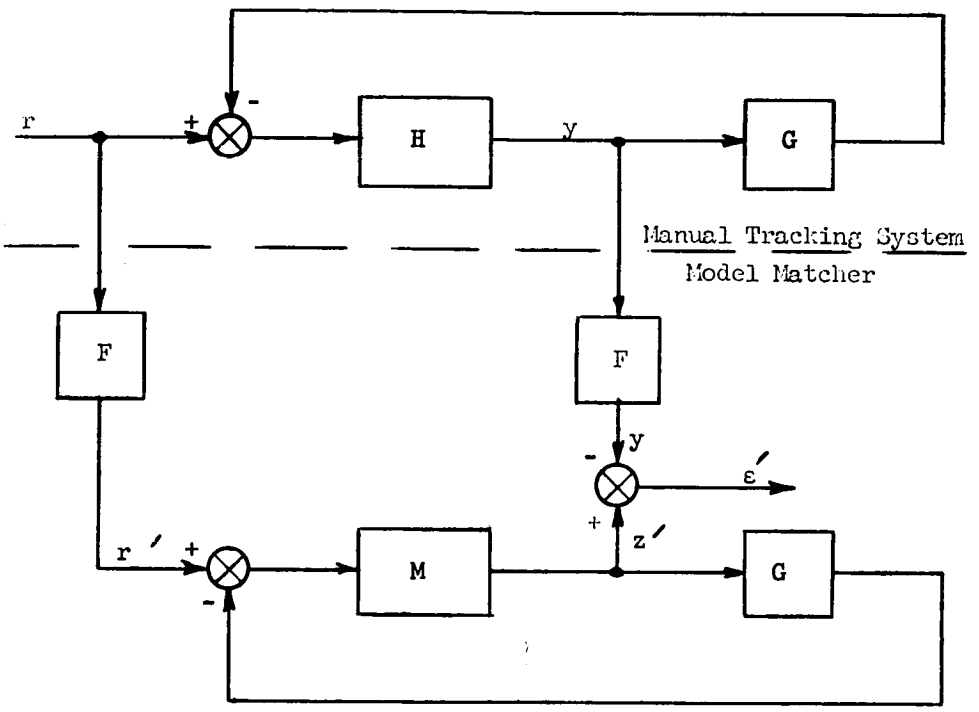

Figure 4-13. Concept of Closed Loop Model Matching with Prefiltering

4.6 Parameter Indeterminacy

4.6.1 Introduction

Parameter indeterminacy difficulties can arise in system identification by model matching techniques. If the excitation signal bandwidth is insufficient or if the system being modeled is actually of lower order than the model, incorrect parameters may be obtained. However, the model obtained will be able to duplicate or match the output of the unknown system and consequently the system identification is unique but the parameter identification is not. Situations where parameter indeterminacy may arise are discussed in the following paragraphs.

4.6.2 Second Order System with Insufficient Excitation Bandwidth

Consider the second order system equation

$$\ddot{y} + a_1\dot{y} + a_2 y = a_3\dot{x} + a_4 x$$

having the transfer function

$$\frac{Y(s)}{X(s)} = \frac{a_3 s + a_4}{s^2 + a_1 s + a_2} \tag{4.7}$$

For input signals of low frequency Equation (4.7) is approximated by

$$\frac{Y(s)}{X(s)} \simeq \frac{a_3 s + a_4}{a_1 s + a_2} \tag{4.8}$$

If the known parameters have values related by

$$\frac{a_3}{a_1} = \frac{a_4}{a_2} = C_1 \tag{4.9}$$

Equation (4.7) simply becomes

$$\frac{Y(s)}{X(s)} = C_1$$

where C_1 is the zero-frequency gain of (4.7).

The corresponding model equation is transformed similarly into

$$\frac{Z}{X}(s) \cong \frac{(\alpha_3 s + \alpha_4)}{(\alpha_1 s + \alpha_2)} \tag{4.10}$$

A set of system parameters which are related in accordance with Equation (4.9) cannot be uniquely identified by model matching because the requirement

$$Z(s) = Y(s)$$

can be satisfied in good approximation by any sets of parameters α_i related by

$$\frac{\alpha_3}{\alpha_1} = \frac{\alpha_4}{\alpha_2} = C_1$$

i.e., the α-parameters will not necessarily be equal to the known a-parameters. For high excitation frequencies the approximations (4.8) and (4.10) are not valid and hence the indeterminacy of parameters α_i will disappear.

Figure 4-14 illustrates a plot of model parameters in the α_1, α_3 plane and in the α_2, α_4 plane. The lines $\alpha_3 = C_1\alpha_1$ and $\alpha_4 = C_1\alpha_2$ are loci of indeterminate parameter pairs. The α_i actually obtained by the computer depend largely on the choice of initial values $\alpha_i(0)$. In practice, even system parameters located in the vicinity of these loci can cause indeterminacy problems on the computer. In the presence of computer noise, a continuous drift of the parameters along the loci, or in their vicinity, is to be anticipated.

4.6.3 Second Order System with Inherent Indeterminacy

Even with sufficient input bandwidth a parameter indeterminacy condition is possible. If the known parameters have values related by

$$a_1 = \frac{a_2 a_3}{a_4} + \frac{a_4}{a_3}$$

Equation (4.7) reduced to

$$\frac{Y(s)}{X(s)} = \frac{a_3}{s + \frac{a_2 a_3}{a_4}}$$

Model matching will only be able to develop the relationships

$$\alpha_3 = a_3$$

$$\frac{\alpha_4}{\alpha_2} = \frac{a_4}{a_2}$$

$$\alpha_1 = \frac{\alpha_2\alpha_3}{\alpha_4} + \frac{\alpha_4}{\alpha_3}$$

Thus, only α_3 may be determined uniquely.

4.6.4 First Order System with Inherent Indeterminacy

A similar problem of parameter indeterminacy can also arise in a first order model matcher. If the system and model equations are given by

$$\dot{y} + b_1 y = b_2\dot{x} + b_3 x$$

$$\dot{z} + \beta_1 z = \beta_2\dot{x} + \beta_3 x$$

having the transfer functions

$$\frac{Y}{X}(s) = \frac{(b_2 s + b_3)}{(s + b_1)}$$

and

$$\frac{Z}{X}(s) = \frac{(\beta_2 s + \beta_3)}{(s + \beta_1)}$$

respectively, parameter indeterminacy will occur in model matching if the system parameters are related by

$$b_2 = \frac{b_3}{b_1} = C_2$$

In this singular case the transfer function is frequency-independent having the gain C_2 at all frequencies.

4.6.5 Excitation with Single Frequency Sinusoid

A parameter indeterminacy will arise in the modeling of any system if the excitation signal is a single frequency sinusoid. For example, if a second order system is being modeled, then only two of the four parameters may be uniquely determined. A complete discussion of this type of indeterminacy may be found in Reference 5.

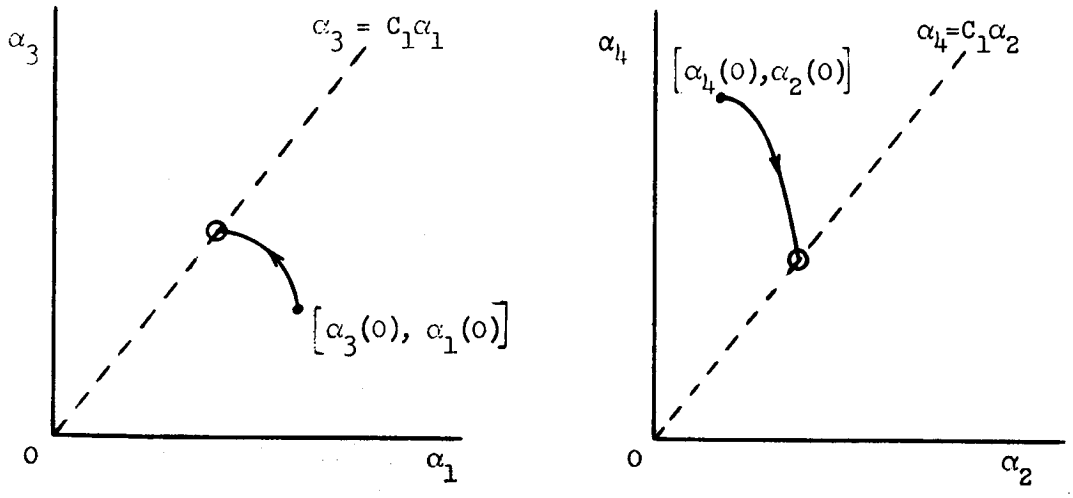

Figure 4-14 Loci of Indeterminate Parameter Pairs in α_1, α_3 and α_2, α_4 Planes

4.7 A Matrix Formulation of the Spectral Technique for the Coupled System

4.7.1 Introduction

Selected portions of the experimental performance data were analyzed using spectral analysis techniques to obtain an independent identification of the human operator's frequency response. Since the spectral technique used in this analysis contains no approximations of the type made in using the iterative model matching technique, then the accuracy of the frequency response obtained will be primarily limited by the number of lag values and data points used in the digital spectral analysis.

4.7.2 The Spectral Analysis

In the two-axis input coupled tracking system shown in Figure 4-15 an asymmetric lattice filter is used to represent the human operator. A spectral analysis is required to uniquely determine each of the four elements of the lattice filter model.

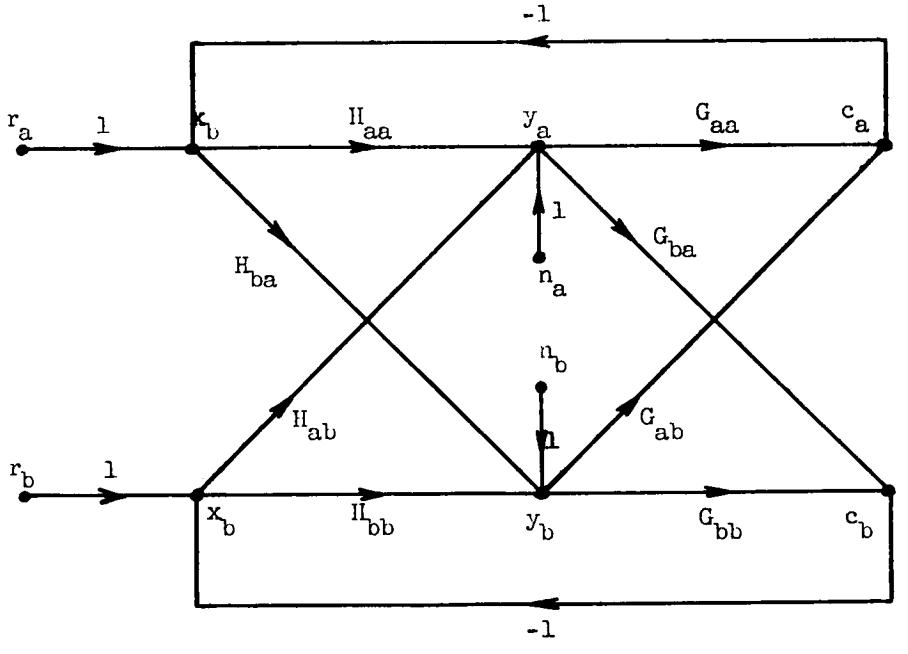

Figure 4-15. Signal Flow Diagram of the Two-axis Input Coupled System

The two-axis system configuration depicted in Figure 4-15 may be simplified by representing the human operator model and the plant dynamics by 2 x 2 matrices as shown below.

$$H = \begin{bmatrix} H_{aa} & H_{ab} \\ H_{ba} & H_{bb} \end{bmatrix} \qquad G = \begin{bmatrix} G_{aa} & G_{ab} \\ G_{ba} & G_{bb} \end{bmatrix}$$

Similarly the signals of the system may be represented by the following vectors:

$$r = \begin{bmatrix} r_a \\ r_b \end{bmatrix} \quad x = \begin{bmatrix} x_a \\ x_b \end{bmatrix} \quad y = \begin{bmatrix} y_a \\ y_b \end{bmatrix} \quad n = \begin{bmatrix} n_a \\ n_b \end{bmatrix} \quad c = \begin{bmatrix} c_a \\ c_b \end{bmatrix}$$

The system shown in Figure 4-15 can now be represented in the simple form shown in Figure 4-16.

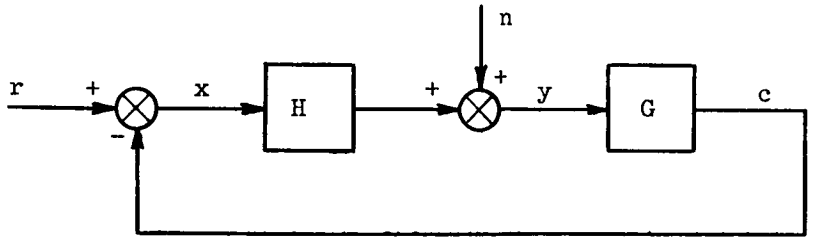

Figure 4-16. The Simplified Two-axis Input Coupled System

It may be shown that the vector x is related to the forcing vectors r and n by the matrix equation

$$x = (I + GH)^{-1}r - (I + GH)^{-1}Gn$$

where I is the identity matrix. The cross spectral density matrix between the vectors x and r can be evaluated as

$$S_{xr} = (I + GH)^{-1}S_{rr} \qquad (4.11)$$

since the vectors n and r are uncorrelated. Solving matrix Equation 4.11 for the matrix H yields

$$H = G^{-1}\left[S_{rr}S_{xr}^{-1} - I\right] \tag{4.12}$$

where

$$S_{rr} = \begin{bmatrix} S_{r_a r_a} & S_{r_a r_b} \\ S_{r_b r_a} & S_{r_b r_b} \end{bmatrix}$$

$$S_{xr} = \begin{bmatrix} S_{x_a r_a} & S_{x_a r_b} \\ S_{x_b r_a} & S_{x_b r_b} \end{bmatrix}$$

Since the spectral matrices S_{rr} and S_{xr} may readily be evaluated from the known vectors r and x, then H may be evaluated without any approximations. Note that this evaluation does not require that the off-diagonal elements of the spectral matrix S_{rr} be zero. The matrix formulation developed above may easily be extended to higher-order systems.

4.7.3 Spectral Program Description

Computation of power spectra of continuous data is performed at TRW Systems by using the IBM 7094 correlation and spectral analysis program. The continuous data must be first digitized and converted into a 7094 compatible format before the spectral analysis program may be run. The analog data records used in the spectral analysis were of 6 minutes duration and were prepared by sequentially recording 1.5 minutes of data obtained in each of the 4 replications for a given task. Only the data in the final performance session was used.

The program evaluates power spectra by first computing the correlation functions and then evaluating their Fourier transforms. Basically, the cross correlation function between two variables x(t) and y(t) is defined by

$$R_{xy}(\tau) = \frac{1}{N} \sum_{n=0}^{N-1} x(nT)y(nT-\tau)$$

where T is the sampling period, N is the total number of data points, and τ is the lag value. Clearly, τ is always equal to an integer number of sampling periods.

The accuracy of the power spectra (and consequently the accuracy of the frequency response) is primarily dependent on the number of lag values and data points used in the analysis. In this analysis the net sampling frequency was 12.5 samples/sec and the number of lag values (m) was 250. The resultant frequency resolution Δf is given by:

$$\Delta f = \frac{1}{2(\Delta t)m} = 0.025 \text{ cps}$$

where Δt is the net sampling period. For 6 minutes of data sampled at a rate of 12.5 samples/sec, the number of data points n is 4500. However, the accuracy of the frequency response is also related to the coherence between the input and output signals (Reference 10). The calculation of the confidence bands on the frequency response is complex since the human operator's coherence is frequency dependent. For illustrative purposes only, the 90% confidence bands on the amplitude ratio and phase were calculated for one task at a frequency of 0.2 cps. At this frequency the coherence between r and y was 0.731 and the resultant frequency response was

$$H(j1.26) = \begin{cases} 0.505 \pm 0.1 \\ -13^{\circ} \pm 12^{\circ} \end{cases}$$

where the amplitude ratio is expressed as a magnitude. A complete evaluation of the confidence bands over the frequency bandwidth of interest was considered to be beyond the scope of this study.

Ideal spectral determination requires that the individual spectra be uniform functions of frequency. Non-uniform spectra were obtained from the human tracking experiment and consequently prewhitening was used to improve the accuracy of the spectral determination.

4.8 Comparison of the Model Matching and Spectral Analysis Techniques

In Section 3.7 approximate human operator models were obtained to describe human performance in a coupled two-axis system using the iterative technique as described in Section 3.4. Since the spectral analysis technique described in Section 4.7 will yield a human operator model without approximations, then this technique was used to check the approximate models obtained. Specifically the average performance of one subject in Task 2 over four replications in the final performance session was checked in this manner.

The iterative technique was used in a closed loop fashion to obtain H_{aa}, H_{bb} and H_{ab}. The describing function H_{ba} was obtained in an open loop manner. Figures 4-17 through 4-24 show the frequency response of the approximate iterative models obtained. For the same data, a set of approximate models was also obtained using a closed loop spectral analysis technique where the describing functions were computed from the equation

$$H_{ij} = \frac{S_{r_j y_i}}{S_{r_j x_j}} \qquad \begin{matrix} i = a, b \\ j = a, b \end{matrix} \tag{4.13}$$

In Equation (4.13) $S_{r_j y_i}$ denotes the cross power density spectrum between the signals r_j and y_i, while H_{ij} represents the required describing function. The frequency responses of the approximate spectral models thus obtained are shown in Figure 4-17 through 4-24.

The approximate models obtained above were compared with theoretically exact models determined by solving the matrix equation

$$H = G^{-1}\left[S_{rr}S_{xr}^{-1} - I\right] \tag{4.14}$$

where the matrices in Equation (4.14) are as defined in Section 4.7.2. Figures 4-17 through 4-24 show the frequency response of the correct spectral models obtained.

In general both approximate models compare favorably with the correct spectral models and consequently the conclusions drawn from the approximate iterative models in Section 3.7 are validated. Large deviations in both the amplitude ratio and phase responses exist above a frequency of 4.0 radians/sec. These deviations are due to the closed loop coherence functions being very small above 4.0 radians/sec. Figure 4-25 shows a typical coherence function $C_{y_b r_a}$ for the describing function H_{ba}. For the describing function H_{ab}, the coherence function $C_{y_a r_b}$ was near zero over the complete frequency range. Since the accuracy of any spectral analysis technique is strongly dependent on the magnitude of the coherence (Reference 10), then large deviations will occur in the amplitude and phase frequency response whenever the coherence is small. In this context the coherence function between two signals x(t) and y(t) is defined by the equation

$$C_{xy}(\omega) = \frac{\left|S_{xy}(j\omega)\right|^2}{S_{xx}(\omega)\, S_{yy}(\omega)}$$

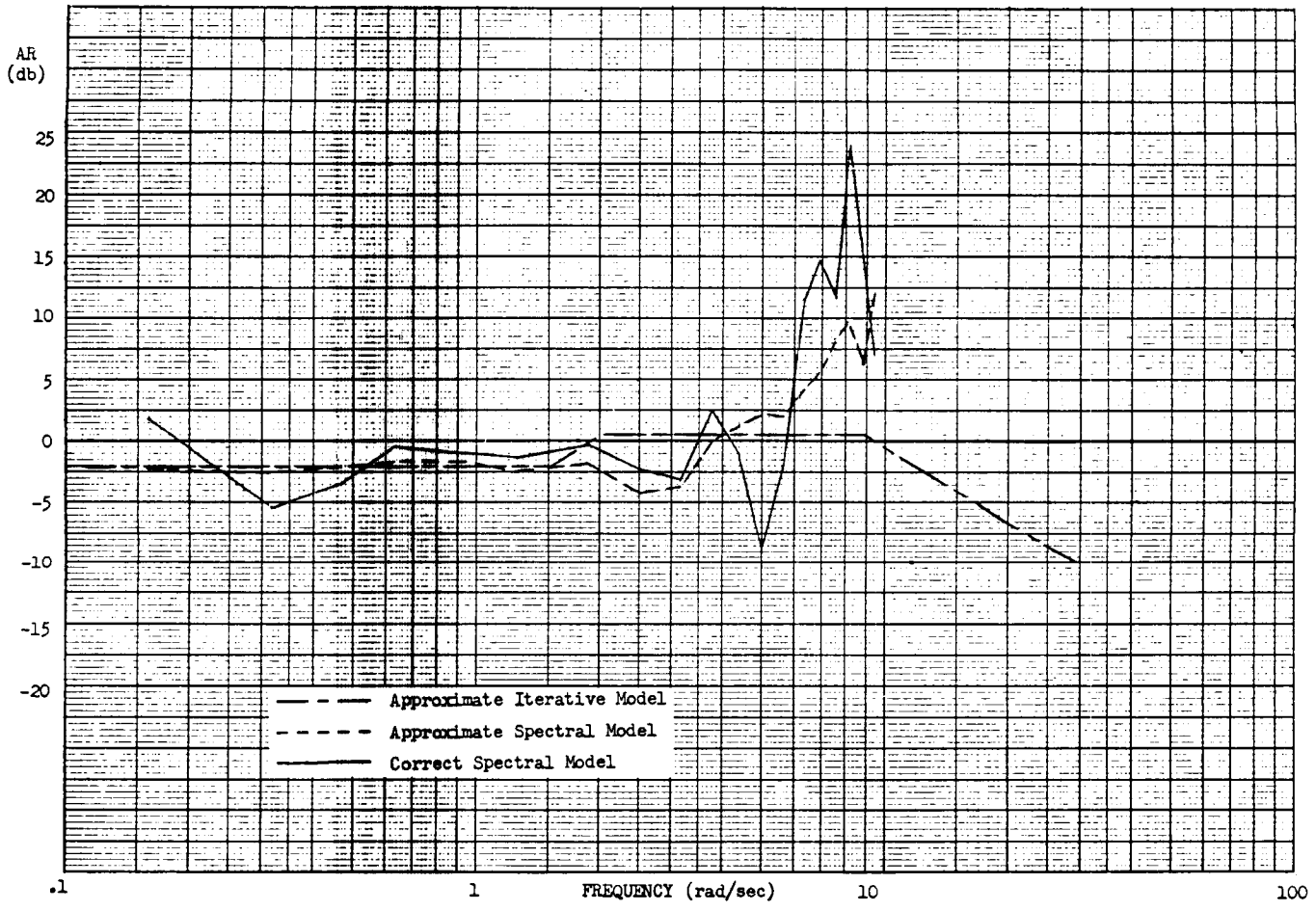

Figure 4-17 Amplitude Ratio Frequency Response (H_{aa})

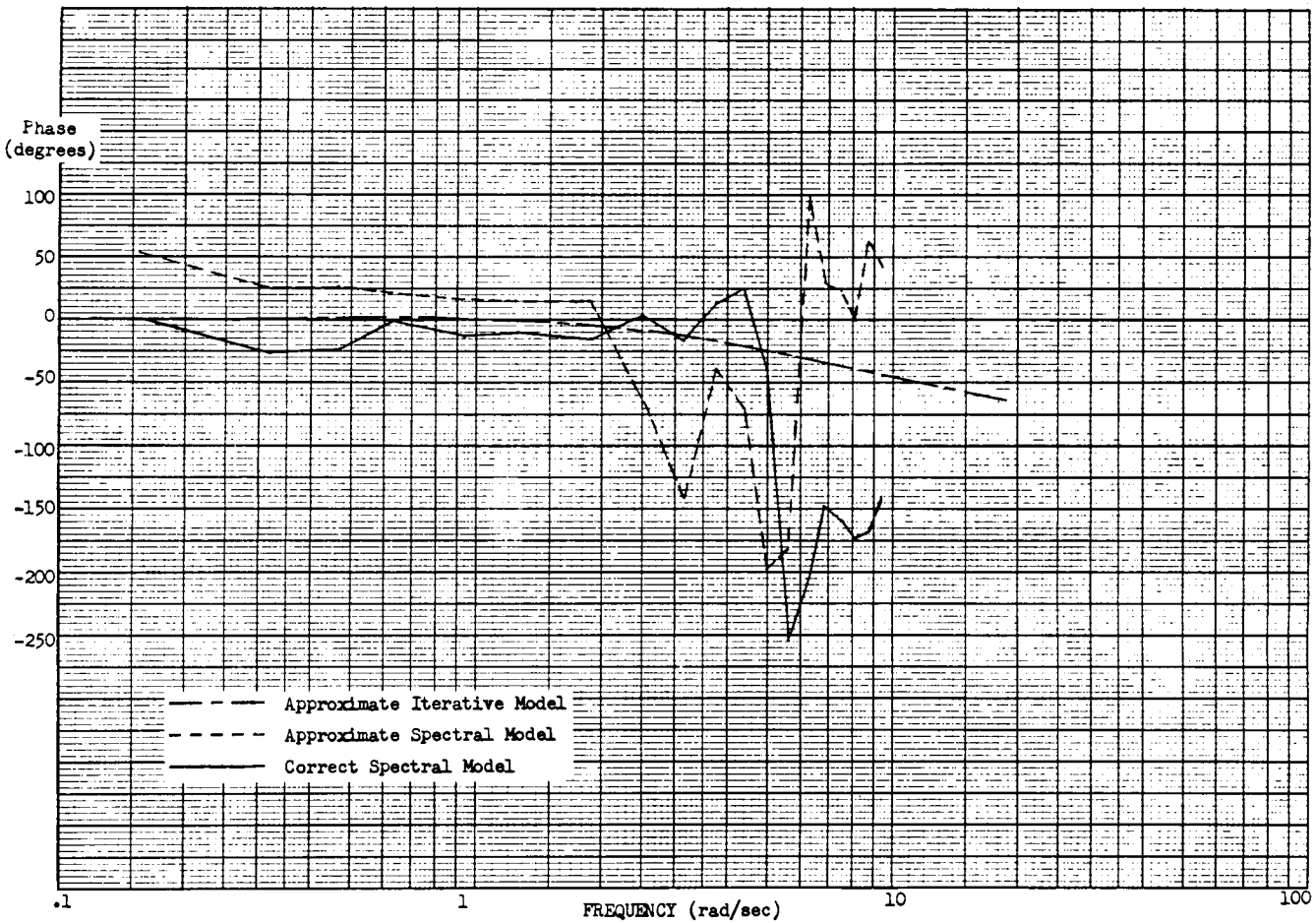

Figure 4-18 Phase Response (H_{aa})

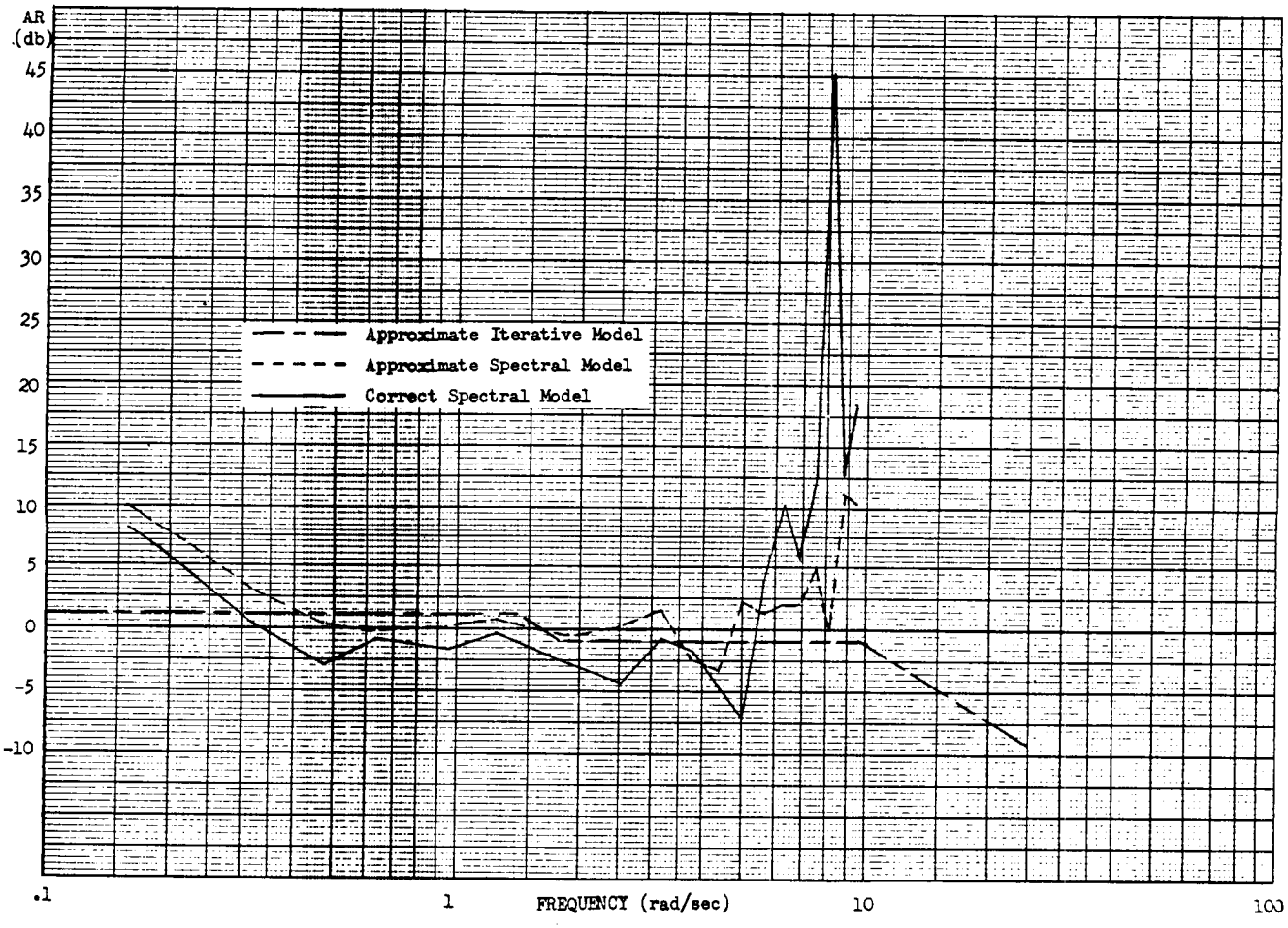

Figure 4-19 Amplitude Ratio Frequency Response (H_{bb})

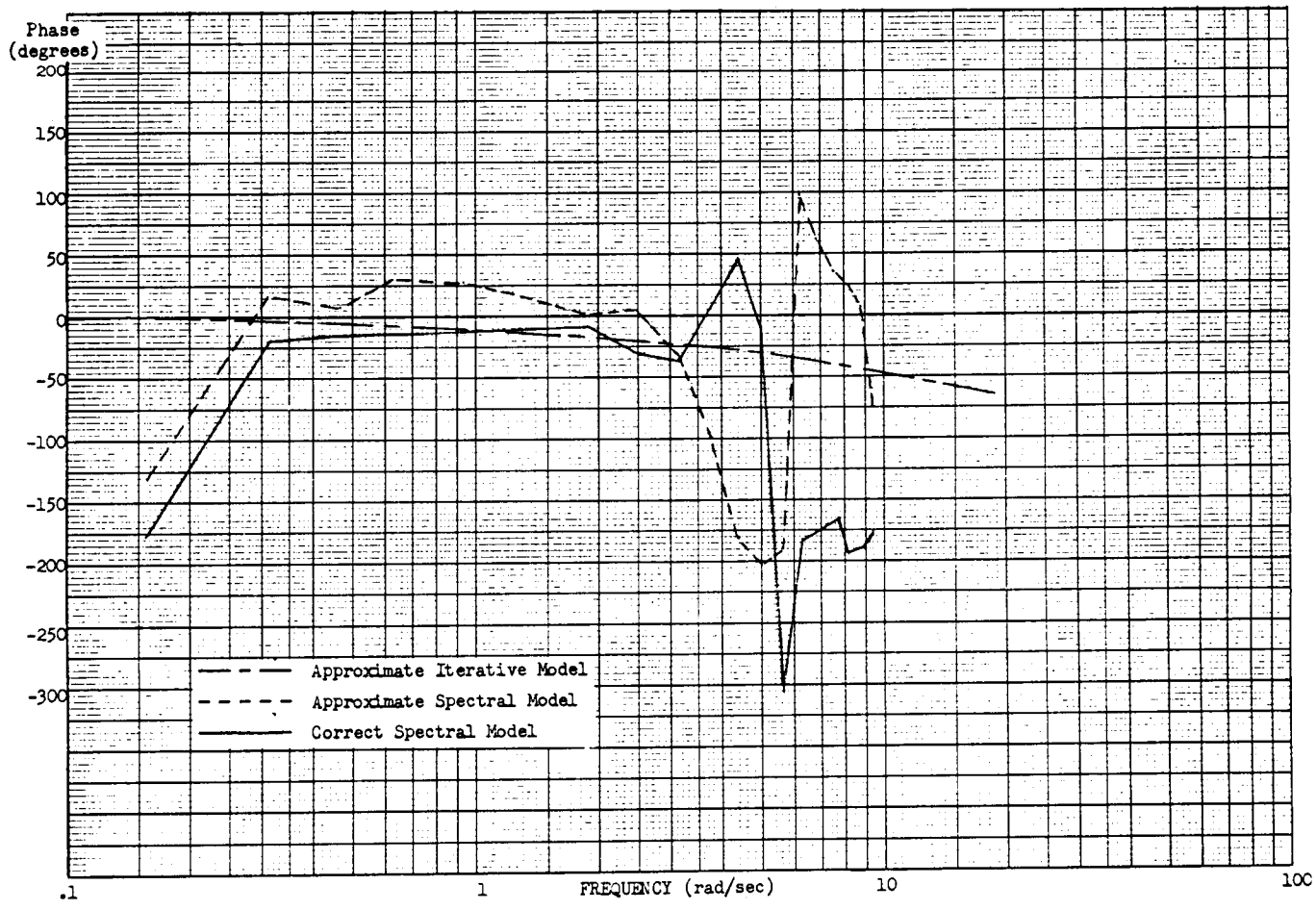

Figure 4-20 Phase Response (H_{bb})

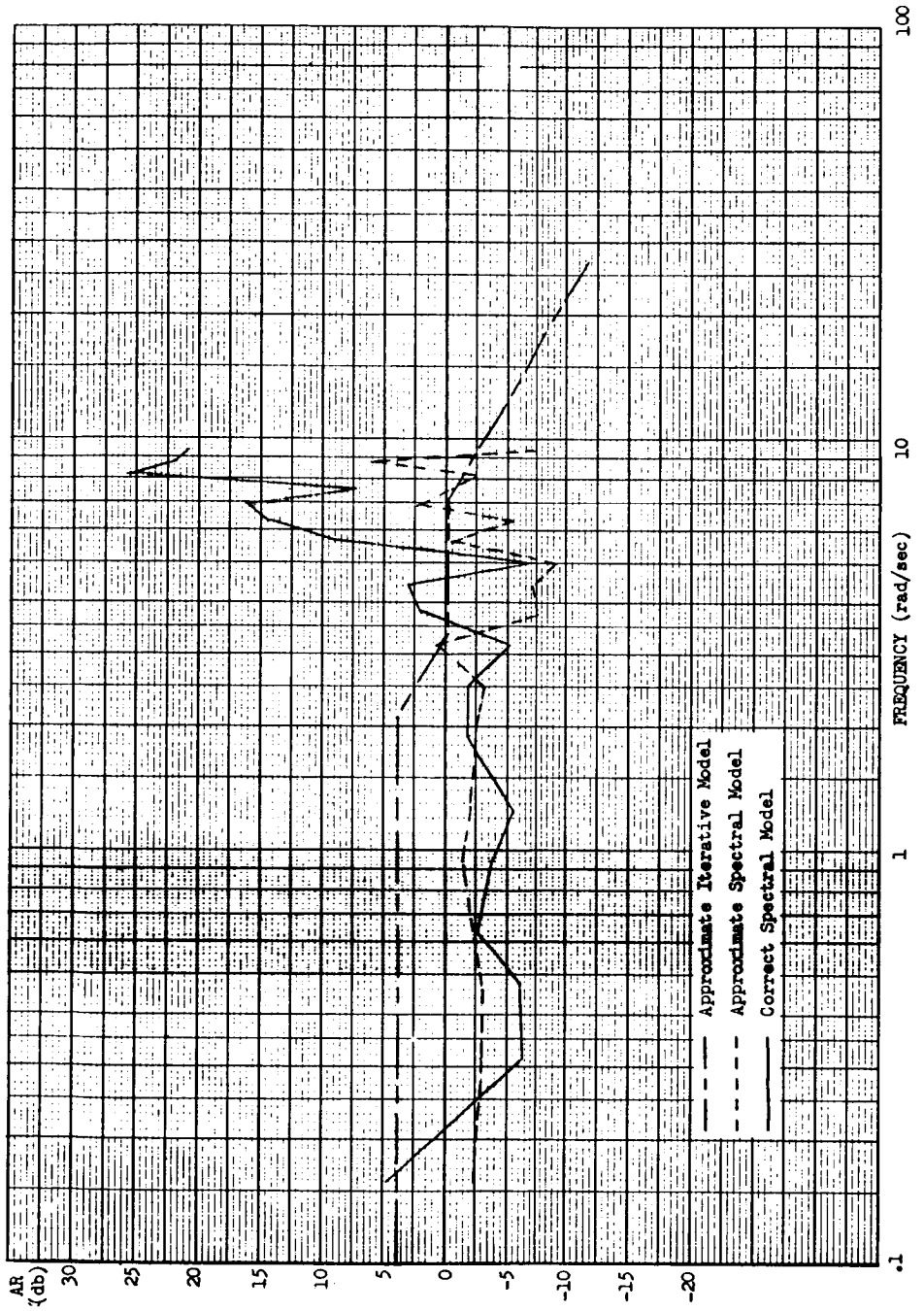

Figure 4-21 Amplitude Ratio Frequency Response (H_{ba})

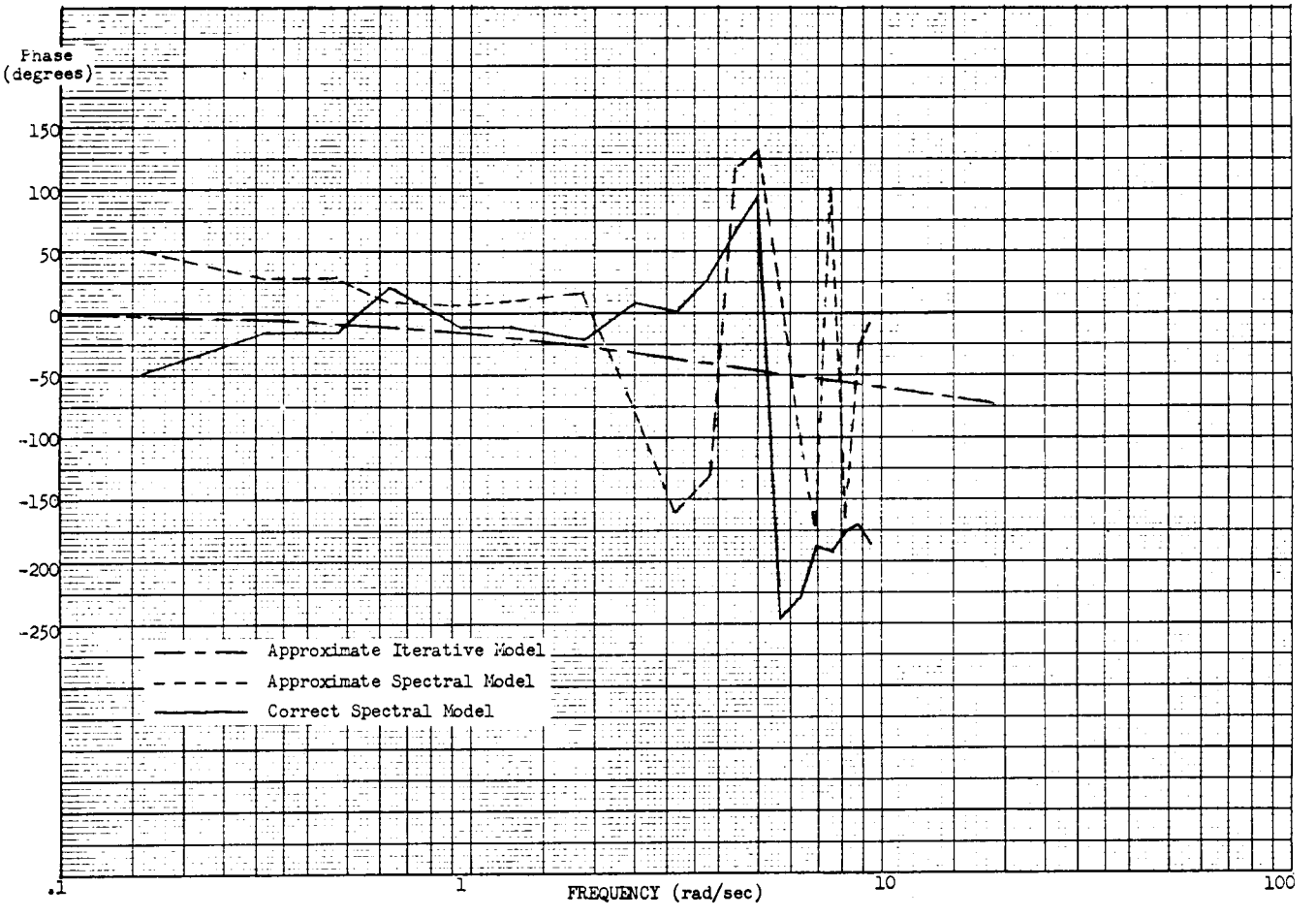

Figure 4-22 Phase Response (H_{ba})

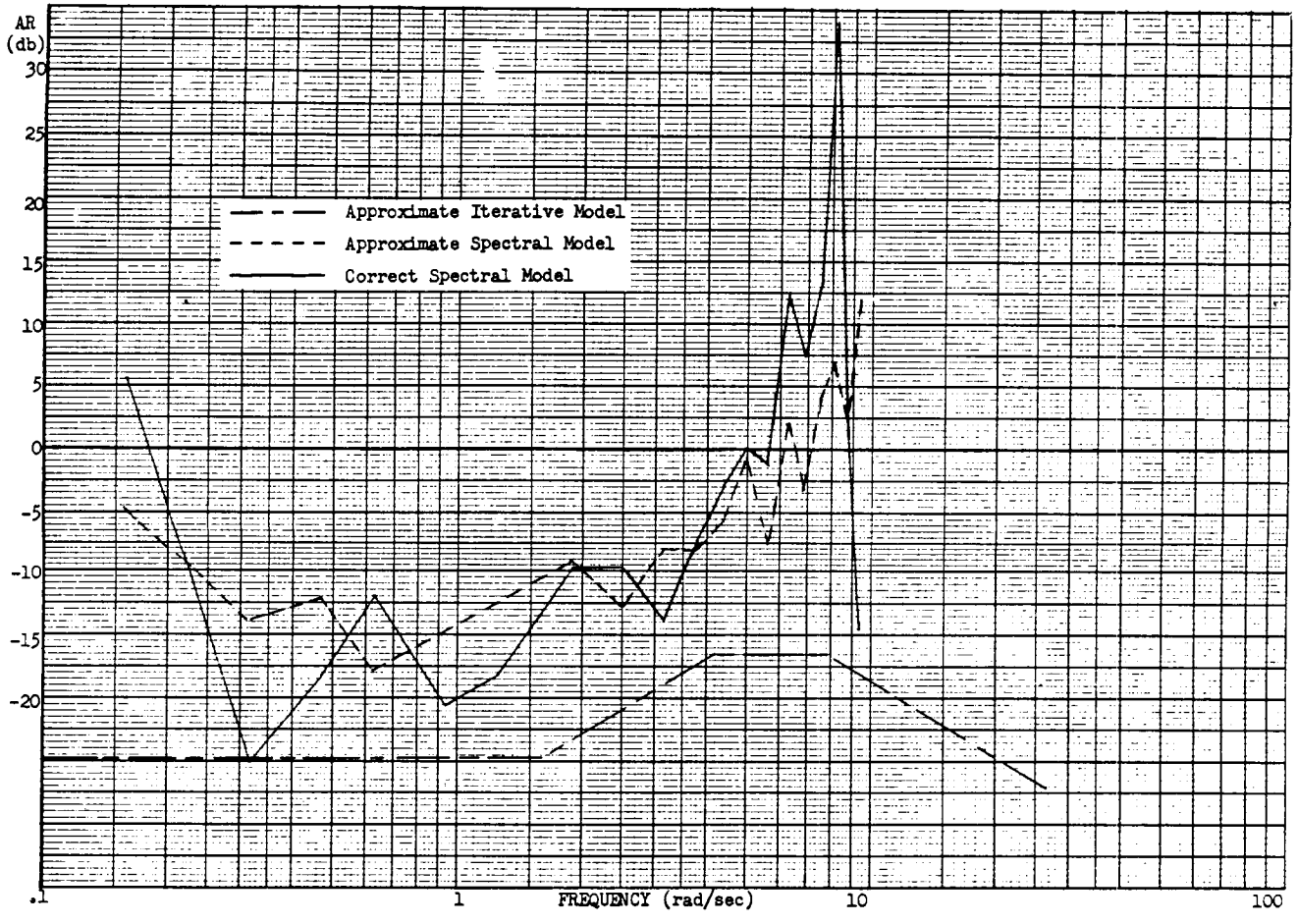

Figure 4-23 Amplitude Ratio Frequency Response (H_{ab})

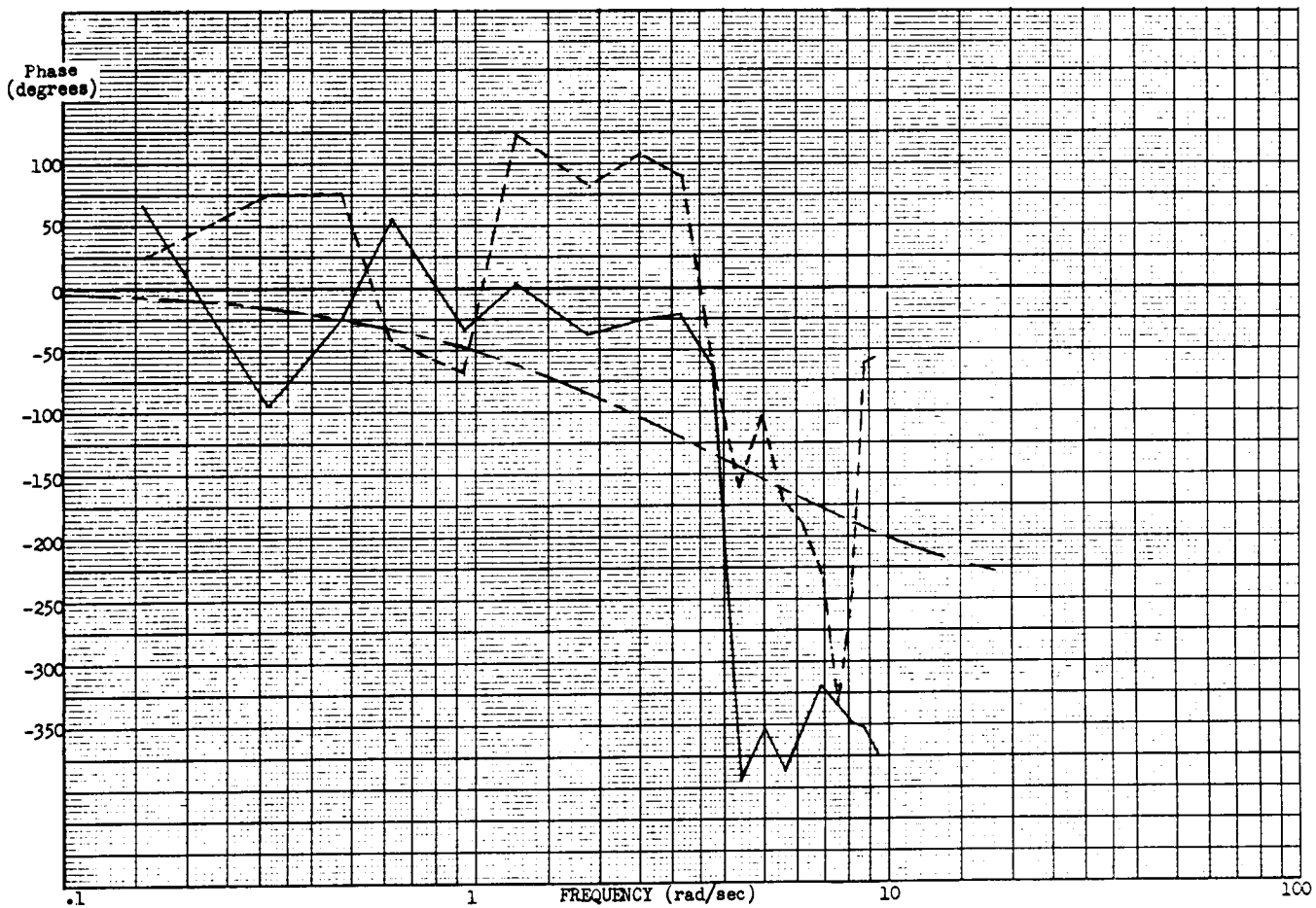

Figure 4-24 Phase Response (H_{ab})

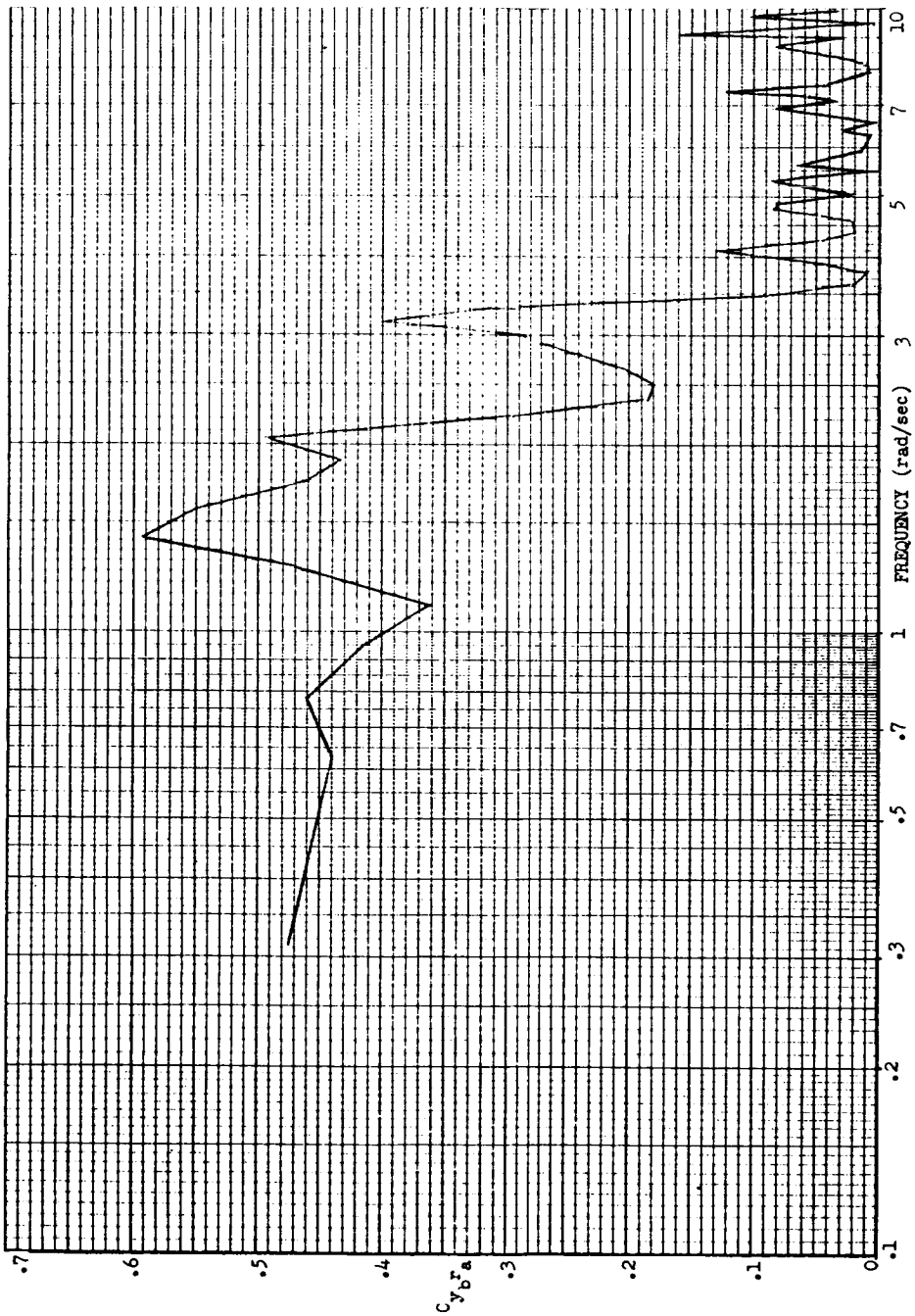

Figure 4-25 A Typical Coherence Function $\left(C_{y_b r_a}\right)$

4.9 Approximate Computation of Human Time Delay

4.9.1 Introduction

One of the major limitations of the model matching methods currently in use is the difficulty encountered in the determination of time delay (reaction time) in human pilot response. Existing methods of implementing the time delay term in the model equation are in general laborious or have extensive equipment requirements. This section of the report describes the experiments performed to evaluate a proposed technique to determine time delay by a first order extrapolation. The proposed method is completely described in Reference 11. A considerable savings in computer equipment requirements is effected since implementation of a time delay term in the computer circuits is not required by this scheme. A brief recapitulation of the method is given in the following paragraphs.

Consider for example the model of the human operator with the input signal delayed τ seconds

$$\dddot{z} + a_1\ddot{z} + a_2\dot{z} = a_3\dot{x}(t-\tau) + a_4x(t-\tau) \tag{4.15}$$

where

- x = input signal to the human operator
- τ = time delay
- z = output of mathematical model
- a_i = model parameters, $i = 1,2,3,4$

The first order extrapolation in the vicinity of $\tau = 0$ yields the equation

$$z_1(t,\tau) = z_0 + \frac{\partial z_0}{\partial \tau}\tau \tag{4.16}$$

(where $z_0 = z_{\tau=0}$) is obtained from

$$\dddot{z}_0 + a_1\ddot{z}_0 + a_2\dot{z}_0 = a_3\dot{x}(t) + a_4x(t) \tag{4.17}$$

The partial derivative $\frac{\partial z_0}{\partial \tau}$ is defined as the influence coefficient u_τ which is obtained from the solution of the equation

$$\ddot{u}_\tau + a_1 \dot{u}_\tau + a_2 u_\tau = - a_3 \ddot{x}(t) - a_4 \dot{x}(t) \tag{4.18}$$

since in the vicinity of $\tau = 0$,

$$\frac{\partial x}{\partial \tau}(t-\tau) \cong - \frac{dx}{dt} = - \dot{x} \tag{4.19}$$

If τ is approximated by the first order extrapolation τ_1, then an improvement should be realized in the model matching accuracy as indicated by the extrapolated error signal

$$\varepsilon_1 = (z_1 - y) = z_0 + \tau_1 u_\tau - y \tag{4.20}$$

where y is the output of the system to be modeled. By using the error squared criterion function

$$f = \tfrac{1}{2} \varepsilon_1^2 \tag{4.21}$$

the approximate steepest descent method yields the following expression for τ_1

$$\dot{\tau}_1 = - k \frac{\partial f}{\partial \tau_1} = - k \varepsilon_1 \frac{\partial \varepsilon_1}{\partial \tau_1} \quad . \tag{4.22}$$

Comparison of Equations 4.17 and 4.18 yields the relationship

$$u_\tau = \frac{\partial z_0}{\partial \tau} \cong - \dot{z}_0 \tag{4.23}$$

in the vicinity of $\tau = 0$.

Equation 4.22 is combined with the definition of ε_1 (Equation 4.20) and Equation 4.23 to give the expression

$$\dot{\tau}_1 = -k \varepsilon_1 u_\tau = + k \varepsilon_1 \dot{z}_0 \tag{4.24}$$

The simultaneous solution of Equations 4.18, 4.20 and 4.23 yields the desired extrapolation approximation. A computer block diagram is shown in Figure 4-26.

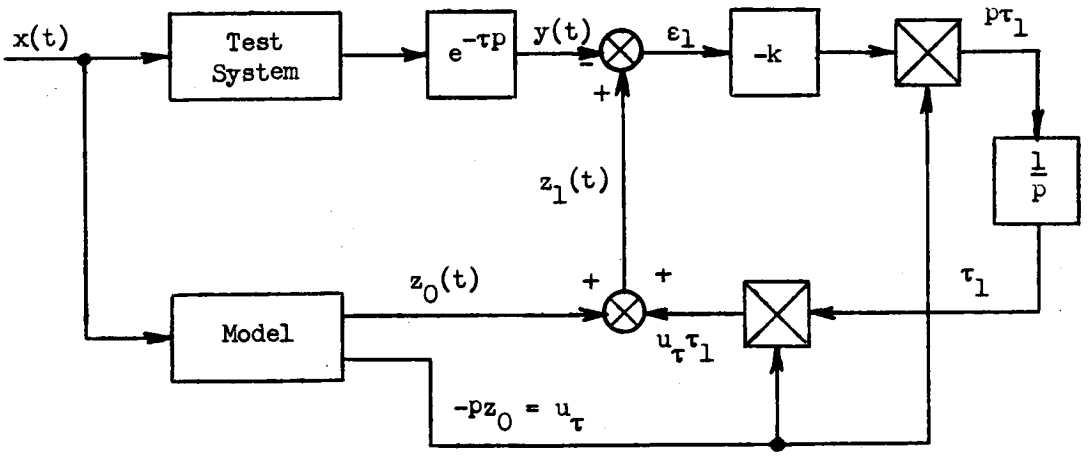

Figure 4-26 Computer Block Diagram for the Determination of τ_1

4.9.2 Experimental Procedure

The approximate computation of the time delay was studied in both an "off" and "on" line sense. In the "off line" case, the τ_1 determination loop operates in an open loop manner as its operation does not influence the value of the model parameters α_i. However in the "on line" case, the τ_1 determination loop does affect the value of the model parameters. For "on line" operation, the extrapolation error signal $\varepsilon_1 = z_1 - y$ is used to determine the α_i parameters rather than the error $\varepsilon = z_0 - y$ used in "off line" operation. The experiments performed to evaluate the τ_1 determination scheme involved the testing of both known systems and human pilot data.

The test configuration was constructed as shown in Figure 4-26. The system to be modeled consisted of the second order differential equation

$$\ddot{y} + a_1\dot{y} + a_2 y = a_3\dot{x}(t-\tau) + a_4 x(t-\tau) \qquad (4.25)$$

where x(t) is a low frequency excitation signal. The pure time delay τ was achieved by the use of a tape recorder delay loop. The model to be obtained was constructed in the form

$$\ddot{z} + \alpha_1 \dot{z} + \alpha_2 z = \alpha_3 \dot{x} + \alpha_4 x \qquad (4.26)$$

No specific allowance for time delay was included in the model. The extrapolation method was expected to indicate the existence of time delay in the system tested without its actual implementation in the model. The experiments for modeling of known systems consisted of continuous "on line" and "off line" operation, as well as iterative "on line" operation. The experiments for modeling of human response were performed using both continuous and iterative "on line" operation.

4.9.3 Results

For the initial test configuration, the α_i parameters of the model were fixed at the values of the corresponding test Equation (4.25) coefficients given in Table 4-7.

Table 4-7
Known System Coefficients

Coefficient	Value
a_1	12
a_2	20
a_3	15
a_4	10
τ	0.4 sec

For this "off line" determination, the resulting value obtained for the extrapolated time delay was $\tau_1 = .331$ sec. For an excitation frequency in the neighborhood of 1.5 rad/sec, the estimated extrapolation error for the technique should be approximately 18% (Reference 11). This agrees closely with the actual error of 20.9% in the value of the time delay obtained.

The "off line" test of the parameter extrapolation was now performed with the α_i parameters adjustable but without the time delay term affecting the model. In all cases, the values of τ_1 obtained were near zero (Table 4-8). It appears that with no feedback to the model from the τ_1 determination loop, the effect of time delay was concealed in the values of the α_i parameters. Since the time delay term was not explicitly included in the model structure, its effect becomes absorbed by the α_i parameters for "off line" operation. These results prompted the "on line" study in which the extrapolated error signal ε_1 replaced the error signal ε for the determination of the α_i parameters. This constituted a feedback signal from the τ_1 determination circuit which would reduce the compensating effect of the "off line" parameter adjustment. However, an improvement in the accuracy of the τ_1 determination was not realized.

Table 4-8

"Off Line" Determination of Known System Parameters

Run No.	α_1	α_2	α_3	α_4	τ_1	x(t)
1	5.1	19.8	-3.0	17.8	0.00	Run 709
2	7.5	18.4	-1.1	17.3	0.01	Run 710
3	8.6	20.4	-1.3	16.9	0.01	Run 711
Values of Known System	12.0	20.0	15.0	10.0	.4	-

In an effort to evaluate the concept of the first order extrapolation and enable the determination of time delay in human systems, an iterative strategy was used. The adjustment loop for the determination of extrapolated τ was disabled. Fixed values of τ_1 were then introduced into the model using the "on line" strategy previously described. For each value of τ_1 selected, the integral of the extrapolated error signal ε_1 and the parameter value α_i were determined over the run length. Figure 4-27 shows that the value of τ could be successfully extracted in this manner for a known system, since the minimum value of the integral of the matching error occurs near $\tau_1 = \tau$. The iterative analysis also demonstrates the compensating effect of the α_i for

terms not included in the model. Figure 4-28 shows this effect. With the time delay term in the model, the α parameters are plotted as a function of fixed values of τ_1. As τ_1 approaches the correct value τ the α_i parameters approach more closely to their corresponding α_i values. The failure of these curves to pass through the correct values of a_i is indicative of the model matching technique inaccuracy discussed in Section 4.5 of this report.

An application of the iterative strategy to human pilot tracking failed to yield a definite value of time delay which would produce a significant improvement in the model. Fixed values of τ_1 were employed with all model parameters varying. The resulting values of the extrapolated error were plotted (Figure 4-29). However the minimum error appeared at $\tau_1 = 0$ and no other well-defined minimum was obtained.

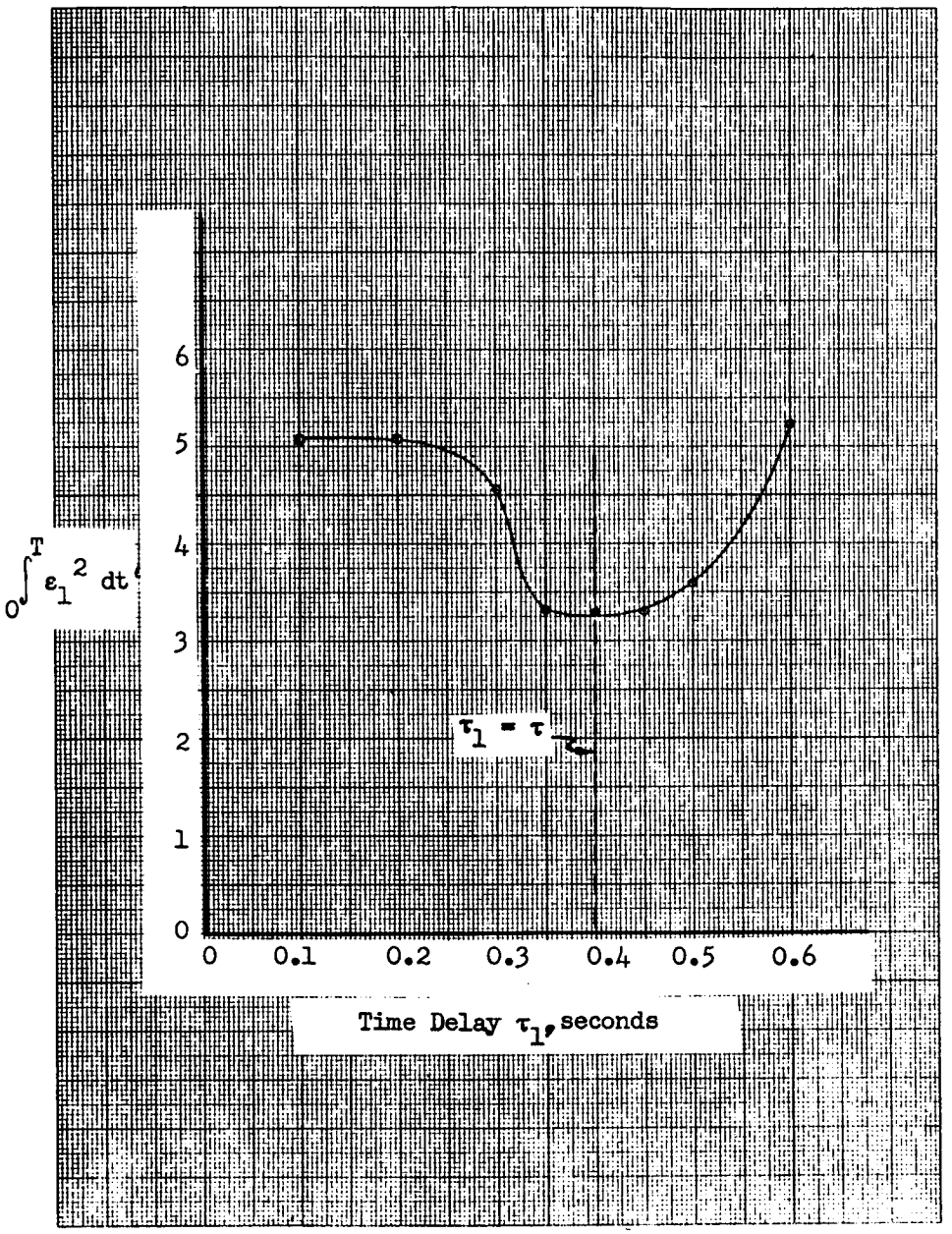

Figure 4-27 Iterative "On Line" Determination of τ_1

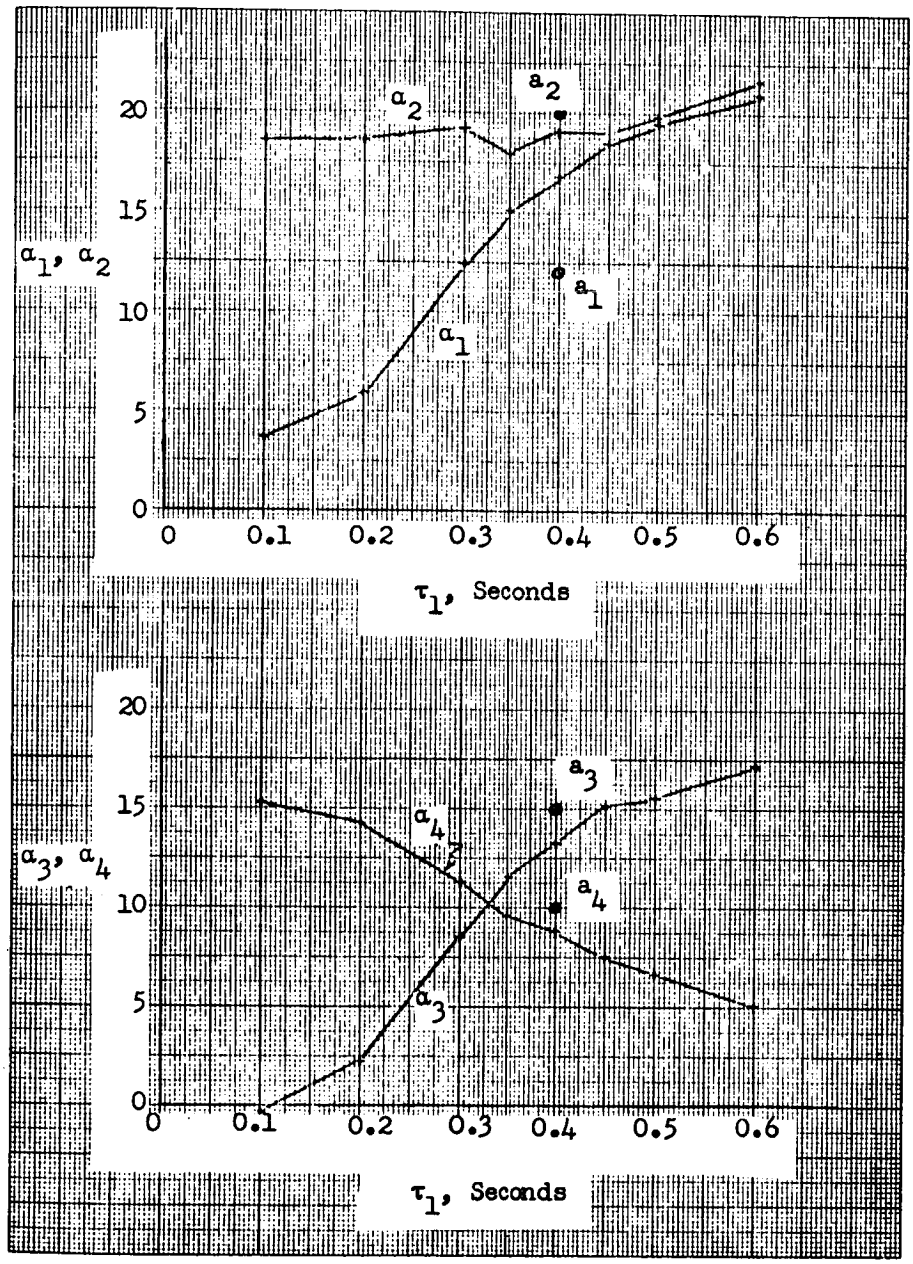

Figure 4-28

Iterative "On Line" Determination of the α_i Parameters

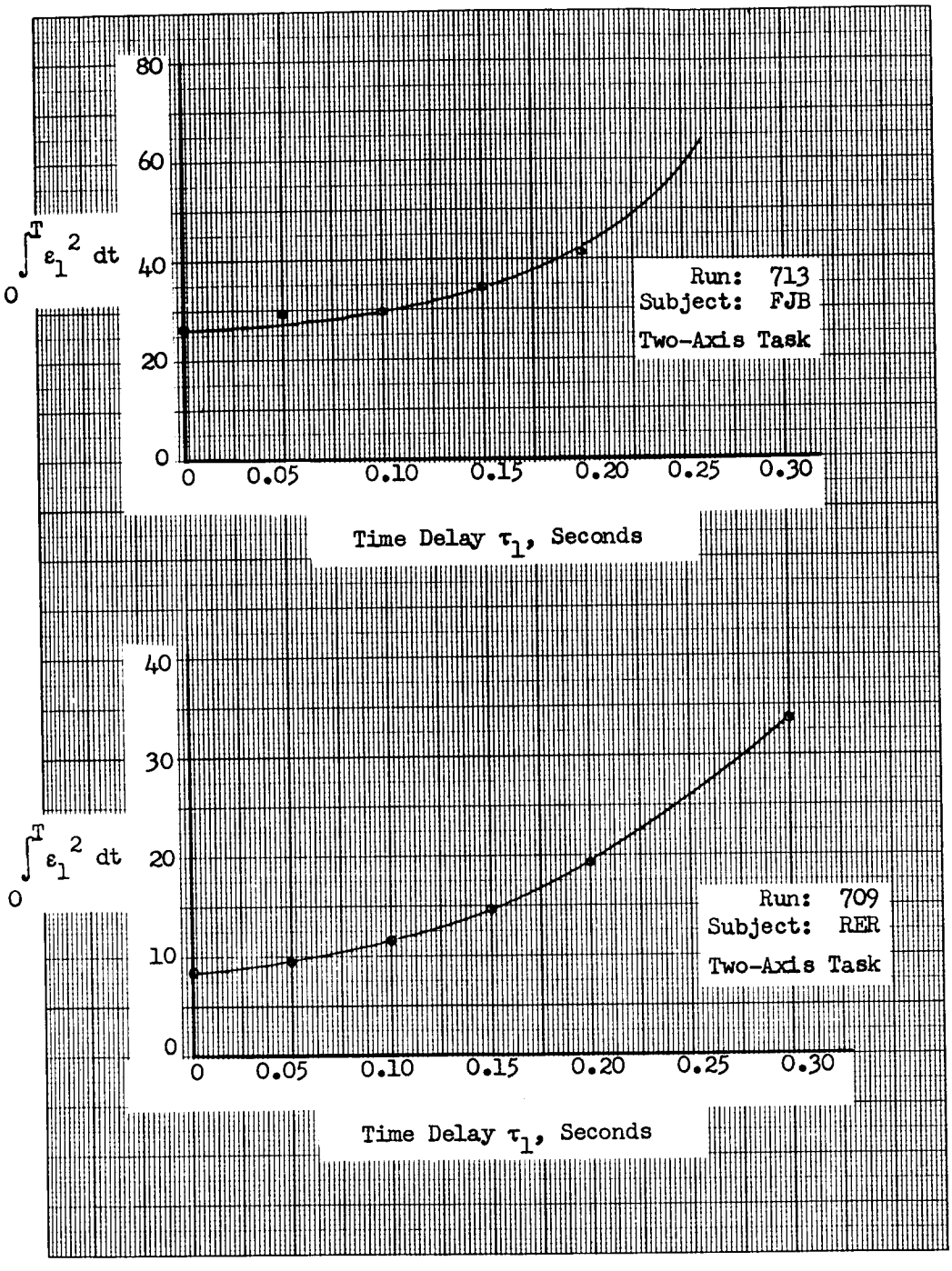

Figure 4-29

Iterative "On Line" Determination of τ_1 for Human Data

4.10 Approximation of Higher Order Model Terms by Extrapolation

4.10.1 Introduction

An approximation technique for parameters associated with higher order terms in the human pilot model was proposed. This scheme resembles the method described for the determination of time delay. This concept has the same analytical basis and form of implementation as the extrapolated approximation of the time delay term. A brief analysis, a comparison with the τ determination method, and a description of the results of test experiments are presented in the following paragraphs.

Consider the example of a third order model of a human pilot

$$\lambda \dddot{z} + \ddot{z} + a_1 \dot{z} + a_2 z = a_3 \dot{x} + a_4 x \qquad (4.27)$$

where λ is a small non-zero parameter. As was the case for the determination of τ, the method of approximation is based on a first order extrapolation in the vicinity of the solution z_0 obtained for $\lambda = 0$:

$$z_1(t,\lambda) = z_0(t) + \frac{\partial z_0}{\partial \lambda} \lambda \qquad (4.28)$$

The effect of λ on the modeling error $\varepsilon = z-y$ is approximated by

$$\varepsilon_1 = z_1 - y = \varepsilon_0 + \frac{\partial z_0}{\partial \lambda} \lambda \qquad (4.29)$$

The term λ can be estimated by an approximate steepest descent optimization by using the equation

$$\dot{\lambda} = - k \frac{\partial f}{\partial \lambda} = -k \varepsilon_1 \frac{\partial \varepsilon_1}{\partial \lambda} = - k \varepsilon_1 u_\lambda \qquad (4.30)$$

where $f = \frac{1}{2}\varepsilon_1^2$ is the error criterion function, $\frac{\partial f}{\partial \lambda}$ is the gradient component, u_λ is the influence coefficient $\frac{\partial z}{\partial \lambda}$, and k is a constant of porportionality. The influence coefficient is obtained by the solution of the equation which results from partial differentiation with respect to λ of Equation 4.27.

$$\lambda \frac{\partial \ddot{z}}{\partial \lambda} + \frac{\partial \dot{z}}{\partial \lambda} + \alpha_1 \frac{\partial \dot{z}}{\partial \lambda} + \alpha_2 \frac{\partial z}{\partial \lambda} = -\ddot{z} \qquad (4.31)$$

Substituting the definition of the influence coefficient, Equation 4.31 becomes

$$\lambda \ddot{u}_\lambda + \dot{u}_\lambda + \alpha_1 \dot{u}_\lambda + a_2 u_\lambda = -\ddot{z} \qquad (4.32)$$

In the vicinity of $\lambda = 0$, Equation 4.32 reduces to

$$\dot{u}_\lambda + \alpha_1 \dot{u}_\lambda + \alpha_2 u_\lambda = -\ddot{z}_0 \qquad (4.33)$$

A comparison of Equation (4.33) and the influence coefficient equation for parameter α_1

$$\ddot{u}_1 + \alpha_1 \dot{u}_1 + \alpha_2 u_1 = -\dot{z}_0 \qquad (4.34)$$

indicates the relationship

$$\dot{u}_1 = u_\lambda \qquad (4.35)$$

A significant equipment savings in the implementation of the λ determination is achieved by the use of Equation 4.35. The computer diagram shown in Figure 4-30 is identical with that employed for the extrapolated time delay τ_1.

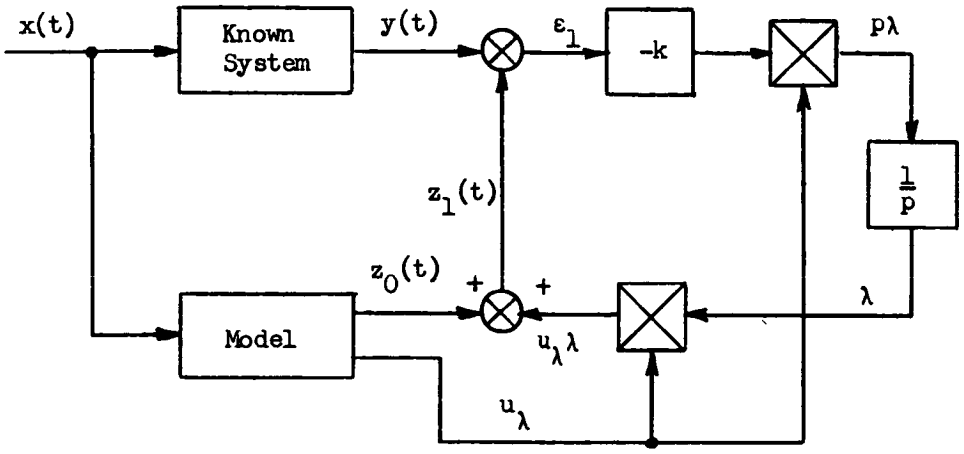

Figure 4-30 Computer Circuit for the Determination of λ

4.10.2 Experimental Procedure and Results

As for the τ_1 determination, experiments were performed on the proposed scheme to evaluate its application to modeling of both a known system and human operator response. "Off line" and "on line" determination of λ was studied for known system responses. The "on line" iterative method previously used for the evaluation of the time delay extrapolation approximation was again used. The results of the known system tests are presented in Table 4-9. The known system employed for test purposes was given by

$$\ddot{y} + \ddot{y} + a_1\dot{y} + a_2 y = a_3\dot{x}(t) + a_4 x(t)$$

where

$a_1 = 12$

$a_2 = 20$

$a_3 = 15$

$a_4 = 10$

ℓ = value shown in Table 4-9

Table 4-9

Determination of Known System Parameters (λ Extrapolation)

Run No.	Model Parameters Obtained					ℓ	
	α_1	α_2	α_3	α_4	λ		
1	12	20	15	10	0.37	0.30	"Off line" α_i fixed at correct values
2	11.9	19.9	15.3	11.2	0.007	0.05	"Off line" α_i adjustment gain K = 2.5
3	12.0	20	15	10	.054	.05	"On line" α_i fixed K = 0
4	11.8	20.8	15.7	12.3	.029	.05	"On line" α_i adjustment gain K = 2.5

The typical results given in the table point out that once again an accurate estimate of extrapolated terms can only be determined when the α_i parameters are fixed at the correct value. Without implementation of the higher order term in the model, the α_i parameters compensate by seeking values other than the corresponding values of the test system.

The experiments on human pilot response data have shown a similar effect. An iterative procedure identical to that employed for time delay determination was used. Figure 4-31, which is a plot of the extrapolated error for various fixed values of λ, shows no well defined minimum other than zero. The existence of a non-zero minimum would indicate an improved model by the inclusion of this higher order term in the model.

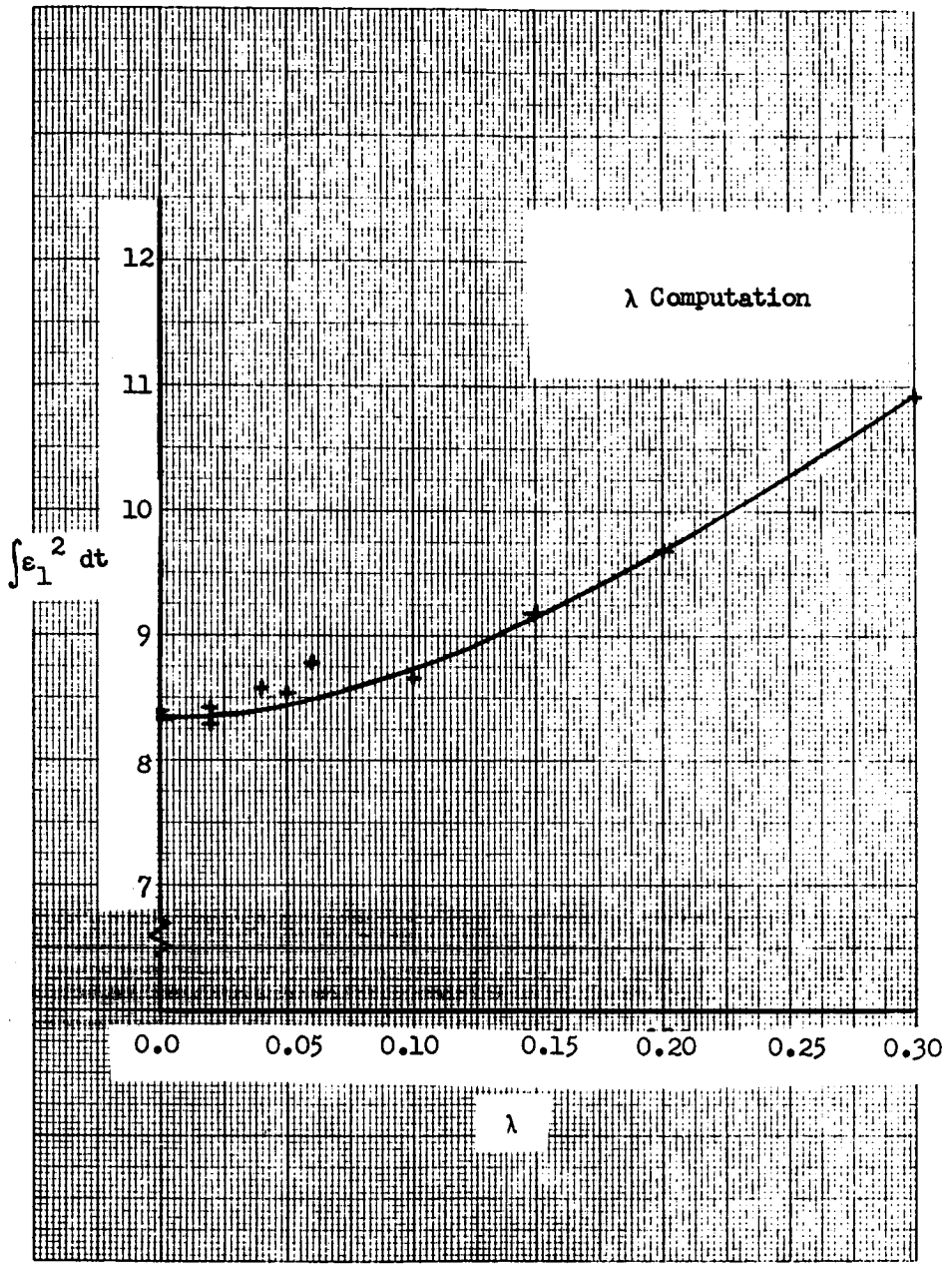

Figure 4-31 Iterative Computation of λ

4.11 Conclusions

The methodology study was primarily concerned with increasing the identification accuracy of model matching techniques and the selection of an optimum technique. A secondary consideration was the development of advanced modeling techniques which would be capable of yielding a more precise model of the human operator. An evaluation of the model matching techniques investigated led to the following conclusions:

1) The iterative technique employing sensitivity equations for the generation of influence coefficients was found to be the most accurate (0.5% overall error for System A). This technique is readily implemented on an analog computer with an interative capability and was considered the optimum technique of all techniques investigated.

2) The identification accuracy is dependent on excitation bandwidth. For the known systems evaluated, an excitation bandwidth greater than the natural frequency of the system being modeled, produced excellent identification accuracy on all internal parameters.

3) Convergence can be improved substantially in iterative techniques by equalizing the parameter adjustment rates and also by limiting the maximum parameter correction per iteration.

4) In modeling of unknown systems, situations may arise where the parameters may be indeterminate. However the model obtained will match the output of the unknown system correctly and consequently the system identification is unique.

5) It is theoretically possible to model the human operator's performance in a coupled system exactly, if a matrix formulation of the spectral analysis technique is used.

6) For the coupled systems investigated, the approximate models of the human operator determined by the iterative techniques compared favorably with the correct spectral models.

7) The extrapolation methods used in extracting an unknown time delay and the coefficient of the third derivative of the response, did not give satisfactory results. However, the model matching techniques were not very accurate at the time of the study and consequently the extrapolation methods may be feasible using the refined techniques just developed.

8) Closed loop model matching will be unstable if during the convergence period, the model parameters assume values which result in a negative phase margin.

9) Prefiltering must be used if accurate closed loop model matching of typical manual control systems is to be performed.

5. CONCLUSIONS

Model matching techniques were used in analyzing human tracking performance in both uncoupled and coupled two-axis systems. Specifically the effects of training, task difficulty and cross-coupling were evaluated by examining the parameters of mathematical models. Analyses of variance were performed in order to obtain statistical significance levels for the major results.

The report is divided into three major sections. The first deals with human performance in single and two-axis compensatory tracking systems where the plant dynamics were identical in both the single-axis system and the symmetrical two-axis system. Second-order dynamics consisting of a pure integration and first-order lag were used. Linear second-order describing functions were used to model the operator's performance. Analysis of system tracking error showed that the rate at which error decreased with training was directly proportional to task difficulty. The amplitude ratio and phase lead of the model describing function increased with training indicating an increase in open loop bandwidth and a decrease in phase margin. Increasing the plant lag time constant resulted in an increase in the model lead time constant and a decrease in the zero frequency gain. No significant difference was found to exist in the tracking error per axis between the two-axis tasks and the single-axis tasks. However the model lead time constant was significantly greater in two-axis tracking.

The second section of the report is concerned with the evaluation of human performance in coupled two-axis systems. Again the plant dynamics were of second-order form and the human operator's performance was modeled by a 2 x 2 matrix whose elements were second-order describing functions. Analysis of the matrix models obtained showed that the human operator can decouple the system for certain forms of cross-coupling. His decoupling performance can be predicted from decoupling equations which are readily derived analytically. Learning was evident for all tasks with the asymmetrical task being the most difficult.

The third section of the report deals with a methodology study of model matching techniques. Analysis of the identification performance of continuous, iterative, and extrapolation techniques showed that the iterative technique using sensitivity equations for the generation of the influence coefficient, was the optimum technique. It is readily implementable on an analog computer with an iterative capability and possesses excellent identification accuracy. Convergence in iterative techniques can be improved substantially by equalizing the parameter adjustment rates and limiting the maximum parameter correction per iteration. Good identification requires that the excitation bandwidth be greater than the natural frequency of the system being modeled. Also prefiltering must be used if accurate closed loop model matching of typical manual control systems is to be performed. Finally, it was shown that the human operator's performance in a coupled system could theoretically be modeled exactly if a matrix formulation of the spectral analysis technique was used.

APPENDIX A

CONVERGENCE STUDY OF FIRST-ORDER MODEL PARAMETERS

A.1 Introduction

An experimental study of the convergence properties of the continuous model matching technique was performed using a first-order system with three parameters. The mathematical model was of the same form as the system and contained the three parameters to be identified. The purpose of the study was to determine the effect of adjustment gain and parameter initial conditions on the convergence characteristics of the model parameters. Convergence was measured by final accuracy of the parameters, time required to reach steady state and repeatability.

Identification was performed using the continuous technique described in Section 4.2 with the slope-limited quadratic criterion function described in the same Section.

If the system and model inputs are denoted by x and their respective outputs by y and z, then the differential equations describing the dependence of y and z on x are given by

$$\dot{y} + b_1 y = b_2 \dot{x} + b_3 x \tag{A.1}$$

$$\dot{z} + \beta_1 z = \beta_2 \dot{x} + \beta_3 x \tag{A.2}$$

where b_1, b_2 and b_3 are the (constant) coefficients of the system and β_1, β_2, and β_3 are the model parameters. The model parameters are adjusted by the model-matcher so as to make $\varepsilon = z-y$ approach zero. For this study the system parameters were chosen to have values representative of comparable human operator models. Specifically these values were

$$b_1 = 40 \text{ sec}^{-1}$$

$$b_2 = 15$$

$$b_3 = 25 \text{ sec}^{-1}$$

Equation (A.1) may be written in the transfer function form

$$\frac{Y}{X}(s) = \frac{K_0(\tau_1 s + 1)}{(\tau_2 s + 1)}$$

where

$$K_0 = \frac{b_3}{b_1} = 0.625$$

$$\tau_1 = \frac{b_2}{b_3} = 0.6 \text{ sec}$$

$$\tau_2 = \frac{1}{b_1} = 0.025 \text{ sec}$$

and s is the Laplace operator. A two minute tape recording of a tracking error history obtained from a compensatory tracking experiment was used as the input x for all phases of the study. The convergence study was initiated by first investigating the repeatability characteristics of the model-matcher for various values of the initial conditions of the β parameters.

A.2 Effect of Initial Parameter Values

A random choice for the initial parameter values will yield a criterion function whose magnitude at t = 0 will also be of a random value. To circumvent this dilemma, the initial conditions were chosen such that the criterion function would have a large initial magnitude by assigning zero initial conditions to β_2 and β_3. The parameter β_1 must be non-zero to keep the model transfer function gain from approaching infinity. Specifically β_1 was initially chosen to have values which were either high or low by 50% with respect to the known value for b_1. With the above described initial conditions, a repeatability experiment was performed on the model-matcher to determine the effect of these initial conditions on the repeatability characteristics. In these experiments, the model-matcher was allowed to operate on the input data for short lengths of time. Model-matcher gains of 30, 60 and 90 were used. Figure A-1 shows the poor repeatability characteristics for the β parameters when $\beta_1(0) = 0.5b_1$ and the adjustment gain

was 60. With $\beta_1(0) = 1.5b_1$, the parameter repeatability was markedly better as shown in Figure A-2. Adjustment gains of 30 and 90 yielded similar results. The reason for this behavior is evident if one notes that $\frac{1}{\beta_1}$ is the model lag time constant (or, β_1 is the model lag break frequency). Making β_1 smaller than the system lag break frequency b_1 means that the frequency content of the model output z is reduced, as compared to the system output and the matching error does not contain enough information to obtain accurate identification. Starting with $\beta_1 > b_1$ is clearly desirable since now the frequency content of z exceeds that of y and the error is sensitive to parameter changes. This observation is further verified in the bandwidth-convergence study discussed in Section 4.5. Initial conditions of $\beta_1(0) = 1.5b_1$ were used in all of the subsequent experimental measurements.

A.3 Long Term Convergence

In operation the model-matcher should cause the β parameters to converge on their true values if sufficient time is available. A typical time history of this process is shown for one parameter in Figure A-3. Note that the parameter converges approximately to the true value in two distinct steps. Initially the convergence is very rapid and consequently this portion of the convergence has been termed short term convergence. After this rapid initial convergence, the parameter requires a long settling time before it reaches a steady-state value (i.e., long term convergence). The initial convergence is rapid because the error ε is large and consequently the slope of the criterion function is large. However, when the error becomes small (point A on Figure A-3), the resultant criterion function has a small slope with respect to ε which decreases the convergence rate.

An experimental study was conducted on the long-term parameter convergence to determine the effect of adjustment gain and matching time on parameter accuracy. Figure A-4 shows the percentage error in the β parameters for the various adjustment gains where the parameter values were determined upon completion of a 2-minute

run. Percentage errors for the equivalent transfer function parameters are also shown in Figure A-4. Clearly, Figure A-4 indicates that the β parameters may be obtained with a percentage accuracy of ±6% or better while the transfer function parameters may be determined to an accuracy of ±4%. In particular the parameter K may be determined to an accuracy of better than 0.5%.

In an attempt to increase the accuracy of the convergence process, the same data was run through the model-matcher a number of times. Four adjustment gains of 10, 30 60 and 90 were used and the final parameter values of one run were made the initial conditions for the subsequent run. Figure A-5 indicates the dependence of β parameter percentage error on the number of replications R as well as the gain used. In general, the percentage error was greater after two replications. In cases where three replications were made, the percentage error had either reached a plateau (for k = 60) or was approaching one (for k = 10). All parameters had approximately the same percentage error and were predominantly negative. Percentage errors were also calculated for the equivalent transfer function parameters and are shown in Figure A-6. Again, the use of replications is apparently not warranted as the accuracy is not increased substantially. The one exception occurs when the gain is 60. Here a definite increase in accuracy for the K and T_1 parameters was obtained if replications were made. Comparison of the accuracies for the β and transfer function parameters indicates that the transfer function parameters are again more accurately determined (especially for K and T_1). This result is due to the fact that the transfer function parameters are ratios of β parameters. Since the β parameters have errors which are consistently negative and approximately equal, it follows that their ratios will be much more accurate with the sole exception of parameter T_2 which is not a ratio but a reciprocal. Figure A-6 clearly shows that T_2 is much less accurate than K or T_1. (See Appendix B for an analysis of these results based on sensitivity considerations.)

A.4 Short Term Convergence

During the long term convergence experiments it was noted that the error was very close to zero at the end of ths short term convergence period. To determine the parameter accuracy at this point, an experiment was conducted in which the short term parameters were found for five randomly chosen points of the same data run previously used. These parameters were then averaged and the RMS value of the percentage error determined. In general, the accuracies were not as good as in the long term case. However, the transfer function parameters with the exception of T_2 were found to be accurate to 5% over all of the adjustment gains used. Figure A-7 compares the accuracy of the β and transfer function parameters. Again, the transfer function parameters are more accurate with the exception of T_2. This may be explained by the same argument used for the long term convergence study. It is important to realize that the short term parameters are accurate to 10% RMS for $k = 90$ as their values may be determined in a second or two while the long term parameters require about 60 seconds.

A.5 Conclusions

An experimental study of the convergence characteristics of the continuous method using a first-order model led to the following conclusions:

1) Parameter adjustment repeatability was good when $\beta_1(0) > b_1$ and $\beta_2(0) = \beta_3(0) = 0$.

2) For long term convergence, the β parameters may be obtained with a percentage accuracy of $\pm 6\%$ while the transfer function parameters may be determined to an accuracy of $\pm 4\%$.

3) Use of replications does not substantially decrease the long term convergence error.

4) No optimum gain was found for long term convergence.

5) For short term convergence, both the β and transfer function parameters may be determined with an accuracy of 10% (RMS) at an adjustment gain of 90.

6) The optimum adjustment gain for short term convergence was 90 (the highest value used).

7) For both long and short term convergence, the transfer function parameters may be obtained with a better percentage accuracy than the β parameters except for the case of T_2 for which no significant difference occurs.

8) The transfer function parameter K may be determined with the greatest precision (0.5% for long term convergence and 2% for short term).

Direct application of these results to the prediction of model-matcher performance on differential equations with unknown coefficients and of an order other than one, cannot be justified from the experiment as the study was only concerned with an equation of order one with known constant coefficients. If the unknown coefficients are slowly time-variant it may be possible for the model-matcher to follow the variation in the unknown parameters with a fair degree of accuracy as the model-matcher does exhibit a good short term parameter convergence accuracy.

An analytical study of the sensitivities of the β and transfer function parameters has been made to explain the difference in behavior of the two sets of parameters. This analysis in general supports the experimental work reported here and may be found in Appendix B.

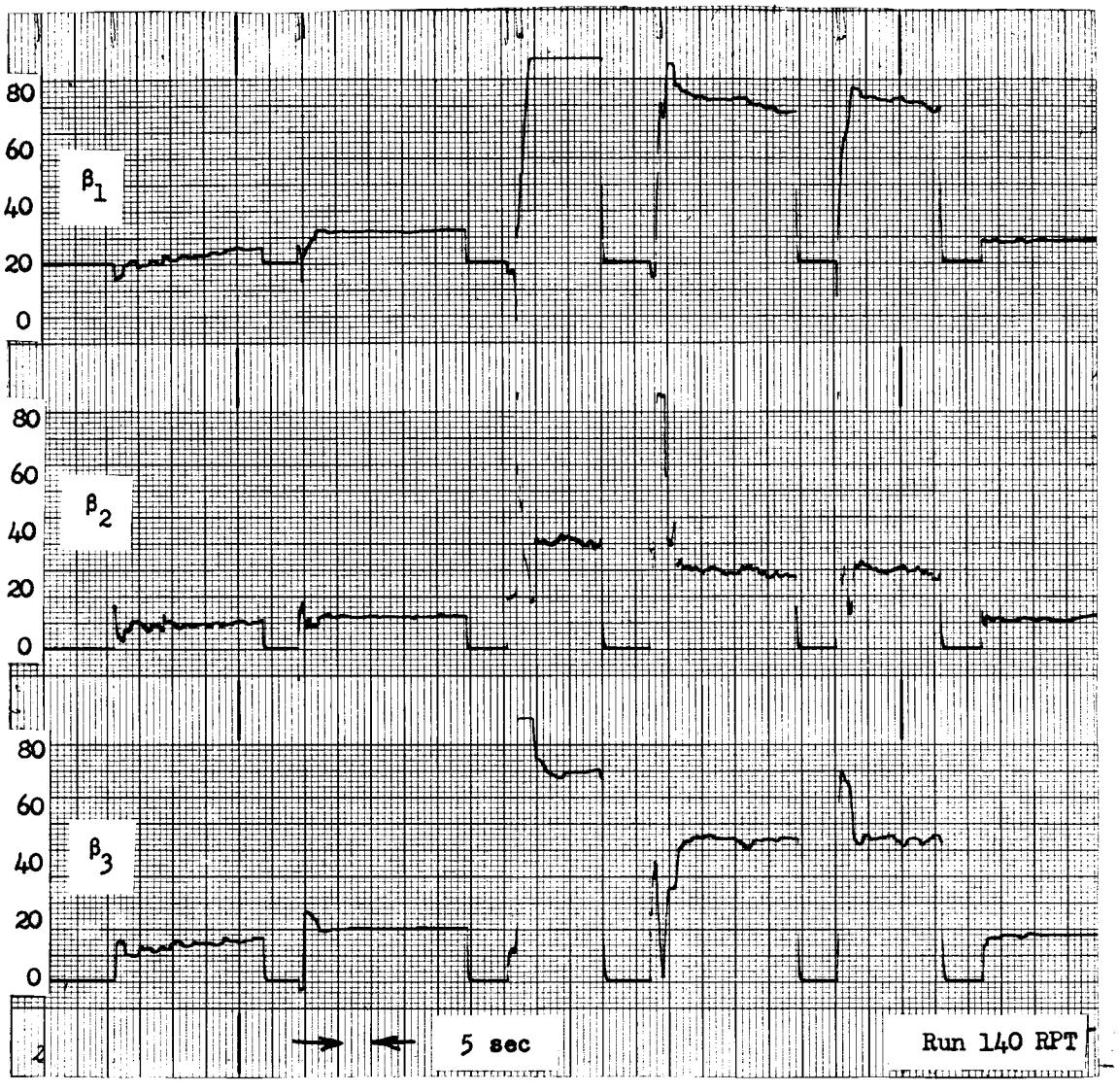

Figure A-1 Parameter Repeatability ($\beta_1(o) = 20$)

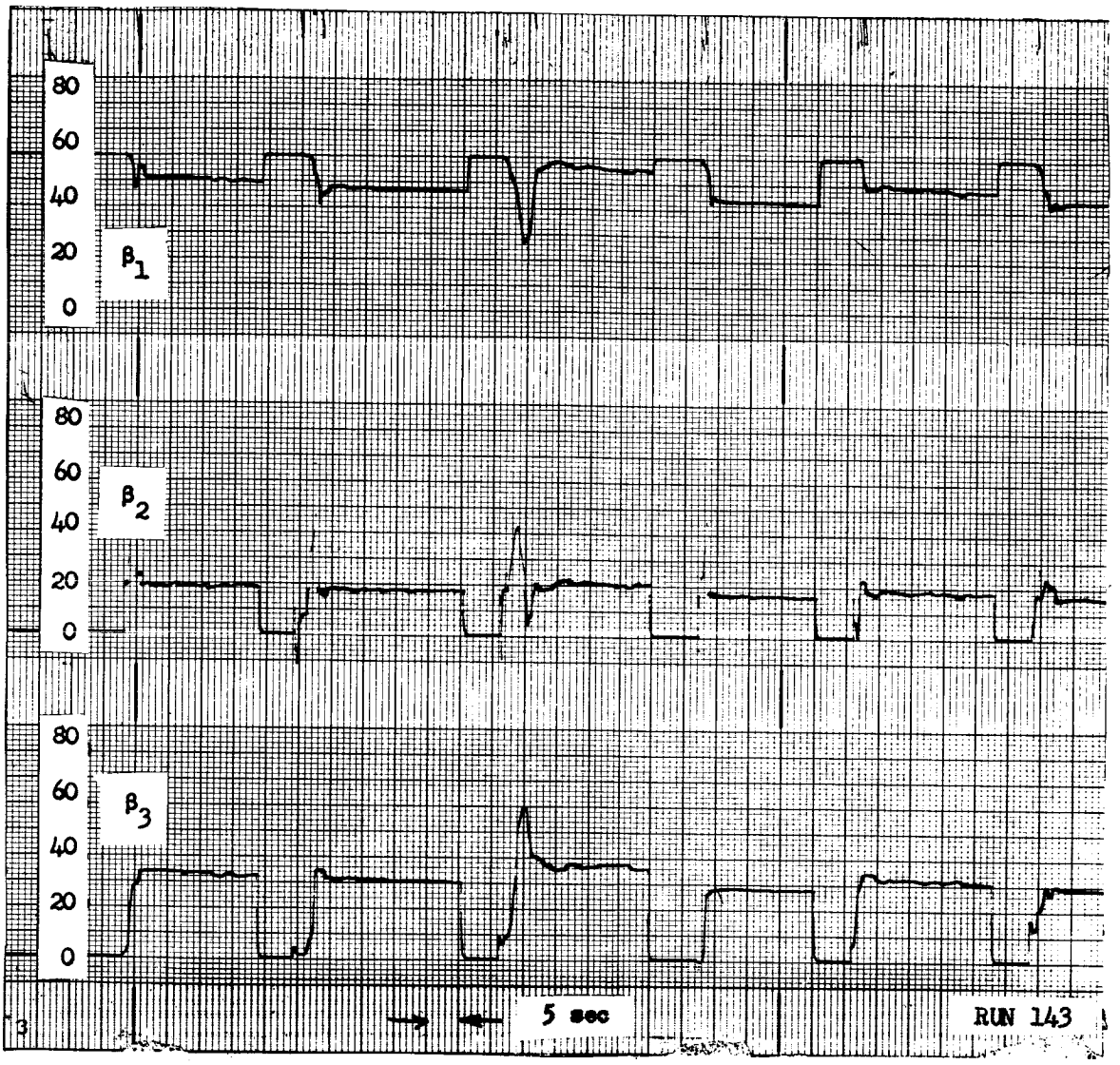

Figure A-2 Parameter Repeatability ($\beta_1(o) = 60$)

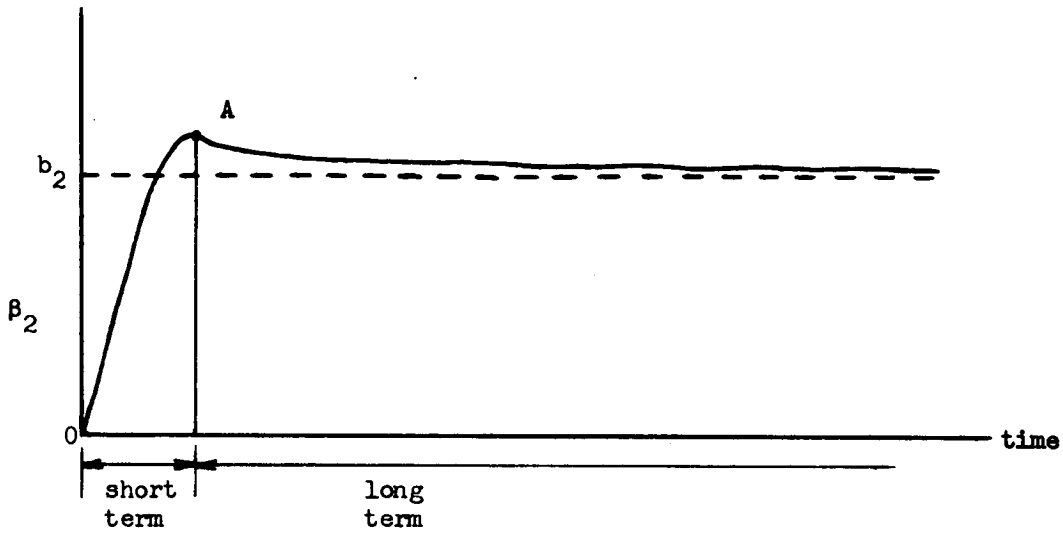

Figure A-3 Parameter Convergence

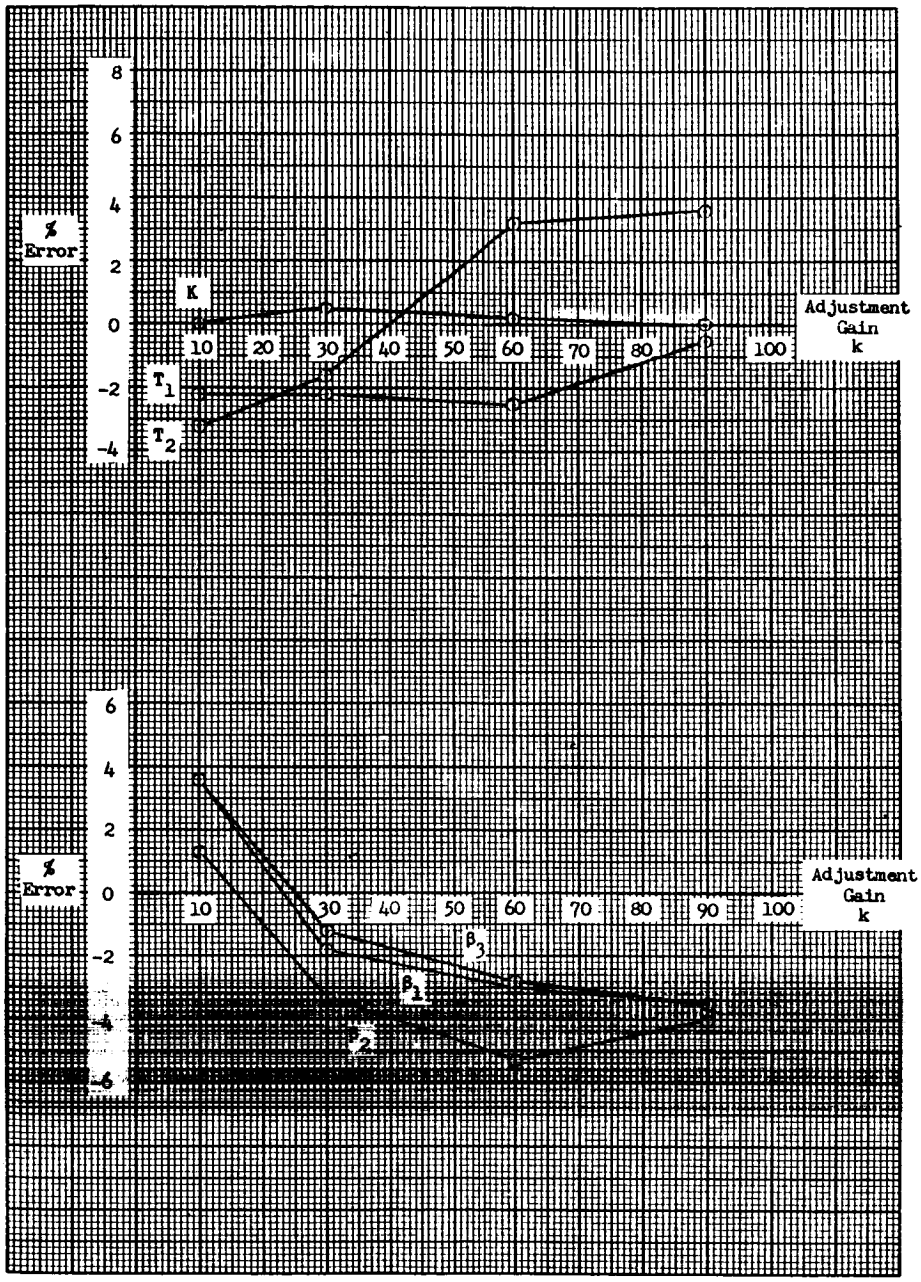

Figure A-4 Effect of Adjustment Gain on Long Term Convergence Accuracy

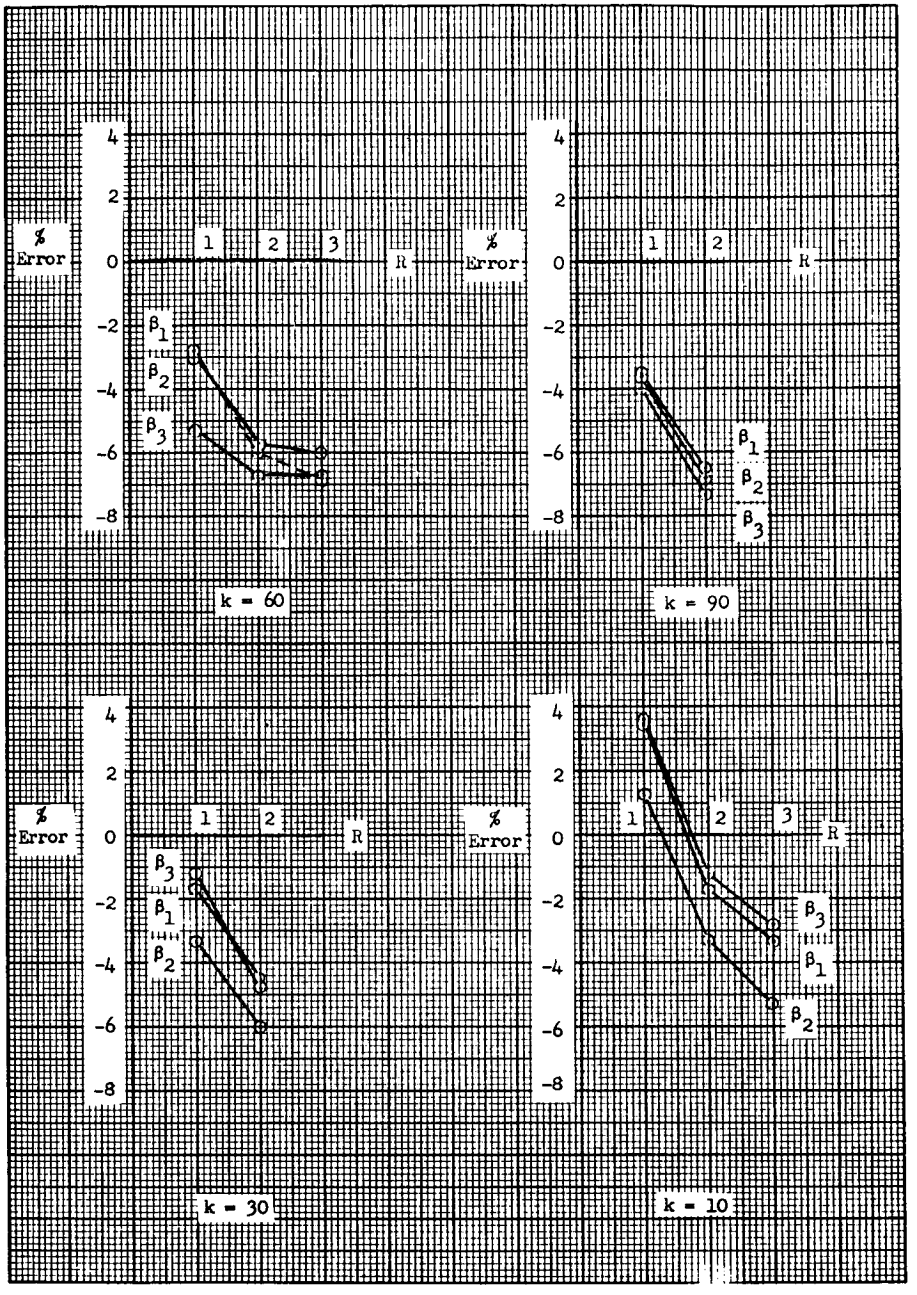

Figure A-5 Effect of Replication on Long Term Convergence Accuracy (β Parameters)

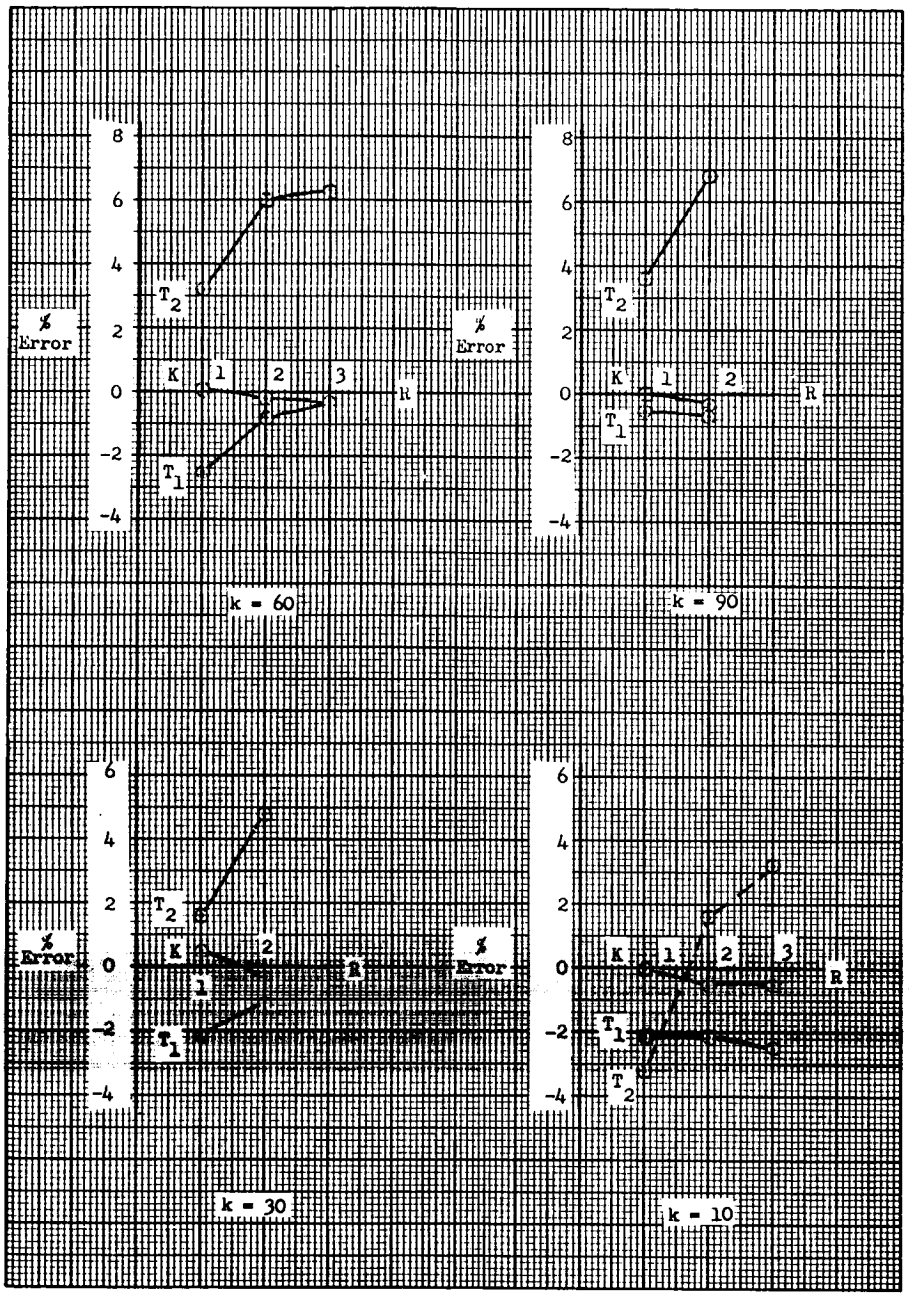

Figure A-6 Effect of Replication on Long Term Convergence Accuracy (Transfer Function Parameters)

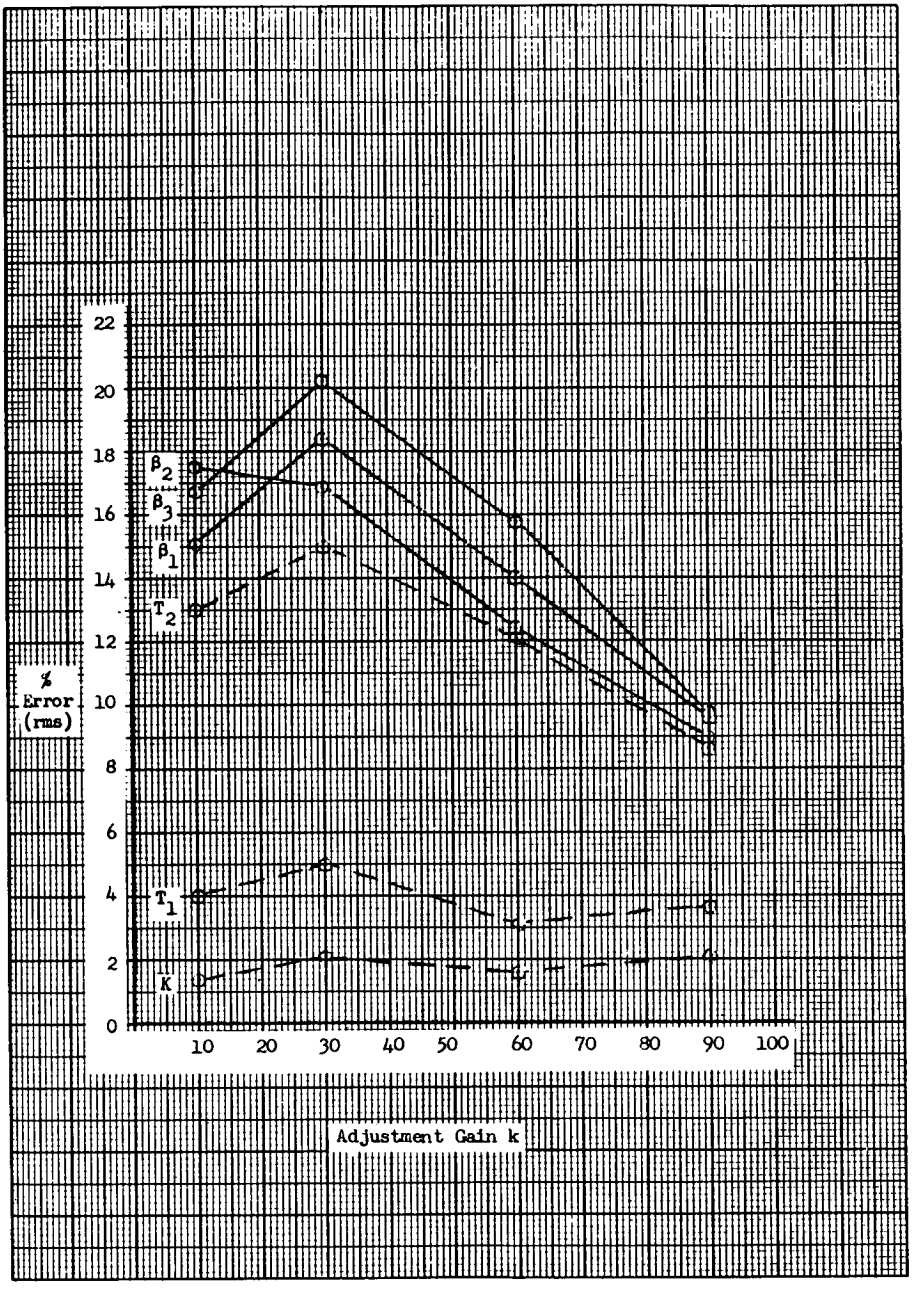

Figure A-7 Effect of Adjustment Gain on Short Term Convergence Accuracy

APPENDIX B

RELATIVE SENSITIVITY OF HUMAN PILOT MODEL PARAMETERS

B.1 Problem Statement

Experimental results indicate that the parameters in a transfer function model of the human operator, especially the steady state gain factor K, tend to be determined with greater precision by the model matching process than the individual coefficients of an equivalent differential equation model. This Appendix shows that this result is traceable to the relative magnitude of the model sensitivities to the various parameters.

The purpose of analyzing these relationships is to confirm the trends exhibited by the experimental results in quantative and qualitative terms, and to find criteria for selecting mathematical model structures that yield to parameter identification processes with higher precision than others. On the basis of this analysis it will also be possible to distinguish between a case of poor computer accuracy and a mathematically unfavorable choice of the task which the computer is asked to perform.

B.2 Equivalent Model Forms

In this discussion we compare the first-order linear model differential equation

$$\dot{z} + \beta_1 z = \beta_2 \dot{x} + \beta_3 x \tag{B.1}$$

having parameters β_i with the equivalent transfer function model

$$\frac{Z}{X} = K \frac{T_1 s + 1}{T_2 s + 1} \tag{B.2}$$

where

$$K = \frac{\beta_3}{\beta_1}, \quad T_1 = \frac{\beta_2}{\beta_3}, \quad T_2 = \frac{1}{\beta_1} \tag{B.3}$$

Both model forms (B.1) and (B.2) have been used interchangeably in previous work. Computer results (Reference 11) show that K is a well-defined parameter, whereas the terms β_1, β_3 which determine K tend to drift simultaneously or yield somewhat inconsistent results in repeated modeling runs of the same human operator tracking data. T_1 and T_2 are also defined with greater relative accuracy than the corresponding β_i terms.

B.3 Sensitivity Equations and Sensitivity Ratios

The influence coefficients $u_i = \partial z/\partial \beta_i$ are obtained by solution of the sensitifity equations derived from (B.1). In transform notation, assuming zero initial values,

$$U_1 = -KT_2 \frac{T_1 s + 1}{(T_2 s + 1)^2} X$$

$$U_2 = \frac{T_2 s}{T_2 s + 1} X = sU_3 \qquad \text{(B.4)}$$

$$U_3 = \frac{T_2}{T_2 s + 1} X$$

Similarly the sensitivity equations for

$$V_0 = \frac{\partial Z}{\partial K}, \quad V_1 = \frac{\partial Z}{\partial T_1}, \quad V_2 = \frac{\partial Z}{\partial T_2}$$

yield

$$V_0 = \frac{T_1 s + 1}{T_2 s + 1} X$$

$$V_1 = K \frac{s}{T_2 s + 1} X \qquad \text{(B.5)}$$

$$V_2 = -K \frac{s(T_1 s + 1)}{(T_2 s + 1)^2} X$$

For simplification of the subsequent discussion we form the sensitivity ratios

$$q_{12} = \frac{U_1}{U_2} = -\frac{K(T_1 s + 1)}{s(T_2 s + 1)} \qquad r_{01} = \frac{V_0}{V_1} = \frac{T_1 s + 1}{Ks}$$

$$q_{13} = \frac{U_1}{U_3} = -\frac{K(T_1 s + 1)}{T_2 s + 1} \qquad r_{02} = \frac{V_0}{V_2} = -\frac{T_2 s + 1}{Ks} \qquad \text{(B.6)}$$

$$q_{23} = \frac{U_2}{U_3} = s \qquad r_{12} = \frac{V_1}{V_2} = -\frac{T_2 s + 1}{T_1 s + 1}$$

These expressions which permit an estimate of the relative magnitude and power of the sensitivities U_i and V_i are illustrated by Bode diagrams shown in Figures B-1 and B-2 respectively, for a typical case where the parameter values are

$$\beta_1 = 40 \text{ sec}^{-1} \qquad K = 0.625$$

$$\beta_2 = 15 \qquad \text{or} \qquad T_1 = 0.600 \text{ sec}$$

$$\beta_3 = 25 \text{ sec}^{-1} \qquad T_2 = 0.025 \text{ sec}$$

(This parameter condition has been the subject of an extensive experimental model matching study and data analysis as reported in Appendix A.)

While r and q give relative sensitivities of the parameters within the models (B.1), (B.2) respectively, the relative sensitivities between the models are expressed by the ratios $\frac{U_3}{V_2}$, $\frac{U_3}{V_1}$, $\frac{U_3}{V_0}$, etc. The term

$$\frac{U_3}{V_0} = \frac{T_2}{T_1 s + 1} \qquad \text{(B.7)}$$

is plotted in Figure B-2. Using this term for calibration the other relative inter-model sensitivities can be deduced.

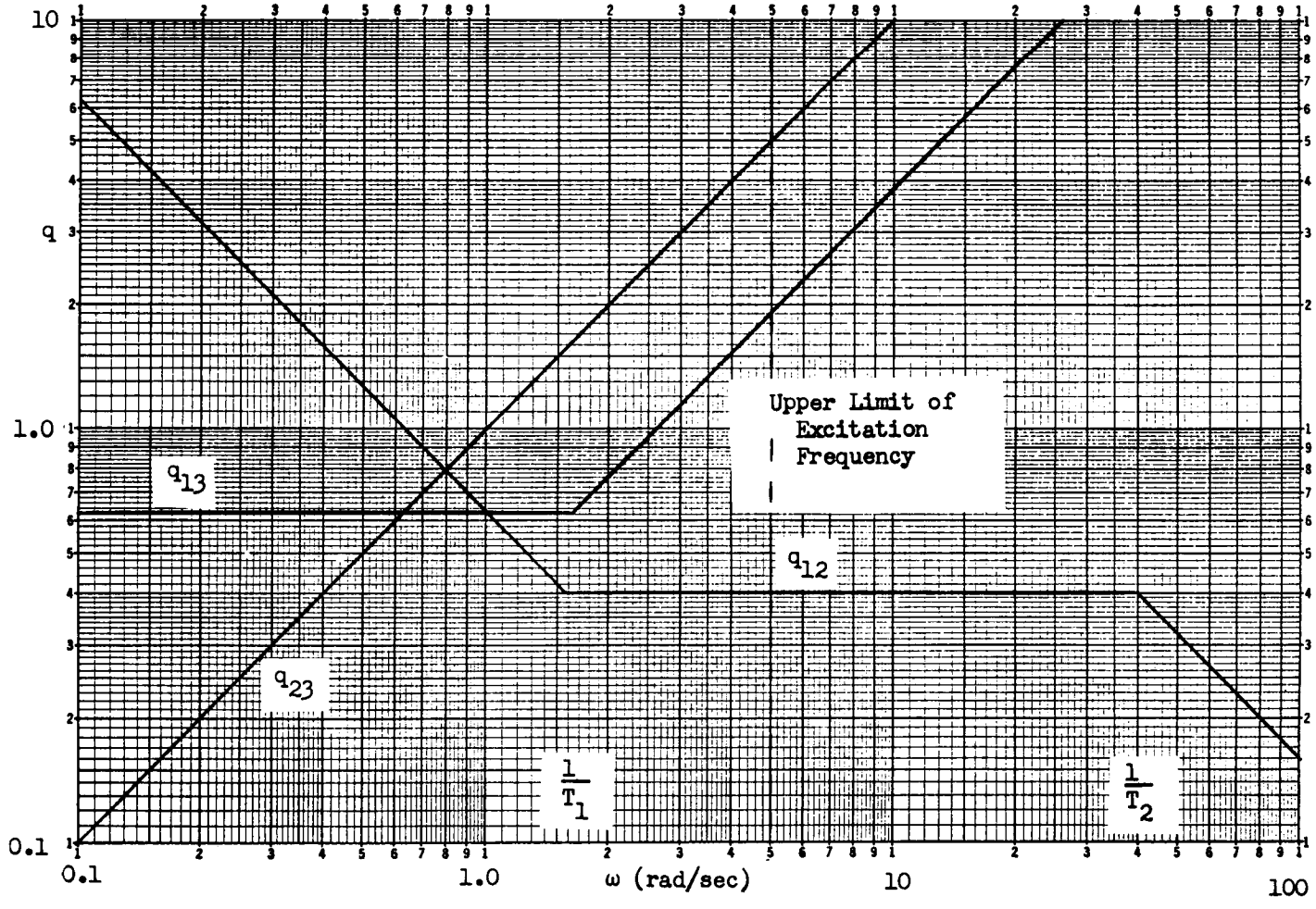

Figure B-1: Frequency Dependence of Sensitivity Ratios q

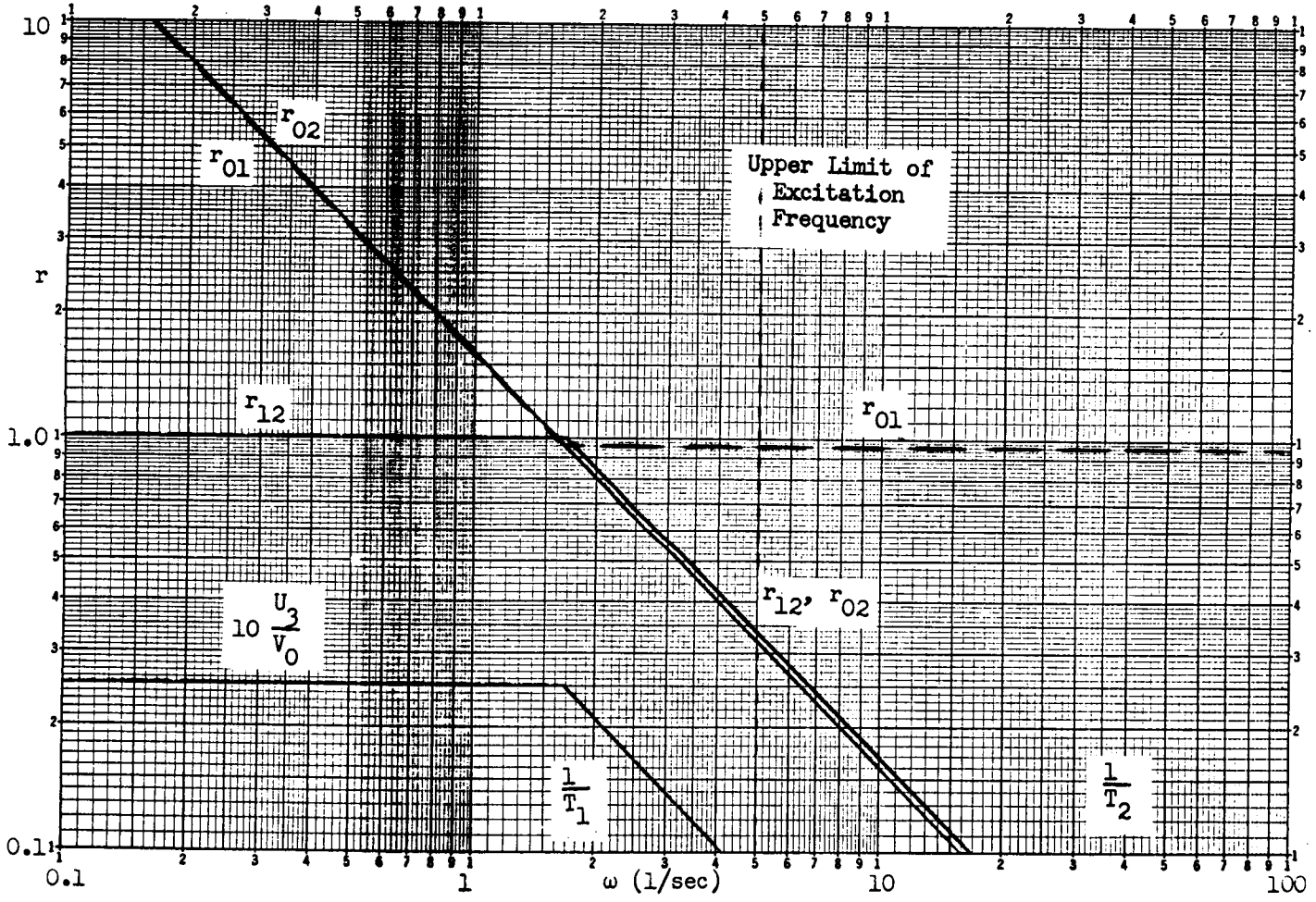

Figure B-2: Frequency Dependence of Sensitivity Ratios r and U_3/V_0

B.4 Discussion

In evaluating the amplitude vs. frequency plots for r and q one must take into account the upper frequency limit of the excitation signal x(t) occurring in human tracking studies. On the basis of past experiments we set the cutoff frequency roughly at $\omega_c = 5$ rad/sec to obtain estimates of relative magnitude of the U_i and V_i. (The resulting estimates reflect this choice of ω_c). In the frequency range of interest the sensitivity ratios behave as follows:

Table B-1

Range of Sensitivity Ratios

Differential Equation Parameters	Transfer Function Parameters
q_{12} ~6.0 ... 0.4	r_{01} ~15 ... 1.0
q_{13} ~0.6 ... 2.0	r_{02} ~15 ... 0.3
q_{23} ~0.1 ... 5.0	r_{12} ~ 1 ... 0.3

Between Models

$$\left|\frac{V_0}{U_3}\right| \sim 40 \quad \ldots \quad 100$$

This leads to the following observations:

1) The parameters β_1, β_2, β_3 have essentially the same degree of sensitivity in the vicinity of $\omega = 1$ rad/sec. This agrees with the findings, in Appendix A, of comparable accuracy of all β's. U_3 dominates U_2, U_1 in the lower frequency region, U_1 dominates U_2 at low frequencies, U_2 dominates U_1 and U_3 at high frequencies. On the average the sensitivities are approximately matched.

2) The parameter sensitivities for K, T_1, T_2 are also of the same order of magnitude near $\omega = 1$ rad/sec. V_0 dominates V_1 and V_2 very distinctly up to frequencies of 1.5 rad/sec. V_1 and V_2 are of similar magnitude, but V_2 tends to dominate V_0 and V_1 in the upper frequency range. The high accuracy of K exhibited in the experimental study confirms this result.

3) The most striking difference in sensitivities is indicated by the behavior of V_0/U_3. Figure B-2 shows that K is determined with an accuracy at least an order of magnitude higher than β_3. This result can also be seen by noting that

$$V_0 \triangleq \frac{\partial Z}{\partial K} = \frac{\partial Z}{\partial\left(\frac{\beta_3}{\beta_1}\right)} \tag{B.8}$$

For constant $\beta_1 = 40$,

$$V_0 = \beta_1 \frac{\partial Z}{\partial \beta_3} = 40\ U_3$$

Furthermore, since near $\omega = 1$ the relative sensitivities of the β_i are comparable, K can be determined much more accurately than all the β_i not only β_3. Thus for the case investigated the steady state gain K is determined with an accuracy at least an order of magnitude higher than the parameters β_i. In view of the values r_{01}, r_{02} and the ratio V_0/U_3 we deduce that T_1 and T_2 should also be considerably more well defined than the β_i's. This finding is confirmed by the experimental results.

Additional insight is gained by noting that

$$\frac{V_1}{U_3} = \frac{K}{T_2} s = 25s$$

$$\frac{V_2}{U_1} = \frac{s}{T_2} = 40s$$

which shows that, except for very low frequencies, V_1 and V_2 dominate over the U's.

4) The above results are largely parameter-dependent. For example, r_{01} is shaped by T_1 and K. Figure B-3 illustrates how r_{01} varies with increases in each of these parameters. As T_1 increases, the dominance of V_0 is enhanced, an increase in K

has the opposite effect. The dominance of V_0 over U_1, U_2, U_3 depends strongly on T_2. For increased T_2 (human pilot lag time constant) to more typical values of 0.1 - 0.2 sec the preponderance of V_0 decreases by an order of magnitude but is still noticeable. T_1 has a much smaller effect on the ratio U_3/V_0 unless T_1 is substantially increased above the 0.6 sec value used in this discussion.

r_{12} and q_{23} are largely uninfluenced by parameter changes.

B.5 Conclusion

The simple analytical method presented here is very useful in detecting sources of parameter definition accuracy or inaccuracy which may otherwise remain obscure. The method can be readily extended to practical problems characterized by second order models, but remains limited to linear structures.

The method serves to pinpoint mathematically favorable model formats or parameter combinations to be selected for the optimization program. As a general method of sensitivity analysis it has a range of applications in control engineering, system optimization, adaptive control, and related fields where it should be further pursued.

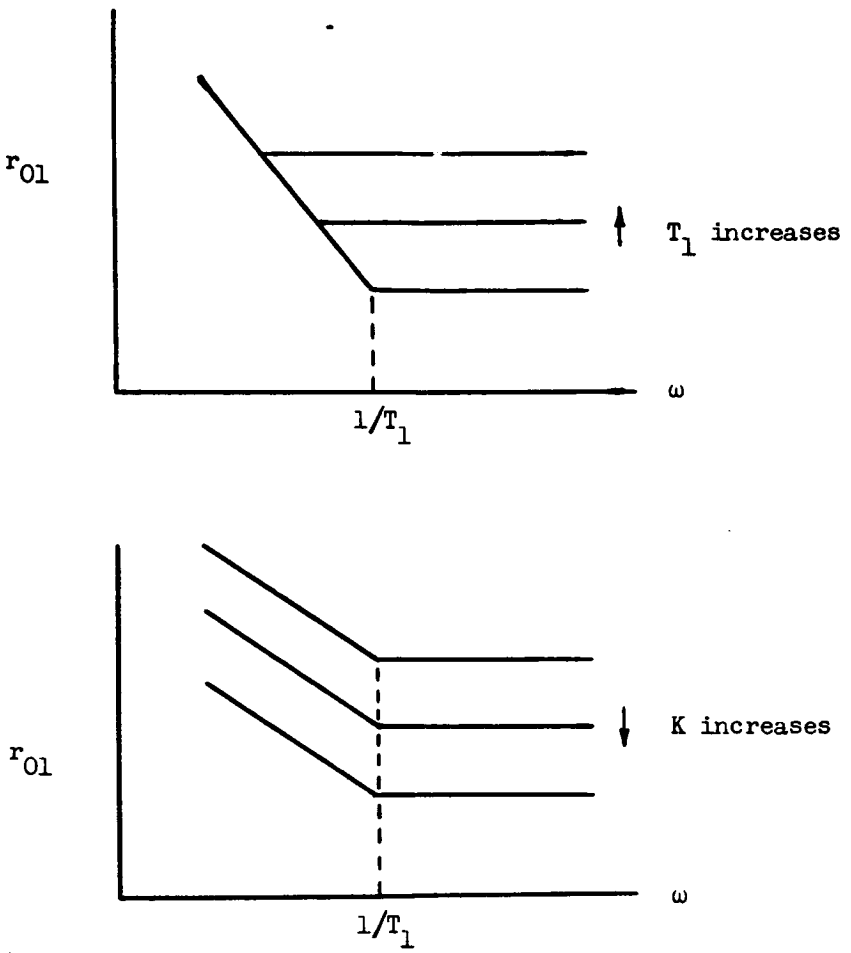

Figure B-3 Parameter Dependence of r_{01}

APPENDIX C

TYPICAL TIME HISTORIES OF THE HUMAN OPERATOR MODEL

Human performance in two-axis systems without cross-coupling was modeled with the conventional second-order model. A continuous model matching technique of the form described in Section 4.2 was used to obtain the model parameters. Figure C-1 shows a typical parameter time history obtained for Task 4. Approximate modeling of human performance in two-axis systems with cross-coupling was accomplished using the iterative model matching technique described in Section 3.4. Figures C-2 through C-5 show a set of typical time histories of the model parameters for one subject's performance in Task 2. Figures C-6 through C-9 show a similar set of time histories obtained for Task 3. The parameter values used in the models were obtained by averaging the model parameters over the last minute of the modeling run. Examination of the time histories shows that parameter convergence was good and that the parameters were stable once convergence was reached. Similar time histories were obtained in the determination of the other models. In general, no difficulties were encountered other than the occasional instability that would arise in closed loop model matching. This instability was due to the model parameters assuming values during the convergence process which would cause a negative phase margin. Prefiltering of the form described in Section 4.5 was used in all closed loop model determinations.

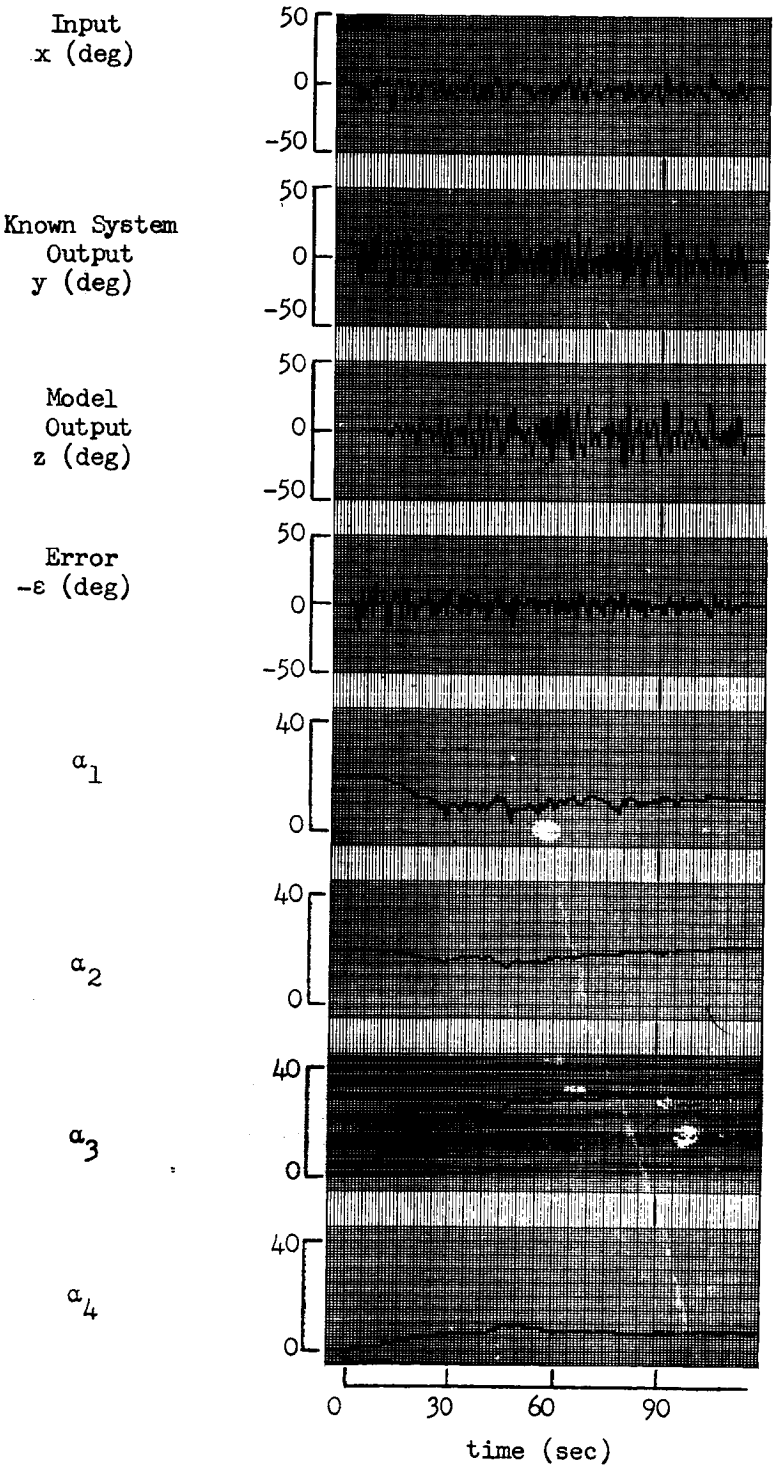

Figure C-1 Parameter Time History for H_{bb} (Task 4 of Uncoupled Experiment)

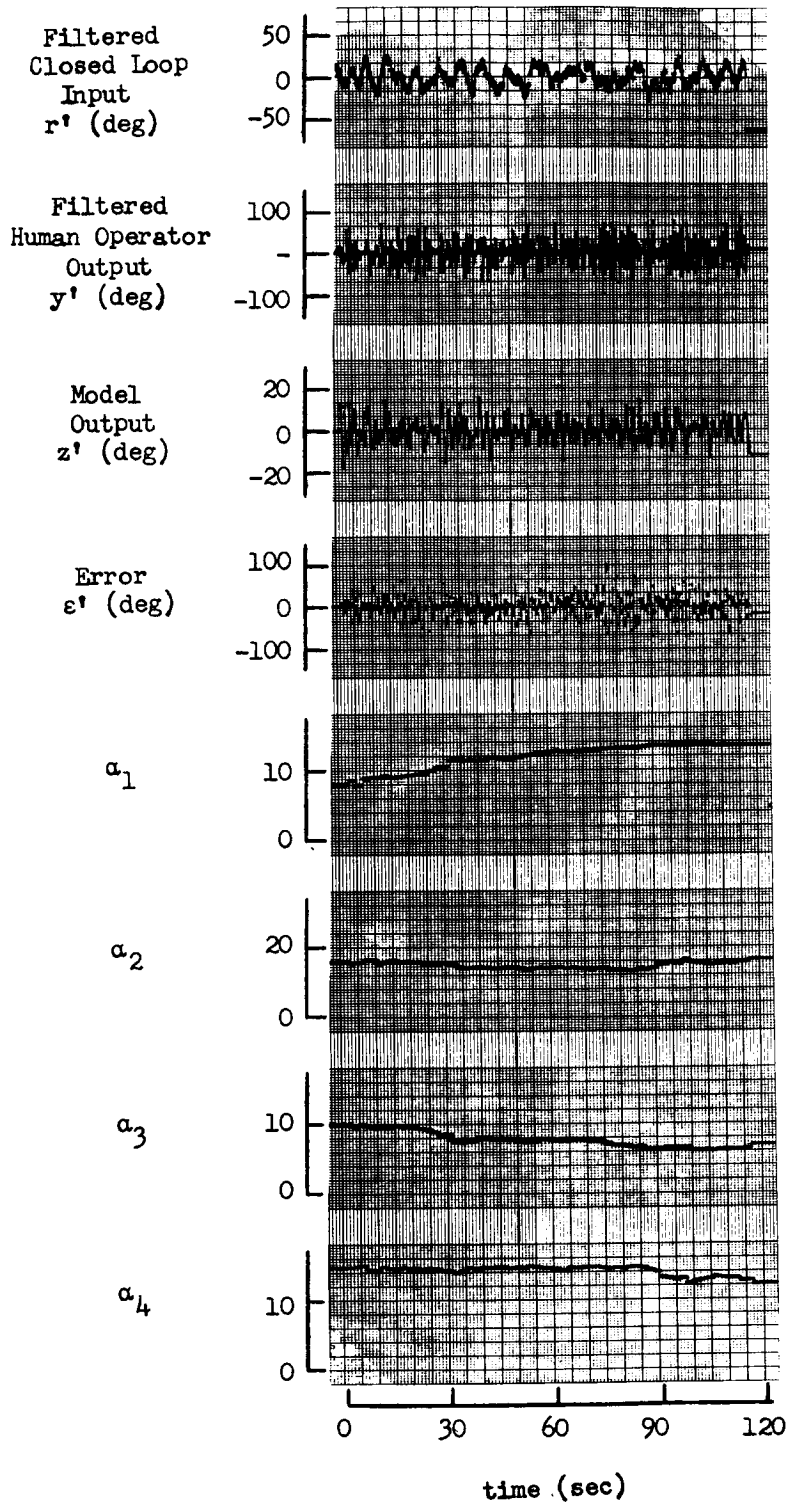

Figure C-2 Parameter Time History for H_{aa} (Task 2 of Coupled Experiment)

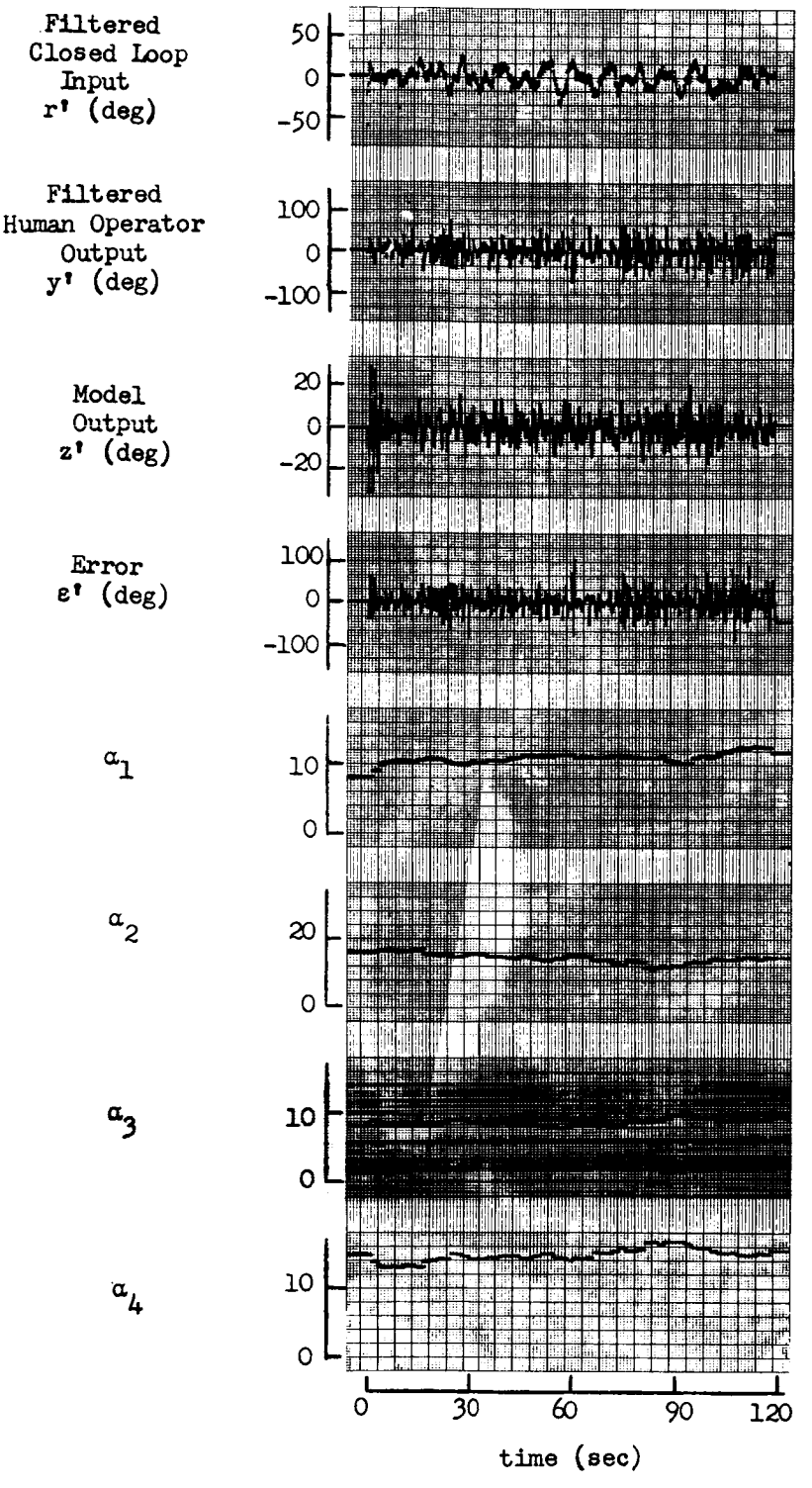

Figure C-3 Parameter Time History for H_{bb} (Task 2 of Coupled Experiment)

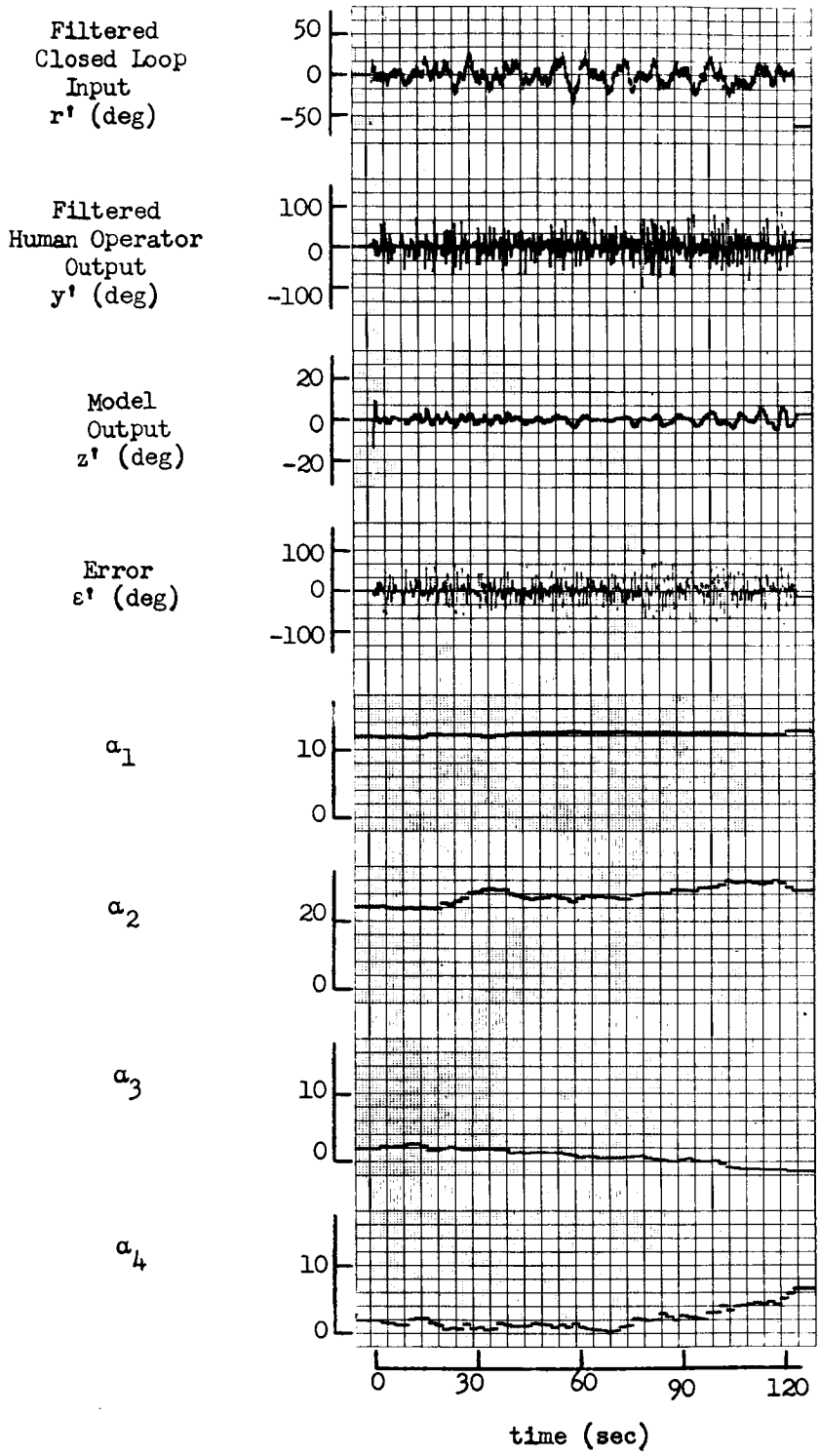

Figure C-4 Parameter Time History for H_{ab} (Task 2 of Coupled Experiment)

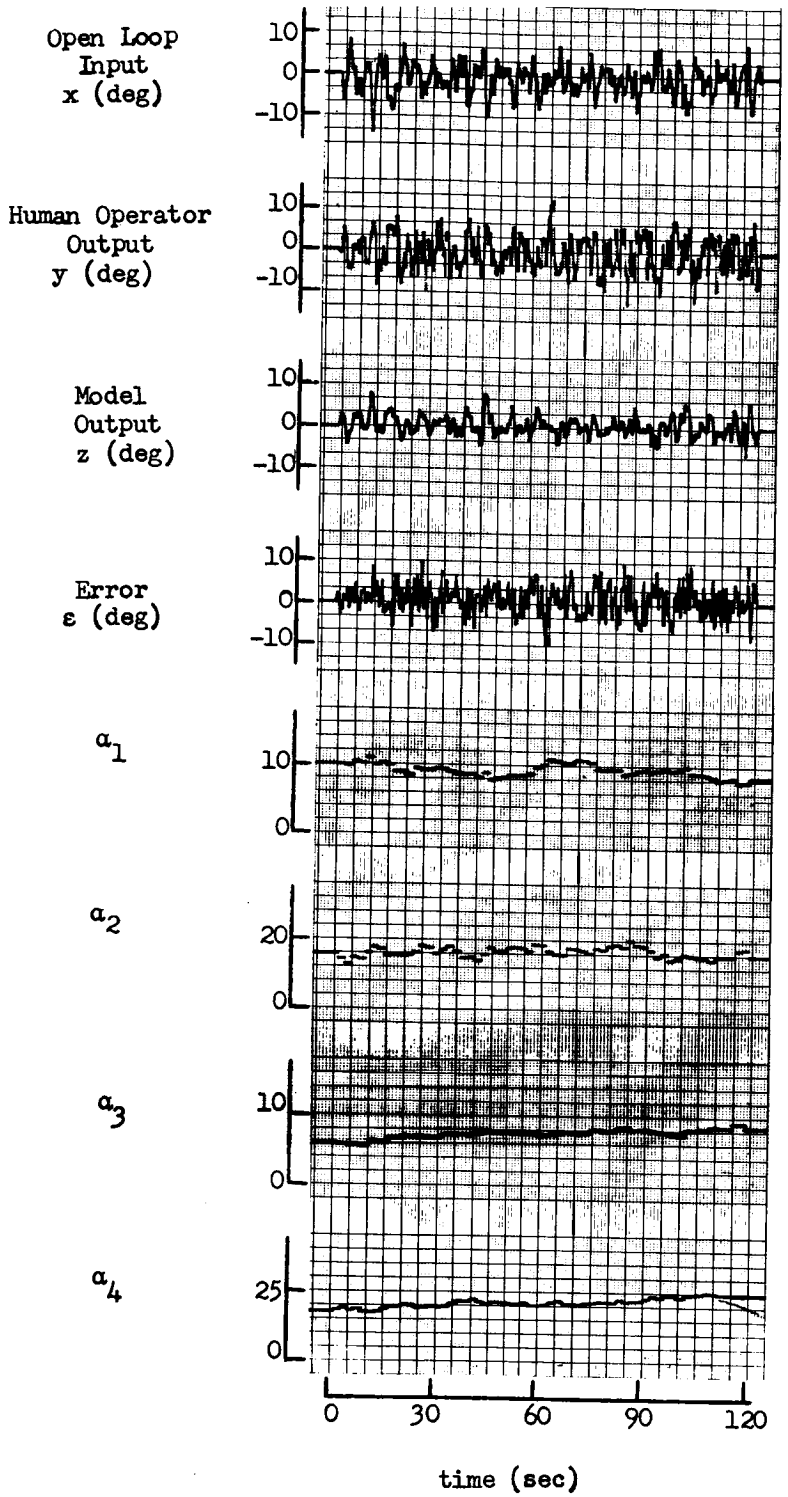

Figure C-5 Parameter Time History for H_{ba} (Task 2 of Coupled Experiment)

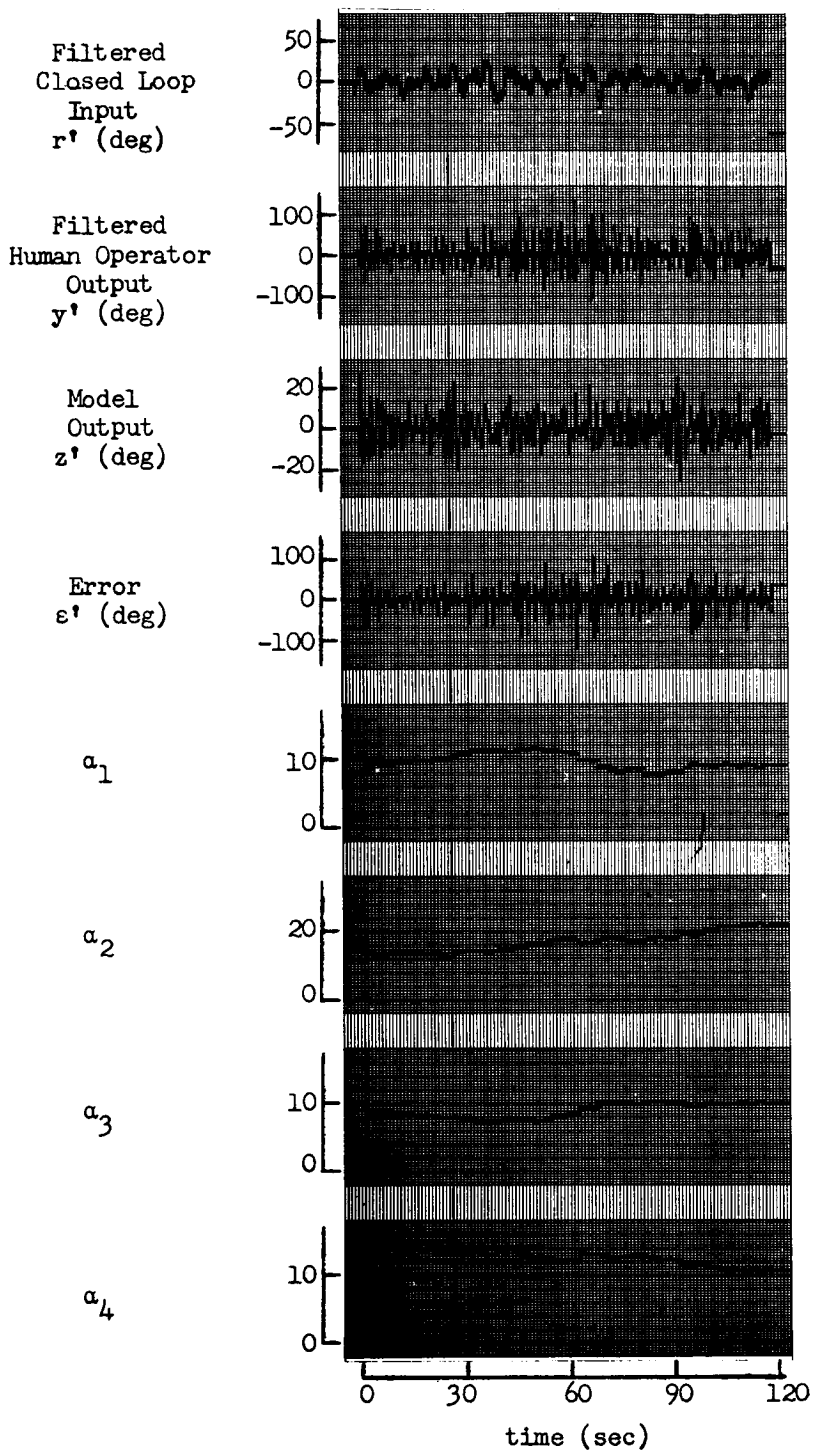

Figure C-6 Parameter Time History for H_{aa} (Task 3 of Coupled Experiment)

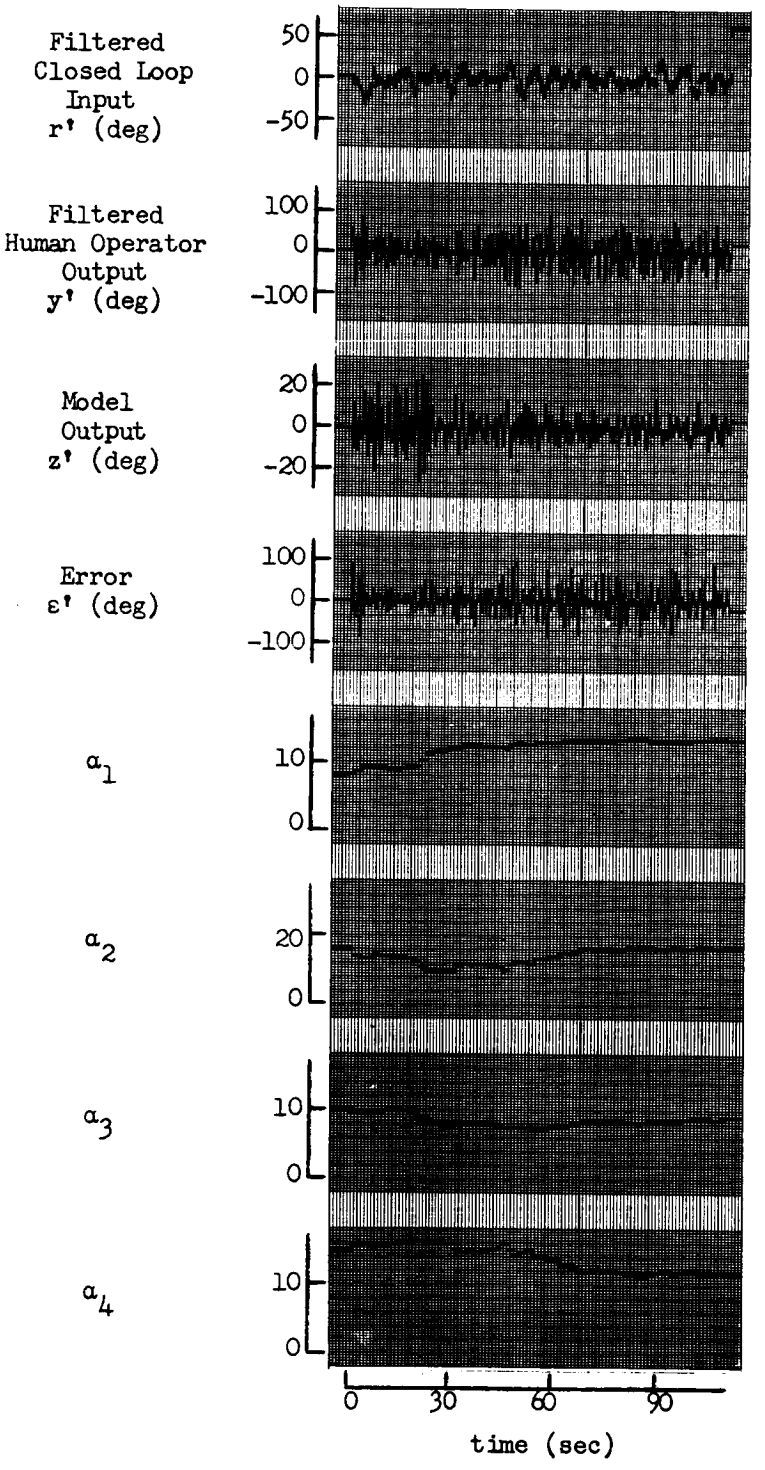

Figure C-7 Parameter Time History for H_{bb} (Task 3 of Coupled Experiment)

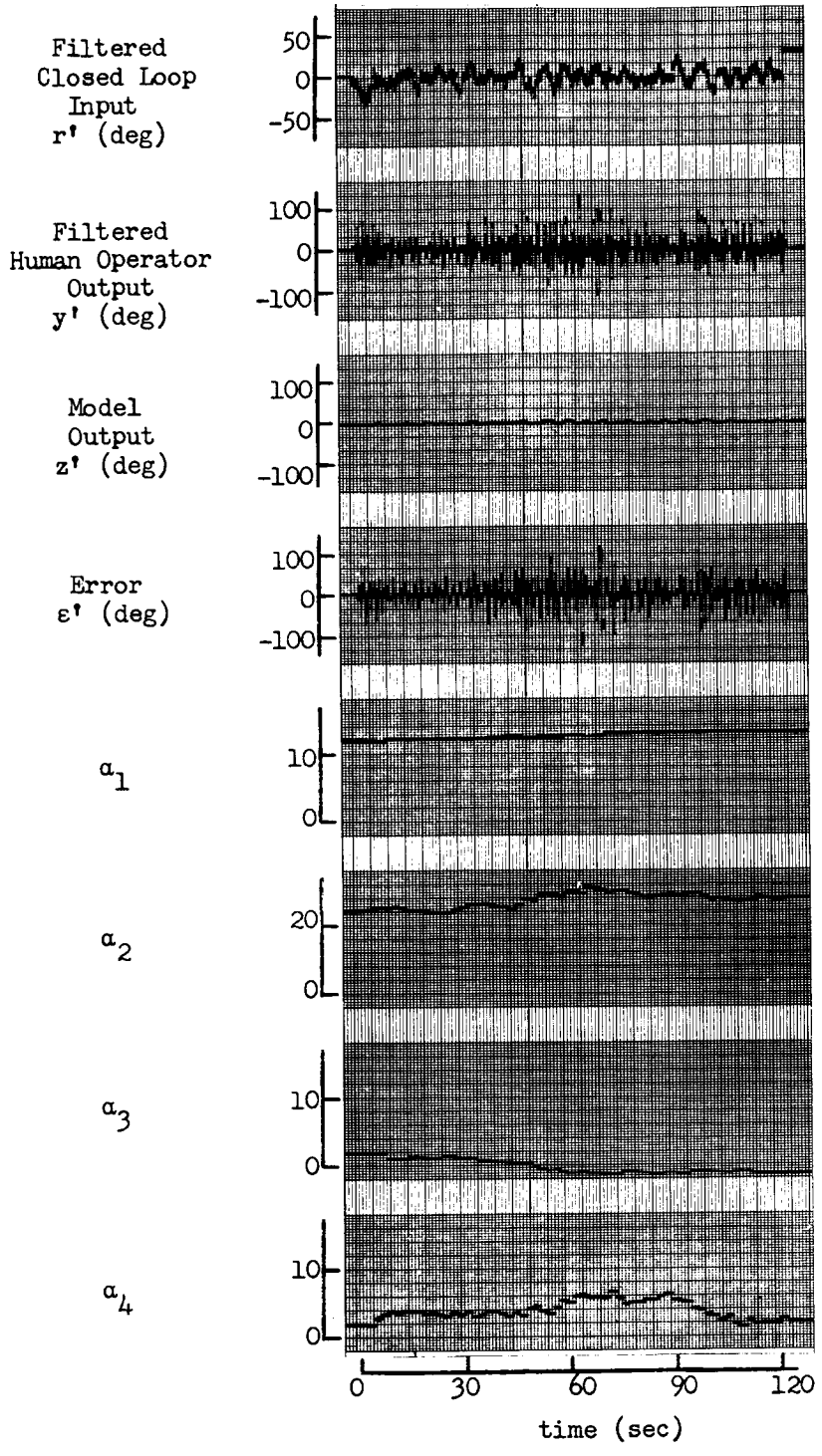

Figure C-8 Parameter Time History for H_{ab} (Task 3 of Coupled Experiment)

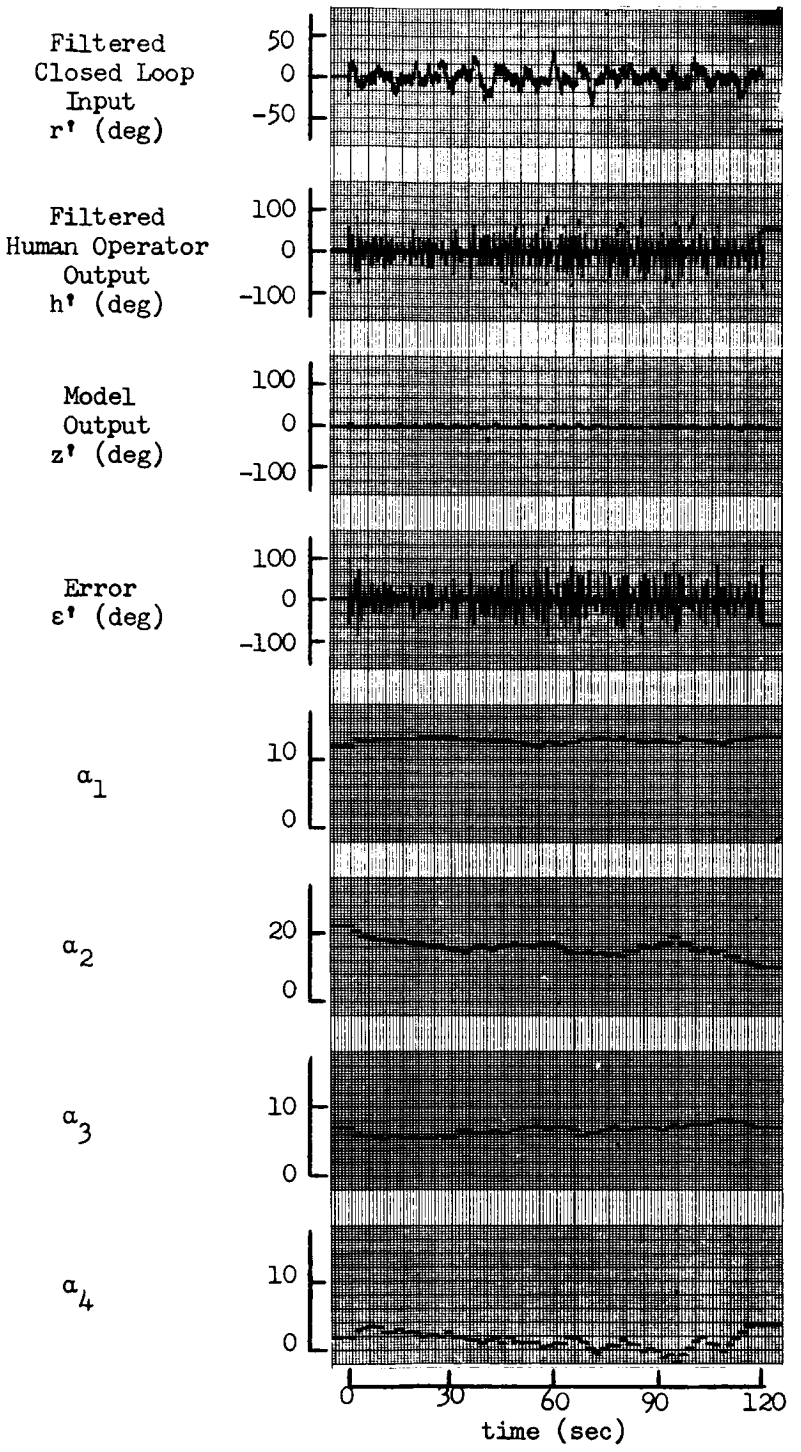

Figure C-9 Parameter Time History for H_{ba} (Task 3 of Coupled Experiment)

REFERENCES

1. Creer, B.Y., Stewart, J.D., Merrick, R.B., and Drinkwater III, F.J., "A Pilot Opinion Study of Lateral Control Requirements for Fighter-Type Aircraft," NASA Memo 1-29-59A, March 1959.

2. Chernikoff, R., Duey, J.W., and Taylor, F.V., "Two-dimensional tracking with identical and different control dynamics in each coordinate," J.Exp.Psych., 1960, 60: 318-322

3. Bolt, Beranek, and Newman, Inc., "Studies of Manual Control Systems," Progress Report No. 7, 10 May 1965.

4. Bolt, Beranek, and Newman, Inc., "Studies of Manual Control Systems," Progress Report No. 5, December 1964

5. Bekey, G.A., Meissinger, H.F., and Rose,R.E., "A Study of Model Matching Techniques for the Determination of Parameters in Human Pilot Models," NASA CR-143, January 1965.

6. Margolis, M. "On the Theory of Process Adaptive Control Systems: the Learning Model Approach, Ph.D. Dissertation, University of California, Los Angeles, June 1960, and Report AF OSR - TN 60 - 618, May 1960.

7. Meissinger, H.F., and Bekey, G.A., "An Analysis of Continuous Parameter Identification Methods, Simulation, February 1966.

8. Humphrey, R.E., "Determination of the Values of Parameters in Mathematical Models of Physical Systems," STL Document 9352.1-258, 6 September 1963.

9. Elkind, J.E., "A Comparison Between Open and Closed-Loop Measurements of Dynamic Systems," Memorandum Report No. 9224-4, Job No. 11093, Bolt, Beranek, and Newman, Inc.

10. Goodman, R. A., "Simultaneous Confidence Bands for Matrix Frequency Response Functions," Rocketdyne Division, North American Aviation Inc., Research Report, 1963

11. Meissinger, H.F., "Study of Model Matching Techniques for the Determination of Parameters in Human Pilot Models," STL Technical Memorandum 4380-6001-RU000, March 25, 1965.

12. Hoffman, L.G., Lion, P.M., and Best, J.J., "Theoretical and Experimental Research on Parameter Tracking Systems," STI Technical Report No. 148-1, October 1965.